NTNU
Norwegian University of
Science and Technology

Thyroid hormone status and thyroid gland histology in PFAS- and mercury contaminated glaucous gulls (*Larus hyperboreus*) from Svalbard

Torunn Slettemark Hovden

Environmental Toxicology and Chemistry
Submission date: May 2018
Supervisor: Bjørn Munro Jenssen, IBI
Co-supervisor: Geir Wing Gabrielsen, Norsk Polarinstitutt

Norwegian University of Science and Technology
Department of Biology

Torunn Slettemark Hovden

Thyroid hormone status and thyroid gland histology in PFAS- and mercury contaminated glaucous gulls (*Larus hyperboreus*) from Svalbard

Master's thesis in Environmental Toxicology

Trondheim

May 2018

Norwegian University of Science and Technology

Department of Biology

NTNU

Cover photo: Glaucous gull in Sassendalen, Svalbard. By Torunn Slettemark Hovden

ACKNOWLEDGEMENTS

I would like to thank my supervisors Bjørn Munro Jenssen, Åse-Karen Mortensen, and Geir Wing Gabrielsen for letting me take part in this huge, interesting, and important project. Thank you all for last-minute feedback. Thank you, Åse-Karen, for being my lab companion and for letting me come with my own ideas, and thank you, Geir, for enthusiasm about my project.

A bunch of people have been involved in the extensive lab work in this project. Thank you Linda Hanssen for supervising me through the PFAS analysis at NILU, and for follow-up afterwards. Thank you to Grethe Stavik Eggen for spending days with the hormone analysis and to Syverin Lierhagen for helping with the elemental analysis. Huge thank you to Christian Sonne for teaching me how to read histology and for helping me find my way through Copenhagen without a smartphone. Betina Gjedstad Andersen also deserves a thank for carrying out the staining of thyroid glands.

Thank you Tomasz Maciej Ciesielski for being a potato, a good hunter, and a statistics wizard.

I am very thankful for having shared these two years with all the wonderful classmates in the envitox-class. A special thank goes to Jose for patiently teaching me SPSS when R had treated me badly and everything seemed terribly dark. Ane and Brenley, huge thanks to you for being there throughout the year to share ups and downs at numerous of lunch dates. A warm thank goes to Brenley also for proofreading.

Finally, thanks to my parents for proofreading and for always supporting me. Thanks also to my flatmates Elin and Ingvild for being such good friends and discussion partners. Lastly, thank you Erling for the artistic touch on my figures and for sharing your inherent understanding for computers. Also, thank you for bearing over with my complicated relationship to gulls.

Trondheim, May 2018
Torunn Slettemark Hovden

ABSTRACT

The glaucous gull (*Larus hyperboreus*) is a scavenger and top predator in the Arctic marine food web. Due to its high trophic position, it is highly exposed to organohalogenated compounds (OHCs) and metals originating from anthropogenic emissions. The high body burden of contaminants is believed to cause adverse health effects, which assumingly affect the species even at the population level. The aim of this project was to investigate the possible effects of per-and polyfluoroalkyl substances (PFASs) and mercury (Hg) on the thyroid hormone system, as expressed by circulating thyroid hormone (TH) and thyroid stimulating hormone (TSH) levels, as well as the histology of the thyroid gland.

Fifteen glaucous gulls were euthanized in Sassendalen and Adventfjorden in Svalbard during the pre-breeding period in April and May 2017. Samples were taken of plasma, feathers, liver, and thyroid gland. PFAS concentrations were quantified in the liver, whereas Hg concentrations were quantified in the liver, feathers, and plasma. TSH and total and unbound fraction of TH were quantified in plasma. As selenium (Se) plays a role both in activation and regulation of THs, and acts as a detoxifying agent for Hg, this element was analysed in the same tissues as Hg. The histology of the thyroid glands was examined for histological changes. Multivariate data analyses were conducted to evaluate associations between Hg, PFASs and thyroid response variables.

Perfluorooctane sulfonate (PFOS) was the dominating PFAS, accounting for 71 % of the PFAS load. Long-chained perfluorinated carboxylates (PFCAs) constituted the remaining 29 % of the load, and there were no major differences between male and female glaucous gulls. Hg levels were highest in feathers of males, whereas liver and plasma concentrations were similar in males and females. Se levels were higher than Hg levels in plasma, feather and liver samples. Normal thyroid tissue was seen in five of fourteen birds. Eight birds had epithelial cell proliferation, and nodular hyperplasia was seen in one bird. The results indicate that Hg might contribute to a high follicle count in thyroid glands. TSH was negatively correlated with PFOS and perfluoro tetradecanoate (PFTeDA), and positively correlated with Se:Hg in liver (all, n=15) and plasma (males, n=7). Overall, the results from the present study indicate that ecological exposure to PFASs and Hg may alter thyroid hormone economy and thyroid histology in glaucous gulls in Svalbard.

SAMANDRAG

Polarmåka (*Larus hyperboreus*) er ein åtseletar og eit rovdyr som er på toppen av næringskjeda i det arktiske marine økosystemet. Menneskelege utslepp av miljøgifter, som organohalogenerte sambindingar (OHCs) og tungmetall, hopar seg opp i den arktiske næringskjeda, og polarmåka, med sitt høge trofiske nivå, er difor eksponert for svært høge konsentrasjonar. Miljøgiftene gir truleg alvorlege helseeffektar, og ein mistenkjer at desse effektane gjev utslag òg på populasjonsnivå. Målet for denne studien var å undersøkje dei moglege verknadene av per- og polyfluorerte stoff (PFAS) og kvikksylv (Hg) på tyroidhormonsystemet hjå polarmåka, uttrykt som blodnivå av tyroidhormon (TH) og tyroidstimulerande hormon (TSH), i tillegg til endringar i histologien til skjoldbruskkjertelen.

Femten polarmåker vart avliva i Sassendalen og Adventfjorden på Svalbard før hekkesesong i månadsskiftet april-mai i 2017. Prøvar vart tekne av blod, fjør, lever og skjoldbruskkjertel. Lever vart analysert for PFAS-ar, medan Hg vart kvantifisert i plasma, fjør og lever. TSH, samt fri og proteinbunden TH vart kvantifiserte i plasma. Plasma, fjør og lever vart òg analyserte for selen (Se), som er viktig for aktivering og regulering av TH, i tillegg til at Se detoksifiserer Hg. Skjoldbruskkjertlane vart undersøkte for histologiske endringar. Multivariat dataanalyse vart nytta for å finne moglege samanhengar mellom Hg, PFAS-ar og responsvariablane knytte til tyroid-tilhøvet.

Perfluoroktylsulfonat (PFOS) stod for 71 % av PFAS-ane, medan langkjeda perfluorinerte karboksylatar (PFCA-ar) utgjorde dei resterande 29 %. Det var ingen store skilnader mellom hannar og hoer i konsentrasjon og fordeling av dei ulike PFAS-ane. Hg-nivået var høgast i fjør frå hannar, medan det ikkje var nokon stor skilnad mellom kjønna sine lever- og plasmakonsentrasjonar. Det var meir Se enn Hg i både plasma, fjør og lever. Fem av fjorten fuglar hadde normalt skjoldbruskkjertel-vev. Åtte fuglar hadde epitelcelleproliferasjon, og éin fugl hadde nodulær hyperplasi. Resultata tyder på at Hg kan ha ein positiv verknad på talet folliklar i skjoldbruskkjertelen. TSH stod i negativ samanheng med PFOS og perfluortetradekanoat (PFTeDA), og i positiv samanheng med Se:Hg i lever (alle fuglar,[♪] n=15) og plasma (hannar, n=7). Alt i alt tyder resultata frå denne studien på at økologisk aktuelle nivå av PFAS-er og Hg i polarmåker på Svalbard kan påverke tyroidhormonbalansen og histologien i skjoldbruskkjertelen.

[♪] små dei er

ABBREVIATIONS

5´D I	Type I deiodinase
5´D II	Type II deiodinase
5´D III	Type III deiodinase
AMAP	Arctic Monitoring and Assessment Program
BCI	Body condition index
BFR	Brominated flame retardent
BM	Body mass
brPFDcA	Branched perfluorodecanoic acid
C	Celcius
CHL	Chlordne
CV	Coefficient of variation
CV-ANOVA	Cross-validated analysis of variance
DDT	Dichlorodiphenyltrichloroethane
DNA	Deoxyribonucleic acid
dw	Dry weight
E	East
EIA	Enzyme immunoessay
F53 b	6:2 Chlorinated polyfluorinated ether sulfonate
FASA	Perfluoralkane sulfonates
FC	Follicular epithelial cell
FG	*Fulmaris glacialis*
FOSA	Perfluorooctane sulfonamide
FT3	Free triiodothyronin
FT4	Free thyroxine
FTH	Free thyroid hormone
FTS	Fluorotelomer sulfonic acid
HCl	Hydrogen chloride
HE	Hematoxylin and eosin stain
Hg	Mercury
HLB	Hydrophilic-lipophilic balance
HNO_3	Nitric acid
HPT	Hypothalamus-pituitary-thyroid
HSI	Hepato somatic index
I	Iodine
ICP-MS	Inductively coupled plasma mass spectrometry
IDL	Instrumental detection limit
IU	International unit
kg	Kilogram
l	liter
LC-MS	Liquid chromatography–mass spectrometry
LH	*Larus hyperboreus*
LOD	Limit of detection
M	Molar
MeHg	Methylmercury
MS/MS	Tandem mass spectrometry
n	Number of observations
N	North

ng	Nanogram
NH_4OAc	Ammonium acetate
NILU	Norwegian Institute for Air Research
nm	Nanometer
nmol	Nanomol
NTNU	Norwegian University of Science and Technology
O-PLS	Orthogonal projection to latent structures
OC	Organochlorine
OHC	Organohalogenated contaminants
p	Probability of rejecting the hypothesis
PC	Principal component
PCA	Principal component analysis
PCB	Polychlorinated biphenyl
PFAS	Per- and polyfluorinated compounds
PFBA	Perfluorobutanoic acid
PFBS	Perfluorobutane sulfonate
PFCA	Perfluorinated carboxylates
PFDA	Perfluorodecanoate
PFDcS	Perfluorodecane sulfonate
PFHpA	Perfluoroheptanoate
PFHpS	Perfluoroheptane sulfonate
PFHxA	Perfluorohexanoate
PFHxDA	Perfluorohexadecanoate
PFNA	Perfluoronanoate
PFNS	Perfluorononane sulfonate
PFOA	Perfluorooctanoate
PFODcA	Perfluorooctadecanoate
PFOS	Perfluorooctane sulfonate
PFPeA	Perfluoro-n-butanoic acid
PFSA	Perfluoroalkyl sulfonates
PFTeDA	Perfluorotetradecanoate
pmol	Pikomol
POP	Persistent Organic Pollutant
PP	Polypropylene
ppm	Parts per million
Q^2	Goodness of prediction coefficient
QQ	Quantile-quantile
r	Correlation coefficient
R^2X	Explained variance
R^2Y	Goodness of fit coefficient
RIA	Radioimmuno assay
RiS	Research in Svalbard
RNA	Ribonucleic acid
ROS	Regression on order statistics
r_P	Pearson correlation coefficient
rpm	Revolutions per minute
r_S	Spearman correlation coefficient
RT	*Rissa tridactyla*
S/N	Signal to noise ratio
SD	Standard deviation

Se	Selenium
SRM	Standard reference material
T3	Triiodothyronine
T4	Thyroxine
TH	Thyroid hormone
TMB	3,3´,5,5´-tetramethylbenzidine
TSH	Thyroid stimulating hormone
TT3	Total triiodothyronine
TT4	Total thyroxine
TTH	Total thyroid hormone
TTR	Transthyretin
UHPLC-MS/MS	Ultrahigh pressure liquid chromatography triple–quadruple mass-spectrometry
UPLC HSS	Ultrahigh pressure liquid chromatography high strength silica
v/v	Volume-volume percent
VIP	Variable importance in projection
ww	Wet weight
µg	Microgram
µl	Microliter
µlU	Micro international unit
µmol	Micromol

Table of contents

1 INTRODUCTION

1.1 Contamination in the Arctic

1.1.1 Persistent organic pollutants in the Arctic

Despite few local sources in the Arctic, this polar region has become a sink for anthropogenic pollution sourced in more southerly latitudes (Letcher et al., 2010). Industrial and agricultural compounds with certain physiochemical characteristics are transported north via complex pathways involving atmospheric and ocean currents and river run-off, influenced by temperature, precipitation, snow cover, and ice cover (AMAP, 2004). These transport systems are dynamic, and may also be modified by climate changes (Alava et al., 2017). The physio chemical properties of contaminants which are transported to the Arctic and taken up in the food chain, are typically semi volatility, persistency, low water solubility, and high lipophilicity (O'Sullivan, 2013). Organochlorinated compounds (OCs) are one big group of such compounds. Marine organisms take up (bioconcentrate) these lipophilic compounds directly from the water, or from their prey. During an organism's lifetime, it accumulates persistent, lipophilic compounds (bioaccumulation), and the concentrations are magnified (biomagnification) up through the food chain (Borgå et al., 2001). Organisms with reduced ability to metabolize foreign compounds, like seabirds, have an increased accumulation (Walker, 1992). High concentrations of persistent organic pollutants (POPs) are therefore found in the Arctic top predators (Gabrielsen, 2007), and concentrations are above threshold levels of toxic effects in certain species (e.g. polar bears (*Ursus maritimus*), glaucous gulls, and ringed seals (*Pusa hispida*)) (De Wit et al., 2005, Dietz et al., 2015). The concentrations of legacy persistent organic pollutants (POPs) have, however, decreased substantially over the last decades partly as a result of international regulations like the Stockholm Convention (Hung et al., 2016). Yet, several compounds, i.e. the so-called emerging contaminants, are not declining in the Arctic: Polybrominated flame retardants (BFRs) like polybrominated diphenyl ethers (PBDEs) now seem to increase again, after a decline at the beginning of the 2000s (Rigét et al., 2016, Sagerup et al., 2010); and PFASs (which are not lipophilic like the other POPs, but rather bind to proteins), show variable trends. However most PFASs increased between the 1970s to the 2000s, and stabilized or decreased after 2004 (Butt et al., 2010, Rigét et al., 2016, Rotander et al., 2012, Routti et al., 2016).

Mercury, a toxic element present in the Arctic due to anthropogenic emissions, increased by 1.6 – 1.7 % yearly from 1892 to 2008 in polar bear hair (Dietz et al., 2011), but recent years have shown more variable temporal trends (Braune et al., 2015). Hg concentrations in eastern parts of the Arctic seabirds now seem to be stable (Braune et al., 2015).

1.1.2 Per- and polyfluorinated compounds (PFASs)

Contrary to the lipophilic chlorinated and brominated POPs, PFASs are not lipid soluble, but bind to the proteins in organisms. The strong electronegativity and small size of the fluorine make the compounds extraordinary stable and both water- and oil repellent (Wang et al., 2017). These properties are the reason why such compounds are so popular in a variety of industrial and consumer applications (Wang et al., 2017, KEMI, 2015). The stability of PFASs also make them resistant to metabolization, and they accumulate in the liver of exposed organisms (Jones et al., 2003). There are two main groups of PFASs, namely perfluorinated sulfonates (PFSAs) and perfluorinated carboxylates (PFCAs). Perfluoroocrane sulfonate (PFOS) belongs to the former group, and is now listed under the Stockholm Convention, but more than 3000 PFASs are still, or have been, on the global market (Wang et al., 2017). Volatile precursors such as fluorotelomer alcohols, are transported to the Arctic with atmospheric transport, while the bulk of PFASs are transported north with ocean currents (Armitage et al., 2009, Butt et al., 2010). Several PFASs are now detected in fairly high concentrations in Arctic wildlife (Haukås et al., 2007, Routti et al., 2016, Butt et al., 2010).

1.1.3 Mercury (Hg)

Elemental mercury (Hg^0) is the predominant form of atmospheric Hg, and its long residence time in the atmosphere makes the element prone to long-range transport far from its emission sources (Schroeder and Munthe, 1998). Iron- and sulphate-reducing bacteria in anaerobic environments sediments can convert inorganic Hg to organic Hg by methylation (Schaefer et al., 2011), and the product – MeHg – is lipophilic, and has strong affinity to soft nucleophiles, thiols, and selenol (Se) groups. MeHg therefore readily binds to both lipids, and cysteine (thiol) and selenocysteine (Se) groups on proteins and enzymes (Khan and Wang, 2009, Mulder et al., 2012) and thereby magnify in the food chain (Braune et al., 2015, Jæger et al., 2009). Since Hg is a toxic element, the Se-Hg interaction detoxifies Hg, and recently more attention has been directed on the detoxifying effect of the Se-Hg antagonism (Khan and Wang, 2009, Mulder et al., 2012). However, Se availability is also affected by this interaction,

which may disrupt the function of Se dependent enzymes like deiodinase, and consequently affect the thyroid hormone homeostasis (Mulder et al., 2012).

1.2 The glaucous gull

1.2.1 Population

The glaucous gull (*Larus hyperboreus*) is an avian predator with circumpolar distribution breeding in the Arctic. Its global population size is estimated to 170 000 – 1 200 000 pairs (Mitchell et al. 2004 in Fauchald et al., 2015), of which 7 000 – 17 000 pairs breed in the Barents Sea region (Anker-Nilssen et al., 2000). The Svalbard population is estimated to 4 000 – 10 000 pairs (Strøm and Descamps, npolar.no), but the population trends in Svalbard are unknown (Artsdatabanken). However, the Bjørnøya population has decreased by 65 % from 1986 to 2006, from 2 000 pairs to 650 pairs (Sagerup et al., 2009 b), and there is concern that increasing exposure to pollutants might contribute to the decrease (Erikstad et al., 2013, Sagerup et al., 2009 b). The species is listed as "near threatened" on the Red list in Svalbard (Fauchald et al., 2015) and "least concern" globally (BirdLife International, 2016, iucnredlist.org).

1.2.2 Biology

Glaucous gulls are opportunistic feeders, predators, and scavengers, feeding on algae, tundra plants, molluscs, fish, birds, eggs, mammals, and crustaceans (Barry and Barry, 1990, Bustnes et al., 2010, Gabrielsen et al., 1995, Lydersen et al., 1985, Løvenskiold, 1964). In autumn, they migrate south to winter in Northern Norway and Iceland, and return to Svalbard in March-April to breed. They breed in all parts of Svalbard, and commonly nest on bird-cliffs, where they lay 1-3 eggs (Løvenskiold, 1964). The oldest recorded glaucous gull on Svalbard lived to be 19 years of age (Strøm and Descamps).

1.2.3 The glaucous gull as a bioindicator species

Since Bourne and Bogan (1972) first reported organochlorine pesticides in glaucous gulls at Bjørnøya forty-six years ago, the glaucous gull has been recognized as a bioindicator species for contamination in the Arctic environment (Verreault et al., 2010). As a top predator, it is exposed to the contaminant load that has biomagnified through the long, Arctic food chain, and reaches some of the highest concentrations of legacy and emerging POPs of all animals in the Arctic (Borgå et al., 2001, Fisk et al., 2001, Gabrielsen et al., 1995, Haukås et al., 2007).

There are indications that glaucous gulls have a restricted capacity for metabolism of OCs (Henriksen et al., 2000), and concentrations of ∑PCB, ∑DDT, and ∑CHL have been reported to be higher than 1 part per million (ppm) in this bird, which is a general threshold level of concern (Letcher et al., 2010). The chronic exposure to POPs is associated with immunological, behavioural, and reproductive effects, as well as reduced survival in glaucous gulls (AMAP, 2004, Erikstad et al., 2013, Letcher et al., 2010, Verreault et al., 2010) but also additional natural stressors like prey abundance, competition, climate change, and pathogens must be considered in the overall picture (Verreault et al., 2010). Still, a clear, causal link between contaminant exposure and health effects in Svalbard glaucous gulls remains to be established (Letcher et al., 2010, Verreault et al., 2010).

1.3 The thyroid hormone system and endocrine disruption

1.3.1 Function and regulation

Thyroid hormones (THs) are required for normal development, growth and metabolism in birds and mammals (Decuypere et al., 2005). They are produced in the thyroid glands located ventrolaterally to the trachea and transported in the vascular system to the target cell (Sturkie, 2012). There are two main forms of thyroid hormones: Thyroxine (T4), which is a precursor hormone, and triiodothyronine (T3), which is the active hormone. They are synthesized by follicular epithelial cells in the thyroid gland and are stored in the colloid-containing follicles within the gland until secretion. Secretion is stimulated by thyroid stimulating hormones (TSH) produced in the pituitary, whose production is stimulated by thyrotropin releasing hormone produced in the hypothalamus (McNabb, 2007, Sturkie, 2012). The entire system of the hypothalamus, pituitary gland, and thyroid gland is called the HPT axis (Figure 1). Secretion of THs is mainly in the form of T4, which has one iodide more than T3. In birds, the circulating concentration of T4 is about ten times the concentration of T3 (Newcomer, 1974).

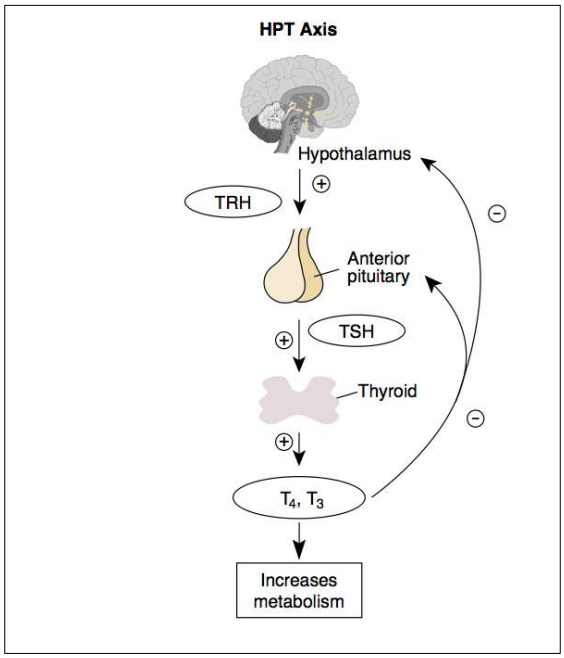

Figure 1. The hypothalamus-pituitary-thyroid (HPT) axis (Embryology, 2012)

Deiodination from T4 to T3 occurs mainly in the liver, but also in target tissues, by the enzyme deiodinase (Reyns et al., 2002). There are different tissue-specific deiodinase enzymes, which provide the opportunity to tissue-specific regulation of thyroid hormone action (Chang et al., 1999). Three key deiodination pathways are present in birds, as well as in mammals: Type I, Type II, and Type III deiodination. Type I deiodinase (5´D I) is present in the liver, kidney, and small intestine, and converts T4 to T3 by outer ring deiodination, as well as converts T4 to rT3 by inner ring deiodination. Type II deiodinase (5´D II) is present in the brain, and converts T4 to T3 by outer ring deiodination, whereas Type III (5´D III) is present in liver and deactivates T3 to inactive T2 (McNabb, 2007). It is assumed that hepatic 5´D1 plays a major role in supplying most of the T3 for circulation in birds (McNabb, 2007).

Only a small fraction – 0.01% - of the total THs in plasma occurs in its free form, as the majority of the THs is bound to transport proteins (Hulbert, 2000). In birds, the main TH binding proteins are transthyretin (TTR) and albumin, the latter being the most important. Only free (unbound) THs are taken up in target cells and trigger cellular responses through the TH receptor (TRs) (Mendel, 1989). Therefore, it is convenient to distinguish between the free fraction and total fraction of THs, abbreviated FT3/FT4 and TT3/TT4, respectively. There are two types of direct responses of THs: metabolic and developmental responses.

Other responses can be indirect effects of THs as well as interactive effects with other hormones (Sturkie, 2012).

A negative feedback mechanism regulates the circulating TH levels to obtain homeostasis: A decrease in circulating THs feeds back to the HPT axis and stimulates the pituitary to release TSH. In response to TSH, the thyroid gland grows, takes up more iodide, and produces THs, as well as releases THs from the colloid storage within the gland, restoring the circulating TH levels. If, however, TH depletion persists, the increased thyroid gland function might not be sufficient to compensate for the TH decrease, and a more chronic state of TH deficiency – hypothyroidism – may arise (McNabb, 2007). Hypothyroidism typically leads to a decrease in the mobilization and metabolism of lipids (McNabb, 2007), and might have severe consequences during the developmental stages of an organism (Dentice et al., 2013).
The feedback mechanism of the HPT axis has a cyclic pattern. In addition, there are TH variations associated with diurnal patterns, temperature conditions, and food related variations (depending on food source, food availability, and iodide availability) (Cogburn and Freeman, 1987, Eales, 1988). Together, these characteristics make circulating TH a variable measurement of TH status. Therefore, interpreting TH levels in relation to contaminant exposure may not give a clear answer about possible thyroid disruption.

1.3.2 Thyroid hormone disruption

A number of chemicals that are released into the environment are known to disrupt the endocrine homeostasis of humans and wildlife (Maqbool et al., 2016). Several lab studies on rats and mice have shown that PCBs, polybrominated biphenyls, and dioxins reduce the circulating T4 levels (Allen-Rowlands et al., 1981, Collins and Capen, 1980, Hallgren et al., 2001, Morse et al., 1992). This relationship is further indicated by several field studies. For example, in birds Melnes et al. (2017) found indications of negative effects of OC exposure on T3 and T4 in female glaucous gulls, but also a contrasting positive association between PFOS and FT3 and TT3 in female gulls. Positive associations between fulmar (*Fulmaris glacialis*) and kittiwake (*Rissa tridactyla*) chick TT4 levels and PFASs have also been reported (Nøst et al., 2012). Furthermore, there are indications that mercury (Hg), and more specifically the selenium to mercury ratio (Se:Hg), might affect circulating TH levels in animals (Mulder et al., 2012, Soldin et al., 2008, Wada et al., 2009). The disruption may occur at several levels of the HPT axis, i.e. synthesis, transport, activation, thyroid receptor binding, metabolism, and elimination of THs. Some studies have investigated the different

compounds' potential to interfere at these levels (Ishihara et al., 2003, Ren et al., 2016, Ucán-Marin et al., 2009, Mortensen, 2015). Other studies have investigated whether the histology of thyroid glands in birds and mammals are affected by exposure to contaminants (Jacobsen et al., 2017, Movasseghi et al., 2017, Sonne et al., 2011, Sonne et al., 2013, Sonne et al., 2010). However, studies on the effects of contaminant exposure on the thyroid function in birds are ambiguous (Dawson, 2000) and more studies are needed to clarify this relationship.

1.4 Aim of study

The aim of this study was to investigate the potential effects of PFASs and mercury on the thyroid hormone system of glaucous gulls from Svalbard, as expressed by changing levels of circulating hormones and changed histology of the thyroid glands. Possible sex differences in thyroid response related to PFAS- and mercury burden were also investigated in the present study.

1.5 Hypothesis

In line with the findings reported by Melnes et al. (2017) and Nøst et al. (2012), it is hypothesized that there is a positive correlation between PFASs and thyroid hormones. Further, it is hypothesized that there is a negative correlation between thyroid hormones and thyroid stimulating hormone, as a result of the feedback mechanism of the HPT axis. It is also hypothesized that there is a negative relationship between Hg levels and T3 levels, and a positive association between Hg and T4 levels, as a result of the inhibiting potential of Hg on deiodinase enzymes (Mulder et al., 2012). Regarding the histology of thyroid glands, my hypothesis is that there is an association between contaminant load and degree of pathology in the glaucous gull thyroids, in line with the findings of Ness et al. (1993).

2 MATERIALS AND METHODS

2.1 Sampling area

Field sampling was conducted in Sassendalen and Adventfjorden, both located near Longyearbyen (78°13'N 15°38'E) on the west coast of Spitsbergen, the largest island of the Svalbard archipelago, Norway. Six glaucous gulls were collected in Brattlidalen in Sassendalen, one close to Fredheim at the mouth of Sassendalen, and eight gulls were collected in Adventfjorden (Figure 2). Sampling was conducted from April 24th – May 9th 2017, during the pre-breeding period. At this time of the year, there is continuous daylight, but the weather conditions may change rapidly between several degrees below zero, no winds, plus degrees, and strong winds.

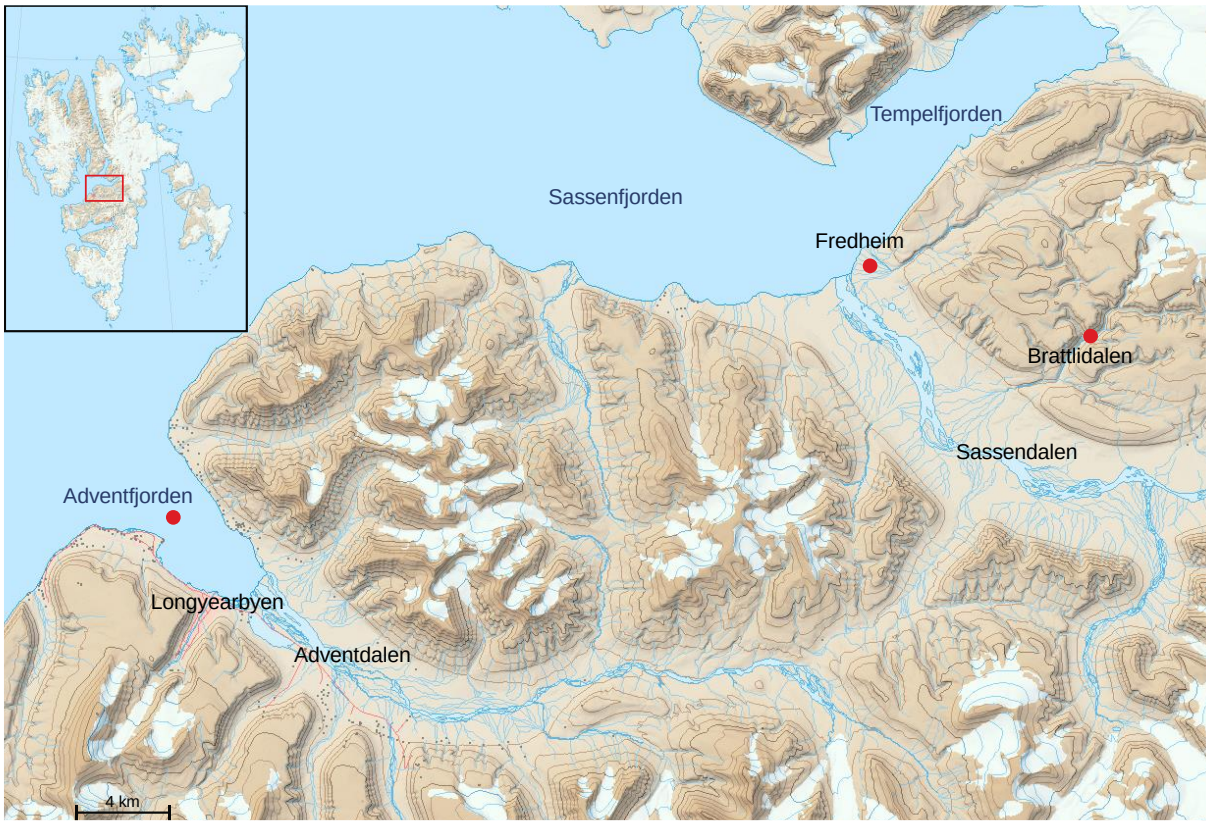

Figure 2. Sampling sites where glaucous gulls were collected in Adventfjorden and Sassendalen, Svalbard, Norway. Red dots mark the sampling sites; Brattlidalen, Fredheim (Sassen), and Adventfjorden.

2.2 Sampling procedure

The glaucous gulls were euthanized by shotgun, followed by decapitation with a heparinized knife. Blood was collected from the birds' necks to a glass beaker and mixed with a few droplets of heparin, transferred to glass centrifuge tubes and centrifuged within 30 minutes after euthanasia (10 minutes, 5 000 rpm). In some cases, only a small amount of blood drained from the neck of the bird, therefore additional blood was collected directly from the heart using a heparinized syringe.

From each glaucous gull we dissected samples from the liver, muscle, kidney, brain, gonad, adrenal gland, thyroid gland, stomach, bile, and adipose tissue. Samples for organic analyses and bioassays (samples of all abovementioned tissues) were wrapped in aluminium foil, whereas samples for metal analyses (samples of liver, kidney, muscle) were packed in plastic bags. Samples of blood and all tissues were rapidly frozen in liquid nitrogen after dissection and packing, prior to storage in a -80°C freezer. Additional samples of muscle and liver were packed in aluminium foil and frozen in ambient air temperatures (-2°C to -8°C) prior to storage in a -20°C freezer. In addition, we collected samples from the gonads, adrenal glands, kidneys, and thyroid glands from each glaucous gull. These samples were stored in 10 % formalin for fixation. Feather samples were stored in paper envelopes.
For each glaucous gull we measured their body mass, liver mass and gonad mass. We also measured tarsus lengths, wing lengths, beak length, and head length of all birds collected prior to dissection. Liver mass of LH3 was eliminated from the data set because of a reading error. Body condition index (BCI) was calculated using the method of Sagerup et al. (2009 a): Principal component analysis was first used to obtain a single measure of size (Jolicoeur and Mosimann, 1960). The first principal component from a PCA of head length and wing length was used as a size index. Size indices were calculated separately for males and females because the two sexes of glaucous gulls are dimorphic. Body mass variables were standardized within each sex. Data for males and females were pooled. Residuals from the linear regression of standardized body mass and size index were used as the BCI, according to the method of Jakob et al. (1996).

Sexing of glaucous gulls was done by gonad identification. Age determination (juvenile/adult) was done visually by recognizing glaucous gulls with a pale plumage as adults (>5 years), and mottled grey and brown as juveniles (Strøm and Descamps, npolar.no).

The project (RiS number 1063) was funded by The Research Council of Norway and approved by the Governor of Svalbard (ref. 17/00414-2). Sampling of the birds was in accordance with the regulations of the Norwegian Animal Welfare Act.

2.3 PFAS analyses

Analyses of hepatic concentrations of 21 per- and polyfluoroalkyl compounds (Table 1) were performed at Norwegian Institute for Air Research (NILU), Framsenteret, Tromsø. The Powley method was applied (Powley et al., 2005), including the main steps homogenization, extraction, clean-up, and LC-MS-analysis. Two reference material samples (500 µl human serum: AM-S-Y1701, positive control) and two blanks (negative control) were run in addition to the 15 liver samples in one batch.

Table 1. The fluorinated compounds analysed in liver from glaucous gulls (*Larus hyperboreus*) living in the Longyearbyen area, Svalbard, in spring 2017. PFSA: perfluoroalkylated sulfonic acid; PFCA: perfluoroalkylated carboxylic acid; FASA: perfluoralkane sulfonates.

Group	Acronym	Analyte	Chain length	Group	Acronym	Analyte	Chain length
PFSA	4:2 FTS	4:2 Fluorotelomer sulfonic acid	6	PFCA	PFBA	Perfluorobutanoic acid	4
	6:2 FTS	6:2 Fluorotelomer sulfonic acid	8		PFPeA	Perfluoro-n-butanoic acid	5
	8:2 FTS	8:2 Fluorotelomer sulfonic acid	10		PFHxA	Perfluorohexanoate	6
	PFBS	Perfluorobutane sulfonate	4		PFHpA	Perfluoroheptanoate	7
	PFHxS	Perfluorohexane sulfonate	6		PFOA	Perfluorooctanoate	8
	PFHpS	Perfluoroheptane sulfonate	7		PFNA	Perfluorononanoate	9
	F-53B	6:2 Chlorinated polyfluorinated ether sulfonate	8		PFDA	Perfluorodecanoate	10
					PFUnDA	Perfluoroundecanoate	11
	PFOS	Perfluorooctane sulfonate	8		PFDoDA	Perfluorododecanoate	12
	PFNS	Perfluorononane sulfonate	9		PFTrDA	Perfluorotridecanoate	13
	PFDcS	Perfluorodecane sulfonate	10		PFTeDA	Perfluorotetradecanoate	14
					PFHxDA	Perfluorohexadecanoate	15
FASA	FOSA	Perfluorooctane sulfonamide	8		PFODcA	Perfluorooctadecanoate	16

Homogenization

Approximately 2 grams (1.61 grams - 2.15 grams) of liver from each bird were cut from the frozen liver samples and homogenized by cutting into tiny pieces using a scalpel. Each liver

sample was transferred to a centrifuge tube (50 ml PP tube, VWR, Germany), and spiked with mass labelled internal standards (20µl 0.5 ng/µl ^{13}C labelled PFAS analyte).

Extraction

LiChrosolv Acetonitrile (8 ml) was added to each tube as solvent. The tubes were capped and vortexed, followed by ultrasonic bath. Vortexing and ultrasonic bath were then repeated twice (sonication at 27°C, 32°C, and 31°C on level 8, all 10 minutes each). Ultrasonic waves increase molecular vibrations and contact between matrix and solvent, facilitating the extraction of PFASs from the matrix.

Clean-up

Samples were centrifuged (2000 rpm, 5 minutes) and the supernatant was transferred to 15 ml PP vials. The supernatant was concentrated to just below 2 ml in RapidVap (Labconco, Kansas City, USA), and acetonitrile was added to exactly 2 ml (LH 8: 2.3 ml). For clean-up of the extracts, adsorption chromatography was applied using fine particulate coal (active carbon treatment); 25 mg ENVI-Carb was weighed into new polypropylene microcentrifuge tubes (1.7 ml) and glacial acetic acid (50 µl) was added, before supernatant solutions were added (0.8 ml) and the tubes were capped and vortexed. The vials were then centrifuged (10 000 rpm, 10 minutes). An aliquot (0.5 ml) of the supernatant was transferred into an autoinjector vial (Chromacol, ThermoFisher Scientific, USA) and recovery standards (20 µl 0.1 ng/µl 3,7-brPFDcA in methanol) were added to allow for determination of the amount of internal standard lost during sample preparation. The samples were then kept cool prior to LC-MS analysis.

Analysis

At the time of analyses, 50 µl of each extract was transferred to autosampler vials with insert and mixed with an equal amount of aqueous ammonium acetate (NH_4OAc, 2 mM in HLB water). The samples were then injected to the UPLC/MS system and the concentrations of PFASs were quantified.

The positive control was provided by AMAP. Internal standards (PFAS standards) were obtained from Wellington Laboratories Inc. (Guelph, Ontario, Canada) and were of >98 %

purity. All solvents used in this work were of Lichrosolv® grade, and were purchased from Merck-Schuchardt (Hohenbrunn, Germany).

Instrumental analyses

PFASs were analysed by ultrahigh pressure liquid chromatography triple–quadrupole mass-spectrometry (UHPLC-MS/MS). Analysis was performed on a Thermo Scientific quaternary Accela 1250 pump (Thermo Fisher Scientific Inc., Waltham, MA, USA) with a PAL Sample Manager (Thermo Fisher Scientific Inc., Waltham, MA, USA) coupled to a Thermo Scientific Vantage MS/MS (Vantage TSQ) (Thermo Fisher Scientific Inc., Waltham, MA, USA); 10 µL was injected on a Waters Acquity UPLC HSS 3 T column (2.1× 100 mm, 1,8 µm) (Waters Corporation, Milford, MA, USA) equipped with a Waters Van guard HSS T3 guard column (2.1× 5 mm, 1.8 µm) (Waters Corporation, Milford, MA, USA). Separation was achieved using 2 mM NH_4OAc in 90:10 methanol/water and 2 mM NH_4OAc in methanol as the mobile phases, as described by Hanssen et al. (2013).

Quantification

Internal standards with known concentrations of ^{13}C –labeled PFASs were analysed together with liver samples for quantification of PFASs. Quantification was conducted using the LCQuan software from Thermo Scientific (Version 2.6) (Thermo Fisher Scientific Inc., Waltham, USA), as described by Hanssen et al. (2013).

Quality control

The blank sample and the control sample described earlier were analysed for quality assurance. No PFASs were detected in the blanks. The concentrations in the control samples were within ± 15 % of reference values, except for PFNA and PFUnDA, for which the mean quantified concentrations were + 19 % and + 21 % of reference values, respectively. Recovery of internal standards were within the guidelines at the NILU laboratory (See Appendix C for details on recovery).

Limit of detection

Limit of detection (LOD) was set to 3 x signal to noise (S/N) ratio, which is common practice at the NILU laboratory, and was 0.10 ng/g ww for all PFASs. When > 50 % of the individuals had detections below LOD for a specific compound, the compound in question was removed from the data set. Consequently, 4:2 FTS, 6:2 FTS, 8:2 FTS, FOSA, PFBS, PFNS, PFDcS,

F53 b, PFBA, PFPeA, PFHxA, PFHpA, PFOA, PFHxDA, and PFODcA were removed from the data set. Concentrations of PFHpS were below LOD in LH3, LH5, LH6, LH14, and LH15. These samples were each assigned a number <LOD calculated in R using the robust regression on order statistics (ROS) method for censored data.

2.4 Element analysis

Plasma, liver and feathers from the 15 glaucous gulls were analysed for elements at Department of Chemistry, NTNU Trondheim, using inductively coupled plasma mass spectrometry (ICP-MS). Since samples introduced to the ICP-MS must be as solution, liver and feathers were treated slightly differently from plasma prior to injection. Feather (app. 100 mg) and liver (app. 500 mg) samples were freeze-dried before digestion with 6 ml 50 % v/v HNO_3 in UltraCLAVE from Milestone (EMLS, Leutkirch, Germany). Feathers were also washed prior to freeze-drying to remove external contaminants. Washing consisted of several steps of flushing with water, acetone, and HNO_3. (See Appendix B for details.) After decomposition, samples were diluted to 60 ml (0.6 M HNO_3) and transferred to 15 ml PP vials for ICP-MS. Plasma samples (app. 1000 mg) were added 2 ml concentrated HNO_3, digested in UltraCLAVE, and diluted to 30 ml (0.6 M HNO_3) before transfer to 15 ml PP vials for ICP-MS. Concentrations of 62 elements in total were quantified, but only Hg and Se were used further in this project.

LOD was calculated for Hg and Se based on both instrumental detection limits (IDLs) and blanks. IDL based detection limit resulted in a higher value (Hg: 0.0319 µg/kg in blood, 0.0005 µg/g in feathers and 0.0001 µg/g in soft tissue; Se: 1.5957 µg/kg in blood, 0.0245 µg/g on feathers and 0.0065 µg/g in soft tissue), and this was used as the LOD. All Hg and Se values in blood, feathers and liver were above detection limit.

2.5 Thyroid hormone analyses

Plasma levels of total and free thyroid hormones (TT3, TT4, FT3, and FT4) were analysed at the Norwegian University of Science and Technology, Trondheim, Norway using commercially available ^{125}I radioimmune assay (RIA) kits manufactured by MP Biomedicals, LCC (New York, USA) (Catalogue No. 06-254215 (TT3), 06B-254011 (TT4), 06B-258709 (FT3), and 06B-257214 (FT4)). The kits are based on the principle that synthetic hormones

labelled with radioactive ^{125}I bind to binding sites in antibody-coated tubes with the same affinity as hormones from the samples, and thereby the quantity of labelled analyte bound to the tube is inversely related to the concentration of unlabelled analyte (natural hormones) in the sample. In short, plasma from glaucous gulls and a tracer solution were added to the test tubes, vortexed an incubated either at room temperature or in water bath at 37 °C. After incubation, the tubes were aspirated and the reactivity was counted using a Packard Cobra-II Auto gamma counter. Standard curves for each hormone were established based on the measured reactivity of the known concentrations in the standards, from which the hormone levels in the plasma samples were quantified.

Assay validation

The RIA kits used for these assays were developed for quantification of human thyroid hormones. To assure for the precision of the kits, quality controls of standard reference material (SRM, Lyphocheck Immunoassay Plus Control Levels 1, 2 and 3. BioRad, California, USA) and chicken plasma were also analysed. Three human serum controls were assayed in each kit. The results were within the acceptable range of the kits.

Quality assurance

Samples were run in triplicates to test the repeatability of the assays, and samples with a coefficient of variance (%CV) >15 were reanalysed. Eventually all triplicates for each TH analysis had a %CV < 15, except for two (LH9 when analysed for FT4; %CV=15.4 and LH11 when analysed for TT4; %CV=17.2). However, these two were not excluded from the data set since the %CVs were so close to 15.

Detection limit was set to the sensitivity limit reported by the kit protocols; 6.7 ng/dl (TT3), 0.76 μg/dl (TT4), 0.06 pg/ml (FT3), and 0.045 ng/dl (FT4). All values were above the sensitivity limits. Units were converted to nmol/L (TT4 and TT3) and pmol/L (FT3 and FT4) using the online converter calculator unitslab.com (unitslab.com, 2018). Average %CV between plasma sample triplicates in each hormone kit was 3.8 for TT3; 8.3 for TT4; 4.7 for FT3; and 7.7 for FT4. Average %CV for the reference material was 7.6 for TT3, 5.4 for TT4, 8.3 for FT3, and 13.7 for FT4.

2.6 Thyroid stimulating hormone analyses

Plasma levels of thyroid stimulating hormone (TSH) were analysed at the Department of Biology, NTNU Trondheim, using the commercially available one-step enzyme immunoassay (EIA) kit Medizym TSH hs, manufactured by Medipan GMBH (Berlin, Germany) (Catalogue No. MP55011). Medizym TSH hs is designed for human serum, but was applied to the glaucous gull plasma as there is no avian TSH specific antibodies available (Troisi et al., 2016) The principle for the EIA system is as follows; TSH from the sample act as antigens and bind to a capture antibody that is coated on the wells of an EIA plate. By adding a second antibody that also binds to the antigen, the whole sandwich complex is immobilized to the plate. By adding a fluorescent substrate solution that binds to the secondary antibody, a colour develops whose intensity is measurable, and directly reflects the THS concentration in the samples.

In short, serum from glaucous gulls was added to the antibody-coated wells in addition to standards and control sera. A conjugate containing a signal antibody coupled with horseradish peroxidase was added to all wells, followed by 1-hour incubation (37°C, shaking) and washing. A fluorescent substrate (3,3´,5,5´-tetramethylbenzidine (TMB) in citrate buffer containing hydrogen peroxidase) was added and the plate was incubated for 15 minutes in the dark, before a stop solution (HCl) was added. The optical density was read at 450 nm using Cytation 5 Cell Imaging Multi-Mode Reader from BioTek Instruments (Vermont, USA). Based on the absorbance of the standards with known concentrations, a standard curve was established and the TSH concentrations were read. All samples were run in duplicates.

Assay validation

To assure for the precision of the kits, quality controls of standard reference material (SRM, Lyphocheck Immunoassay Plus Control Levels 1, 2 and 3. BioRad, California, USA) and chicken plasma were also analysed. The results were within the acceptable range of the kits.

Quality assurance

A quality control followed the Mezidym TSH kit and comparing the reported concentration with the analysed concentration verified the quality of the analyses. Samples were run in duplicates to test the repeatability of the assays. Eight of the 15 samples had CV values higher than 15 %, but since these concentrations were in a low concentration range (0.007-0.093

µlU/ml), and the respective standard deviations were so low (0.0276 at the highest) none of these samples were excluded. Average %CV between plasma sample triplicates was 17.6 for TSH.

2.7 Thyroid gland histology

Thyroid glands were fixated for two days in 10 % formalin before changing solution to ethanol. The tissue was then kept in ethanol until preparation for histology, which was done at Copenhagen University, Section for Experimental Animal Models at the Department of Veterinary and Animal Sciences. Thyroid glands from all birds were prepared for histology reading except for the LH12 thyroid gland, which was lost in field. The glands were examined grossly and trimmed before being enclosed in embedding cassettes and stored in formalin while waiting for further processing. The glands were then washed and dehydrated in a series of alcohol solutions of increasing alcohol concentrations using Excelsior ™ Tissue Processor (Thermo Scientific, Waltham, USA) before they were embedded in melted paraffin. After being cooled down, the glands were sectioned at 1µm in a slicing machine (microtome) using Microm HM 440 E Microtome (GMI, Minneapolis, USA). Single sections were placed on glass microscope slides and rehydrated before staining, firstly with hematoxylin and then with eosin (HE stain) using a linear stainer (Leica ST4040, Nussloch, Germany). Hematoxylin has high affinity to nuclear DNA and areas of the cell containing cytoplasmic RNA, whereas the counterstain eosin colours other structures, like intra- and extracellular proteins and the cytoplasm. The combined staining effect of hematoxylin and eosin colours histology slides in different shades of violet (Ross and Pawlina, 2006).

Stained thyroid gland slides were brought to Aarhus University, Institute for Bioscience, campus Roskilde, for examination and classification. The slides were examined at 200 x magnification using a Leica DC300 microscope (Leica microsystems, Cambridge, UK). Thyroid glands were examined for epithelial cell proliferation and nodular hyperplasia, and assigned three categorical classes based on their histological appearance; Class A for normal thyroid tissue; Class B for moderate histological changes; and Class C for pronounced histological changes. The microscope was coupled to a computer using TWAIN driver software IM50, and density of follicles was estimated by counting the number of follicles on the computer screen (showing fields of 326 x 244 µm) in 20 semi-independent fields at 200 x magnification. The first field was selected by locating the approximate centre of the thyroid

gland. The following fields were selected by moving the field stepwise to the right until the edge was reached, always keeping the reading field within the organ. Then the field was moved up one step and stepwise to the left until the edge on the other side was reached. This procedure was followed until the whole gland was covered. Only whole, clearly marked follicles were counted. All fields counted were photographed (Appendix L). A follicle count mean was calculated for each individual.

2.8 Plasma protein

Due to accidental dilutions of blood samples by body fluids in the field, total plasma protein was analysed. The number of diluted samples is unknown. This lead to a replacement of the planned response variable (hormone concentrations) with hormone to protein ratio (TH:protein & TSH:protein) as the new response variable. Protein analysis was done by PhD candidate Åse-Karen Mortensen at Department of Biology, NTNU Trondheim, using Bradford assay. A detectable colour shift forms the basis of the Bradford principle. A protonated dye in the Bradford reagent, Brilliant Blue G-250, is red under acidic conditions, but turns blue when it is not protonated. When the dye binds to proteins, it converts to the blue form, which is detectable at 595 nm (Bradford, 1976). The light intensity measured by a microplate reader is proportional to protein concentration in the sample, and using prediluted standards with known concentrations, light intensities from the samples are convertible to protein concentrations.

In short, 5 µl of prediluted standards (Bradford bovine serum albumin stock, 14 mg/ml) and plasma samples were added to a 96 well plate in triplicates before 250 µl Bradford reagent was added to all wells. The plate was read in a Cytation 5 Cell Imaging Multi-Mode Reader microplate reader (BioTek Instruments, Vermont, USA) after 5 minutes, and protein concentrations were provided directly. The linear concentration range is 0.1 – 1.4 mg/ml protein. All sample concentrations were within this range.

2.9 Statistical methods

Data plotting was done in Excel (Microsoft Excel 16.12), and statistical analyses were done in SPSS (IBM SPSS Statistics 25, New York, USA). Orthogonal projection to latent structures

(O-PLS) was done in Simca (15.0.0.4783, Umetrics, Umeå, Sweden) and the ROS method for censored data was carried out in R (3.4.1 GUI 1.70 El Capitan).
The data was tested for normality using Shapiro Wilk's normality test. Statistical significance was set to $p \leq 0.05$ and p values were two-tailed. All variables were normally distributed except for TSH:protein and Se:Hg plasma (n=15), TT4:protein and TSH:protein (males), and liver, HSI, FT3:protein, TT3:protein, and TSH:protein (females). TSH:protein had two outliers (LH9 and LH14) which were two orders of magnitude higher than the other individuals. However, since nothing notable had happened to these samples in field nor in the lab, they were regarded biological outliers, and were kept in the data set. See Appendix J for an overview of all variables and their p value from the Shapiro-Wilk normality test. All variables were also visually investigated for normal distribution through quantile-quantile (QQ) plots.

Pearson correlation analysis was applied to test for bivariate correlation between all normally distributed variables. Variables that were not normally distributed were tested using Spearman rank correlation. Correlation is given as r_p (Pearson correlation coefficient) or r_S (Spearman correlation coefficient) and the significance level is given as p value. Since the data set included multiple variables and few observations (n=15), significance level was not corrected by Bonferroni correction or other correction methods. This was in order to avoid producing false negatives, as recommended by Moran (2003).

Differences in biometric variables between sexes were tested using t-test (in Excel) for normally distributed data, and Mann-Whitney Utest (in SPSS) for non-normally distributed data.

2.9.1 Principal component analysis

Principal component analyses (PCA) were performed in SPSS to investigate the relationships between hepatic PFAS concentrations, Hg concentrations in plasma, feathers, and liver, Se:Hg ratios in plasma, feathers and liver, biometric measurements, and plasma ratios of THs and TSH to protein. PCA is commonly used to reduce a large number of variables to a low-dimensional plane in order to help with multivariate data interpretation (Eriksson et al., 2013). The two first, most significant components, PC1 and PC2, were extracted and loadings (representing variables) and scores (representing observations/individuals) were plotted in a 2-dimensional space.

A score plot is a plot where each individual (here: each glaucous gull) is shown in a low-dimensional plane, where the individual's positioning on the plane reflects how the sum of its multiple variables are loaded into this new plane. A loading plot shows which variables are influential to the model (e.g. specific compounds or biometric measures). Both for score plot and loading plot, the distance from a data point to the origin, and the relative positioning of data points in the plot, indicate the properties of the data point and how it relates to other data points in the plot. Variables on opposite sides of the origin are negatively correlated to each other, and variables far from the origin have big influence on the model. Individuals that are clustered together have similar properties, whereas individuals far from each other have dissimilar properties (Eriksson et al., 2013).

2.9.2 Orthogonal projection to latent structures (O-PLS)

O-PLS modelling was conducted to model the influence of X-variables (PFAS levels, Hg levels, Se:Hg ratios, and biometric variables) on the Y-values (TH:protein ratio and TSH:protein ratio) in the glaucous gulls. Variables were $\log_{10}$-transformed in case of skewed data (applied to TSH:protein only) and all variables were centred and scaled to unit variance. The models obtained were visualized in regression coefficient (CoeffCS) plots, and variable importance in projection (VIP) plots. The VIP values were used to optimize the models and select the most important variables in explaining the variation in Y. *X*-variables with a VIP-value < 0.5 were considered less important in explaining the variance in thyroid hormones and were excluded. *X*-variables were thereafter excluded manually one by one until a significant model was achieved (p<0.05). Analysis of variance-testing of cross-validated predictive residuals (CV-ANOVA) was used to cross-validate that the results were reliable according to Lundstedt's guidelines of acceptable R^2 and Q^2 values in biological data (Lundstedt et al., 1998); $R^2 > 0.7$ and $Q^2 > 0.4$. O-PLS was done by researcher Tomasz Maciej Ciesielski at the Department of Biology, NTNU, Trondheim.

3 RESULTS

3.1 Biometric results

Males of glaucous gulls had a significantly higher body weight than females (18.5 %, p<0.001) (Table 2). Sex differences were also significant for the other size related biometrics (head, wing, and tarsus lengths) with males being larger than females, but there was no difference in body condition index (BCI) (p=1). There was a significant sex difference in HSI (p=0.01), but there was no significant difference between liver masses (p=0.99). Individual biometric measures can be found in Appendix A.

Table 2. Mean, standard deviation (SD), median, and range of biological variables of male (n=7) and female (n=8) glaucous gulls (*Larus hyperboreus*) from Sassendalen and Adventfjorden, Svalbard, in April and May 2017. Significant differences (p <0.05) and (p <0.001) are denoted with one * and two ** asterisks, respectively.

	Males			Females		
	Mean ± SD	Median	Range	Mean ± SD	Median	Range
Body mass (g) **	1839 ± 94.4	1875	1685 - 1950	1499 ± 108	1475	1340 - 1687
Head length (mm) *	147.2 ± 4.6	145.5	141.6 - 154.26	133.7 ± 5.2	132.2	128.93 - 145.48
Wing length (mm) **	46.3 ± 0.6	46.2	45.65 - 47.2	44.5 ± 0.8	44.8	43.10 - 45.20
Tarsus length (mm) *	78.6 ± 3.0	78.2	75.48 - 84.55	75.9 ± 2.3	75.9	72.26 - 79.90
BCI	0 ± 0.8	-0.1	-1.38 - 0.92	0 ± 1	0	-1.40 - 1.04
Liver mass (g)	45.0 ± 15.0	42.7	33.3 - 76.25	39.8 ± 6.8	38.3	34.30 - 55.45
Hepato somatic index *	2.46 ± 0.9	2.2	1.74 - 4.36	2.7 ± 0.4	2.6	2.36 - 3.49

3.2 Contaminants

Nine different compounds of individual PFASs were detected and quantified, of which three were perfluoroalkylated sulfonic acids (PFSA; PFHxS, PFHpS, and PFOS) and six were perfluoroalkylated carboxylic acids (PFCA; PFNA, PFDA, PFUnDA, PFDoDA, PFTrDA, and PFTrDA). All hepatic PFAS concentrations are presented in Table 3 (ng/g ww) as well as the sums of sulfonates and carboxylates. Females of glaucous gulls had significantly higher concentrations of PFHpS than males (p = 0.029). There were no sex differences in concentrations of the other PFASs. Therefore, a table showing mean, SD, median, and range for all individuals together was made (Table 3). Concentrations of PFHpS, $PFOS_{lin}$, ∑PFOS, and ∑PFSA were significantly higher in livers from Class A glaucous gulls (gulls with normal

thyroid tissue in the thyroid gland) than Class B glaucous gulls (gulls with moderate histological changes in the thyroid glands) (Table Z; see *3.4 Thyroid gland histology*). Glaucous gulls in Class A had, in general, higher PFAS levels than those in Class B, but there were no other significant differences between Class A and Class B. Class C (pronounced histological changes) was not considered since it consisted of only one bird.

The results from Se and Hg in plasma, feathers and liver are presented in Table 3 (µg/g dw), as well as the molar ratio between Se and Hg. Males had significantly higher Hg concentrations in feathers than females (p = 0.007). There were no statistically significant differences in Hg concentrations between glaucous gulls in histology Class A and Class B (Table Z; See *3.4 Thyroid gland histology*).

Table 3. Mean ± standard deviation (SD), minimum, and maximum concentrations (ng/g ww) of individual PFASs, ∑PFSA, and ∑PFCA in liver from glaucous gull males (n=7) and females (n=8) sampled in April – May 2017 in Sassendalen and Adventfjorden, Svalbard. Hg and Se concentrations (µg/g ww) in plasma, feathers, and liver are also presented, as well as their ratio on molar basis. Significant differences (p <0.05) between sexes are denoted with black up-pointing triangle ▲. Significant differences (p <0.05) between histology classes A and B are denoted with white down-pointing triangle ▽.

	Males				Females				All individuals			
Compound	N	Mean ± SD	Median	Range	N	Mean ± SD	Median	Range	N	Mean ± SD	Median	Range
PFHxS (ng/g)	7	0.23 ± 0.15	0.19	0.03 - 0.45	8	0.25 ± 0.15	0.22	0.07 - 0.58	15	0.24 ± 0.15	0.21	0.03 - 0.58
PFHpS (ng/g) ▽	7	0.08 ± 0.03	0.08	0.045 - 0.14	8	0.14 ± 0.05	0.15	0.06 - 0.19	15	0.11 ± 0.05	0.10	0.05 - 0.19
PFOSlin (ng/g) ▽	7	23.54 ± 10.05	20.16	13.21 - 42.72	8	24.13 ± 12.44	21.88	9.24 - 48.25	15	23.86 ± 10.99	20.61	9.24 - 48.25
∑PFOS (ng/g) ▽	7	25.89 ± 11.10	22.69	13.81 - 47.10	8	26.83 ± 13.26	24.06	11.84 - 52.73	15	26.39 ± 11.87	22.69	11.84 - 52.73
PFNA (ng/g)	7	2.16 ± 0.80	2.43	0.91 - 3.20	8	2.57 ± 1.36	2.53	0.96 - 5.02	15	2.38 ± 1.12	2.46	0.91 - 5.02
PFDA (ng/g)	7	1.97 ± 0.61	1.87	1.20 - 2.75	8	1.65 ± 0.96	1.60	0.58 - 3.48	15	1.18 ± 0.81	1.87	0.58 - 3.48
PFUnDA (ng/g)	7	4.32 ± 1.27	4.63	2.42 - 5.88	8	3.23 ±1.42	3.18	1.49 - 5.38	15	3.74 ± 1.42	3.58	1.49 - 5.88
PFDoDA(ng/g)	7	0.73 ± 0.18	0.73	0.50 - 0.98	8	0.58 ± 0.20	0.64	0.22 - 0.81	15	0.65 ± 0.20	0.66	0.22 - 0.98
PFTrDA (ng/g)	7	1.91 ± 0.39	2.03	1.32 - 2.50	8	1.55 ± 0.52	1.75	0.71 - 2.24	15	1.72 ± 0.48	1.79	0.71 - 2.50
PFTeDA (ng/g)	7	0.34 ± 0.08	0.32	0.25 - 2.48	8	0.33 ± 0.12	0.33	0.12 - 0.54	15	0.33 ± 0.10	0.32	0.12 - 0.54
∑PFSA (ng/g) ▽	7	26.24 ± 11.12	22.91	13.93 - 47.32	8	27.25 ± 13.27	24.31	12.56 - 53.33	15	26.78 ± 11.89	22.91	12.56 - 53.33
∑PFCA (ng/g)	7	11.44 ± 3.21	12.18	6.88 - 15.32	8	9.91 ± 4.00	9.62	4.74 - 16.87	15	10.62 ± 3.61	11.03	4.74 - 16.87
Hg plasma (µg/g)	7	0.01 ± 0.00	0.01	0.009 - 0.015	8	0.01 ±0.00	0.01	0.01 - 0.02	15	0.01 ± 0.00	0.01	0.01 - 0.02
Hg feathers (µg/g) ▲	7	4.62 ± 1.83	5.15	1.40 - 6.57	8	2.19 ± 1.07	1.95	0.85 - 4.15	15	3.32 ± 1.89	3.06	0.85 - 6.57
Hg liver (µg/g)	7	3.44 ± 1.22	2.87	2.02 - 5.55	8	3.10 ± 1.27	3.26	1.08 - 5.32	15	3.26 ± 1.22	2.94	1.08 - 5.55
Se plasma (µg/g)	7	0.29 ± 0.10	0.26	0.18 - 0.47	8	0.31 ± 0.09	0.32	0.17 - 0.43	15	0.30 ± 0.09	0.30	0.17 - 0.47
Se feathers (µg/g)	7	1.17 ± 0.40	1.12	0.77 - 1.95	8	0.93 ±0.10	0.92	0.75 - 1.10	15	1.04 ± 0.30	0.95	0.75 - 1.95
Se liver (µg/g)	7	5.74 ± 1.97	5.58	3.01 - 8.36	8	5.26 ± 1.38	5.01	2.78 - 7.27	15	5.48 ± 1.64	5.30	2.78 - 8.36
Se:Hg ratio plasma	7	62.48 ± 26.65	52.69	37.99 - 112.87	8	72.20 ± 35.67	53.20	46.88 - 145.84	15	67.66 ± 31.08	52.69	37.99 - 145.84
Se:Hg ratio feather	7	0.75 ± 0.39	0.64	0.40 - 1.55	8	1.32 ± 0.62	1.25	0.53 - 2.25	15	1.06 ± 0.59	0.88	0.40 - 2.25
Se:Hg ratio liver	7	4.69 ± 2.19	3.87	1.71 - 7.73	8	5.12 ± 2.94	4.25	2.21 - 11.35	15	4.92 ± 2.53	4.05	1.71 - 11.35

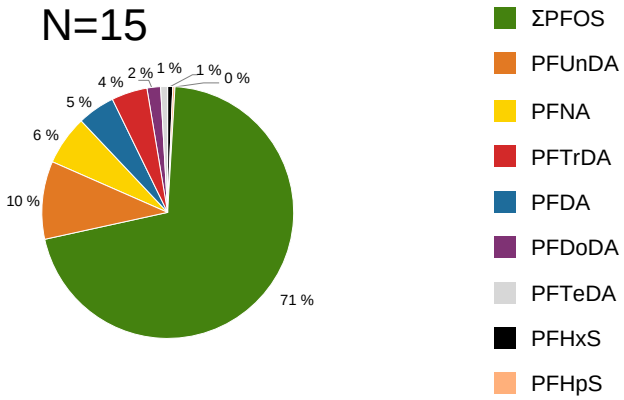

Figure 3. Contribution of the fluorinated compounds to the total PFAS burden in livers of glaucous gulls (*Larus hyperboreus*) collected in Sassendalen and Adventfjorden, Svalbard, in April and May 2017. 10.1 % of ∑PFOS is branched, the remaining 89.9 % is linear PFOS.

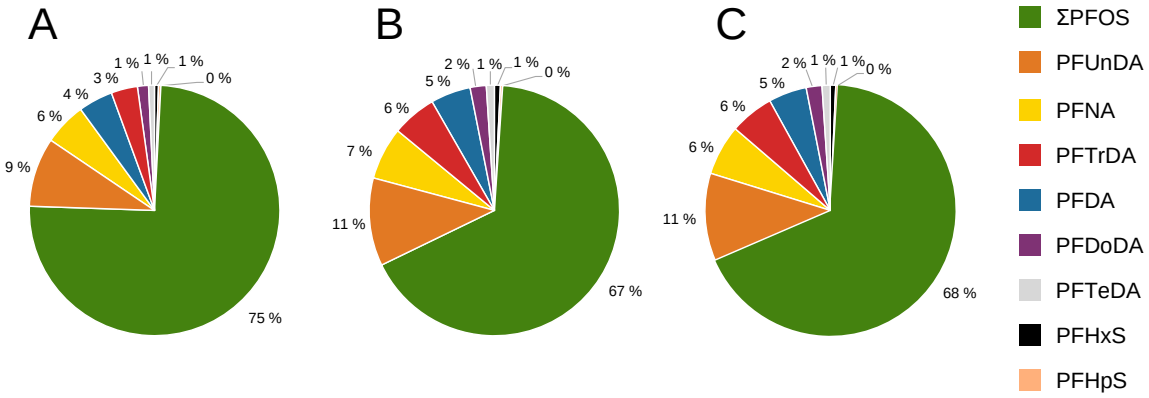

Figure 4. Contribution of the flourinated compounds to the total PFAS burden in livers of glaucous gulls (*Larus hyperboreus*) collected in Sassendalen and Adventfjorden, Svalbard, in April and May 2017. A: Histology Class A. (n=5); B: Class B. (n=8); C: Class C (n=1). The percentage of ∑PFOS which is branched, is (ClassA) 9.51 %, (Class B) 10.71 %, and (Class C) 7.2 %. The remaining PFOS is linear.

The PFAS, Hg, and Se concentrations in each individual are presented in Appendix D and Appendix E. A table showing the class wise contaminant levels is presented in Appendix F.

3.3 Thyroid hormones and thyroid stimulating hormone

Concentrations of THs ranged from 0.66 – 7.32 nmol/L (TT3), 17.12 – 57.57 nmol/L (TT4), 1.00 – 16.62 pmol/L (FT3), and 7.56 – 33.53 pmol/L (FT4) in plasma, whereas circulating concentrations of TSH ranged from 0.01 – 2.06 µlU/ml (Table 4). There were statistically no significant differences between males and females regarding circulating TH levels or TSH levels (p=0.54, 0.54, 0.54, 0.41, and 0.96 for TT3, TT4, FT3, FT4, and TSH, respectively).

The ratios TH:protein and TSH:protein were calculated to avoid the effects of having diluted some of the blood samples in the field. The TH:protein ratios ranged from 0.05 – 0.24 µmol:mg (TT3:protein), 0.57 – 2.63 µmol:mg (TT4:protein), 0.07 – 0.55 nmol:mg (FT3:protein), and 0.27 – 1.38 nmol:mg (FT4:protein), whereas the TSH:protein ranged from 0.18 – 69.00 mIU:mg. There were statistically no significant differences between males and females with respect to TH:protein or TSH:protein ratios, nor between glaucous gulls in histology class A and B (Table 4; See *3.4 Thyroid gland histology*).

Individual TH levels, TSH levels, TH:protein ratios, and TSH:protein ratios are found in Appendix G.

Table 4. A: Mean concentration of TT3 (nmol/L), TT4 (nmol/L), FT3 (pmol/L), FT4 (pmol/L), TSH (µIU/ml), and total protein (mg/ml) in plasma from glaucous gull (*Larus hyperboreus*) males and females captured in Sassendalen and Adventfjorden, Svalbard, in April and May 2017. SD, median, minimum and maximum concentrations are also shown. B: Mean, SD, median, minimum and maximum ratio between circulating TH &TSH concentrations and total protein concentration (TT3:protein and TT4:protein: µmol:mg; FT3 and FT4: nmol:mg; TSH:protein: µlU:mg). There were no significant differences between males and females, nor between histology Class A and Class B. C: Mean, SD, median and range of follicle counts in 20 fields à 326 x 244 µm in the thyroid glands.

		Males			Females			All individuals		
		Mean ± SD	Median	Range	Mean ± SD	Median	Range	Mean ± SD	Median	Range
A	TT3 (nmol/L)	3.30 ± 1.50	3.51	0.66 - 4.75	3.24 ± 1.74	2.69	1.89 - 7.32	3.27 ± 1.57	2.74	0.66 - 7.32
	TT4 (nmol/L)	28.51 ± 5.60	29.94	18.43 - 34.15	35.34 ± 14.31	35.81	17.12 - 57.57	32.15 ± 11.33	30.84	17.12 - 57.57
	FT3 (pmol/L)	8.43 ± 4.41	9.12	1.00 - 13.10	6.99 ± 4.34	6.01	2.26 - 16.63	7.66 ± 4.28	6.90	1.00 - 16.62
	FT4 (pmol/L)	14.16 ± 2.44	13.70	10.61 - 17.74	17.14 ± 8.90	17.01	7.56 - 33.54	15.75 ± 6.67	14.60	7.56 - 33.53
	TSH (µlU/ml)	0.06 ± 0.11	0.02	0.01 - 0.32	0.27 ± 0.72	0.01	0.01 - 2.06	0.17 ± 0.53	0.02	0.01 - 2.06
	Total protein (mg/ml)	24.00 ± 5.86	24.40	13.00 - 32.30	27.84 ± 4.79	28.90	20.70 - 36.00	26.05 ± 5.49	25.80	13.00 -36.00
B	TT3:protein ratio (µmol:mg)	0.13 ± 0.05	0.14	0.05 - 0.2	0.12 ± 0.06	0.10	0.08 - 0.24	0.12 ± 0.05	0.10	0.05 - 0.24
	TT4:protein ratio (µmol:mg)	1.29 ± 0.61	1.10	0.82 - 2.63	1.31 ± 0.61	1.14	0.57 - 2.37	1.30 ± 0.58	1.10	0.57 - 2.63
	FT3:protein ratio (nmol:mg)	0.33 ± 0.15	0.35	0.08 - 0.50	0.25 ± 0.14	0.20	0.11 - 0.55	0.29 ± 0.15	0.24	0.07 - 0.55
	FT4:protein ratio (nmol:mg)	0.63 ± 0.23	0.64	0.33 - 1.05	0.63 ± 0.38	0.51	0.27 - 1.38	0.63 ± 0.30	0.57	0.27 - 1.38
	TSH:protein ratio (mIU:mg)	2.59 ± 5.00	0.72	0.23 - 13.92	9.08 ± 24.21	0.55	0.18 - 69.00	6.05 ± 17.75	0.67	0.18 - 69.00
C	Follicle count	22.1 ± 4.9	21.7	16.2 - 28.7	24.2 ± 6.9	21.8	16.6 - 35.7	23.1 ± 5.9	21.8	16.2 - 35.7

3.4 Thyroid gland histology

Normal, active thyroid tissue was found in five of the 14 glaucous gulls (Figure 5), whereas the thyroid glands of the nine remaining gulls (five males and four females) showed follicular epithelial cell proliferation (Figure 6, Table 5). Nodular hyperplasia was identified in one of these gulls (LH6), characterized by an area with extensive epithelial cell proliferation and unclear follicles containing sparse amounts of colloid (Figure 7). Inflammation was not seen in any of the thyroid glands. Overall, five gulls were assigned Class A (normal thyroid tissue), eight gulls were assigned Class B (moderate histological changes), and one gull was assigned Class C (pronounced histological changes).

Mean follicle count in each gland's 20 fields à 326 x 244 μm was 23.13 ± 5.86 follicles (Median: 21.78; Range: 16.2-35.7). Mean follicle count in thyroids from Class A was 20.1 ± 4,1 follicles; Class B: 25.2 ±; 6.5 follicles; and Class C: 21.8 follicles (Appendix H). Mean follicle count for each thyroid gland ± SD as well as histological features of each gland are presented in Table 5.

Table 5. Presence of histological changes in 15 glaucous gulls (*Larus hyperboreus*) collected in Sassendalen and Adventfjorden, Svalbard, in April and May 2017. Nodular hyperplasia: Benign follicular lesions resulting from cell proliferation. Mean follicle count was calculated based on average follicle count in 20 fields of 326 x 244 μm in each thyroid gland.

	Sex	Epithelial cell proliferation	Nodular hyperplasia	Classification	Mean follicle count ± SD
LH01	F	-	-	A	16.55 ± 5.52
LH02	M	-	-	A	26.95 ± 12.43
LH03	M	x	-	B	28.70 ± 3.61
LH04	F	-	-	A	20.50 ± 4.61
LH05	F	x	-	B	27.60 ± 5.10
LH06	F	x	x	C	21.85 ± 9.80
LH07	F	x	-	B	29.15 ± 5.59
LH08	M	x	-	B	25.10 ± 5.47
LH09	F	x	-	B	35.65 ± 8.15
LH10	F	-	-	A	17.80 ± 3.46
LH11	M	x	-	B	16.20 ± 4.81
LH12	F	n/a	n/a	n/a	n/a
LH13	M	-	-	A	18.80 ± 5.04
LH14	M	x	-	B	21.70 ± 5.00
LH15	M	x	-	B	17.25 ± 5.99

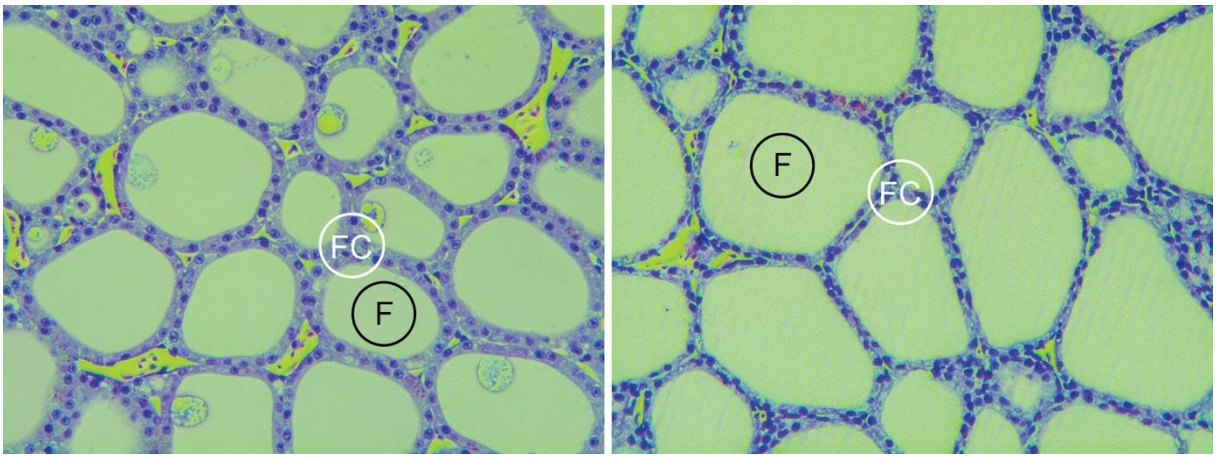

Figure 5. Normal thyroid tissue in glaucous gulls (*Larus hyperboreus*) collected on Svalbard in April and May 2017. The micrographs show colloid containing follicles (F) of similar size surrounded by a single layer of follicular epithelial cells (FC). Left: LH1 (female) with active thyroid tissue; the follicles are lined with high, cuboidal epithelium. Secretory droplets can be seen in several follicles. Right: LH13 (male) with mostly inactive thyroid tissue. HE x 200, 326 x 244 µm.

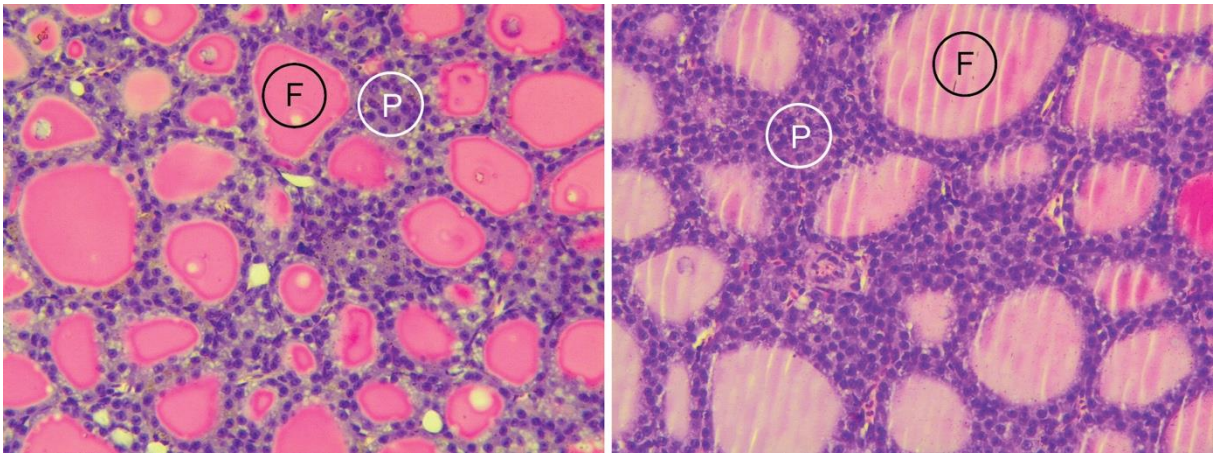

Figure 6. Follicular epithelial cell proliferation (P) in glaucous gulls (*Larus hyperboreus*) collected on Svalbard in April and May 2017. The micrographs also show follicles (F) of varying size. Left: LH5 (female). Right: LH15 (male). HE x 200, 326 x 244 µm.

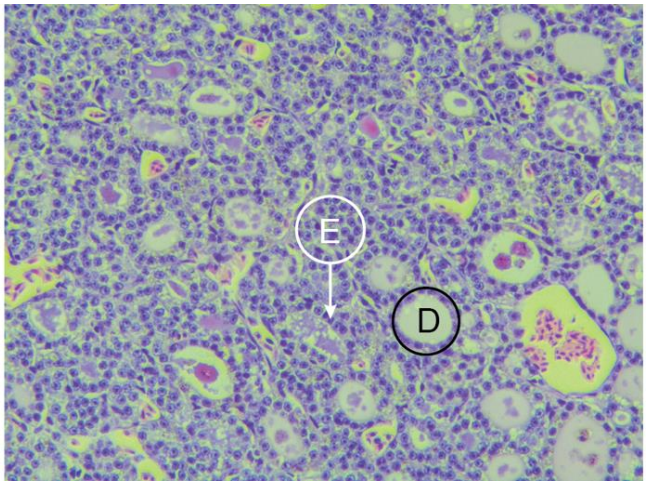

Figure 7. Nodular hyperplasia in LH6 (female) (*Larus hyperboreus*) collected in Sassendalen, Svalbard in April 2017. Extensive epithelial cell proliferation and unclear follicles containing sparse amounts of colloid (D). E: highly active hyperplastic cuboidal epithelium. HE x 200, 326 x 244 µm.

3.5 Relationships between contaminants and thyroid status

3.5.1 Principal component analyses and correlations

Principal component analyses (PCA) were performed to visualize the two-dimensional relationship between biometric variables, PFASs, Hg, Se:Hg, THs, TSHs, and thyroid gland follicle density. Three separate PCA plots were made; one including only males, one including only females, and one including all individuals. A score plot highlighting sampling area was performed (see Appendix I), but as there were no clear groupings between gulls collected in Sassendalen and Adventfjorden, all 15 gulls were regarded as one population.

The two principal components in the PCA including all individuals explained 35.3 % (PC1) and 16.4 % (PC2) of the variation in the data set (51.7 % in total). PC3 (not shown here) explained 14.4 % of the variation in the data set. The loading plot is shown in figure 8A. The PCA indicates a negative relationship between most PFASs and TSH along PC1, in addition to a positive relationship between Se:Hg in liver and TSH. Along PC2, the plot indicates a negative relationship between body size and Se:Hg ratio in feathers.

The negative relationship between PFASs and TSH (n=15, Figure 8A) was confirmed by Spearman correlation only for $PFOS_{lin}$, ∑PFOS (p=0.035, r_s=-0.546 and p=0.046, r_s=-0.521, respectively), PFTeDA, and ∑PFSAs (p=0.010, r_s=-0.639 and p=0.046, r_s=-0.521, respectively) (Table 8) (Appendix K). TSH associations with the remaining PFASs were all negative, but not significant. The positive association between TSH and Se:Hg in liver was also confirmed by Spearman correlations (p=0.028, r_s=0.564). Further, the negative relationship indicated by the PCA along PC2 between body size and PFHpS was confirmed by Pearson correlation analyses for body mass (BM) and wing length (p=0.028, r_p=-0.564 and p=0.003, r_p=-0.712, respectively).

Despite a close positioning on the PCA plot (Figure 8A), BCI and $Se:Hg_{plasma}$ were negatively correlated: p=0.028, r_s=-0.564. Further, follicle count and TSH:protein were positively correlated; p=0.022, r_s=0.605. Follicle count was also positively correlated to Hg_{plasma} (p=0.007, r_p=0.686). All correlations between contaminants, thyroid variables, BM, and BCI can be found in Appendix K.

A score plot highlighting the individual sexes was made (n=15, Figure 8B). This separated males and females in two groups on opposite sides of PC1, and principal component analyses and correlation tests were therefore later performed for the two sexes individually.

A score plot highlighting the histology classes was made (Figure 8C, n=14). Data points for the three histology classes were rather mixed, so no separate loading plots were made for the individual classes.

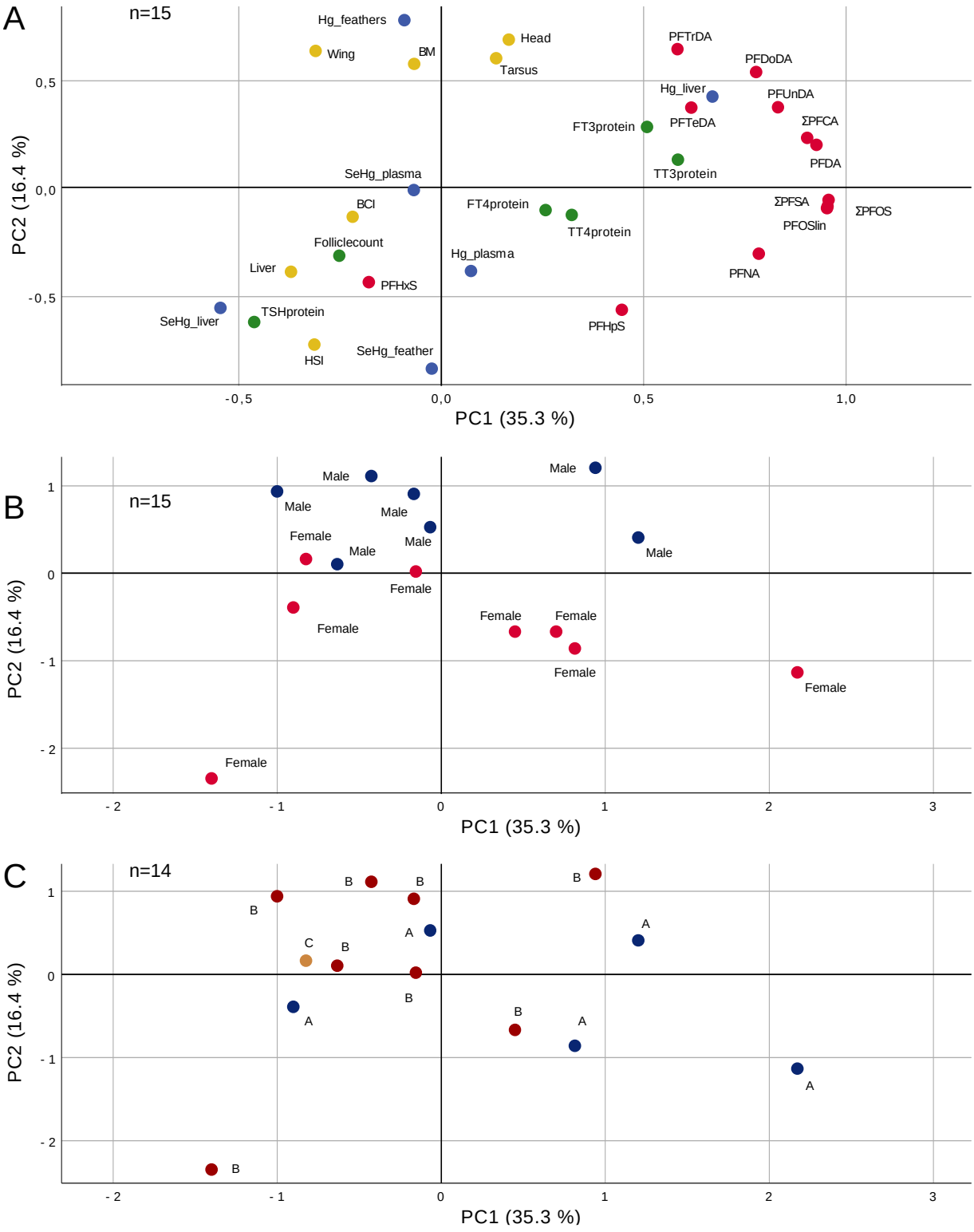

Figure 8. Loading plot (A) of biometric variables, contaminant levels, and thyroid related variables, and score plots (B and C) for n=15 glaucous gulls (*Larus hyperboreus*) (males and females) captured in Sassendalen and Adventfjorden, Svalbard, in April and May 2017. Component 1 explains 35.3 % of the variation in the data set; component 2 explains 16.4 % of the variation in the data set. A: The different colours highlight the subgroups in the plot: PFASs (red), TH related variables (green), Hg related variables (blue), biometric variables (yellow). B: Data labels differentiate between males (blue) and females (red). C: Data labels indicate the histology class each individual belongs to; A (blue), B (red), or C (yellow). Thyroid gland from LH12 was lost in the field and is not included in the score plot.

The PCA including only males (Figure 9) (n=7) indicates the same negative relationship between PFASs and TSH along PC1 (40.1 %), as was indicated for all individuals together. This association was, however, not significant when tested with Spearman correlation analysis. Further, the PCA for males indicates a positive association between Se:Hg ratio in plasma and TSH, but this was not confirmed by correlation analysis either. PC2 (21.2 %) indicates a significant negative relationship between T4 and T3 (TT4:protein and TT3:protein: p=0.040, r_p=-0.777). T4 is also negatively correlated to follicle count (FT4:protein and follicle count: p=0.030, r_p=-0.802) and Hg in feathers (FT4:protein and $Hg_{feathers}$: p=0.004, r_p=-0.914; TT4:protein and $Hg_{feathers}$: p=0.030, r_p=-0.803). Further, a positive relationship is indicated between follicle count and Hg in feathers (p=0.021, r_p=0.831), whereas a negative relationship is indicated between follicle count and BCI (p=0.044, r_p=-0.768). Body size measures are more spread in this loading plot.

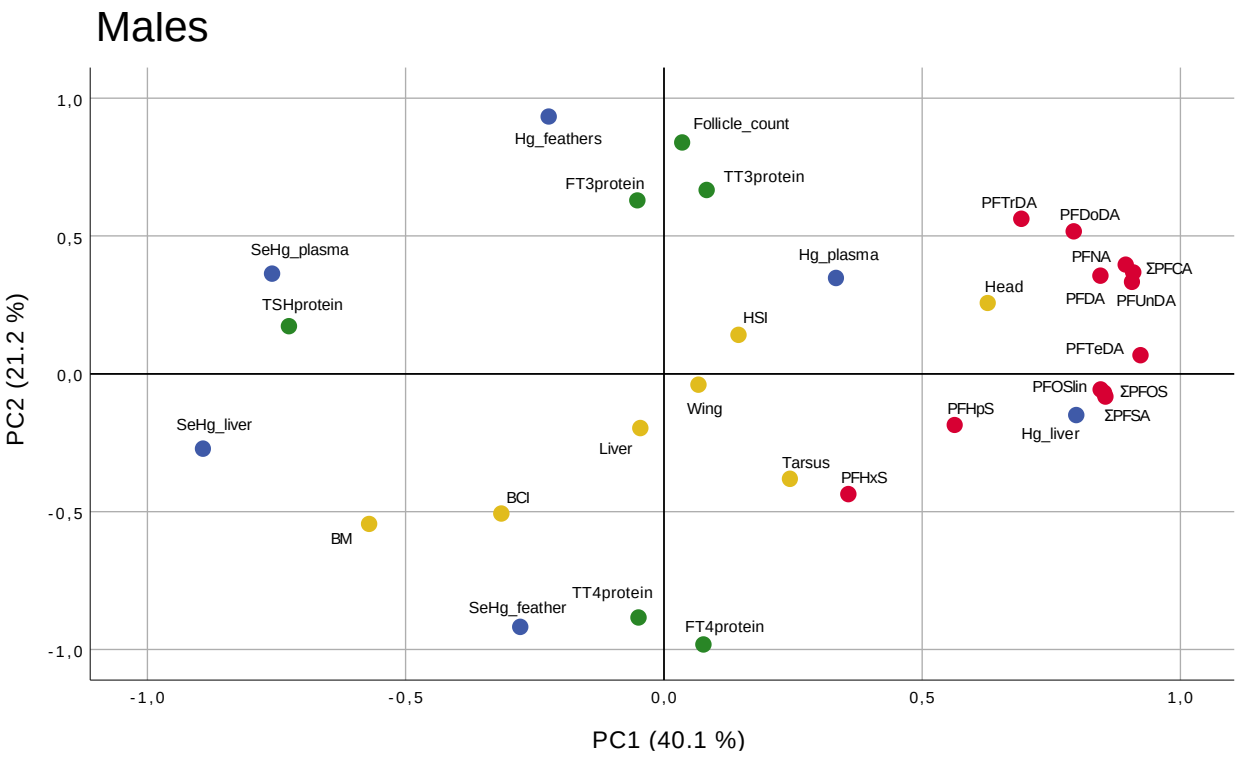

Figure 9. Loading plot of biometric variables, contaminant levels, and thyroid related variables in glaucous gull (*Larus hyperboreus*) males captured in Sassendalen and Adventdalen, Svalbard, in April and May 2017. PC1 explains 40.1 % of the variation in the data set; PC2 explains 21.2 % of the variation in the data set. The different colours highlight the subgroups in the plot: PFASs (red), thyroid hormone related variables (green), mercury related variables (blue), and biometric variables (yellow).

The loading plot for female glaucous gulls (Figure 10) (PC1: 42.6 %, PC2: 23.7 %) also has a grouping of the PFASs, which seems to be negatively related with TSH:protein, and the correlation between PFTeDA and TSH:protein was significant (p=0.047, r_s=-0.714) (Table 6). Both biometric variables and Hg related variables are spread out in the plot. There were positive correlations between TT3 and PFNA (p=0.047, r_s=0.714), and TT4 and PFDoDA (p=0.040, r_p=0.730). In addition, there was a negative, significant correlation between BCI and Se:Hg in plasma: p=0.003, r_p=-0.891. See Appendix K for all correlations.

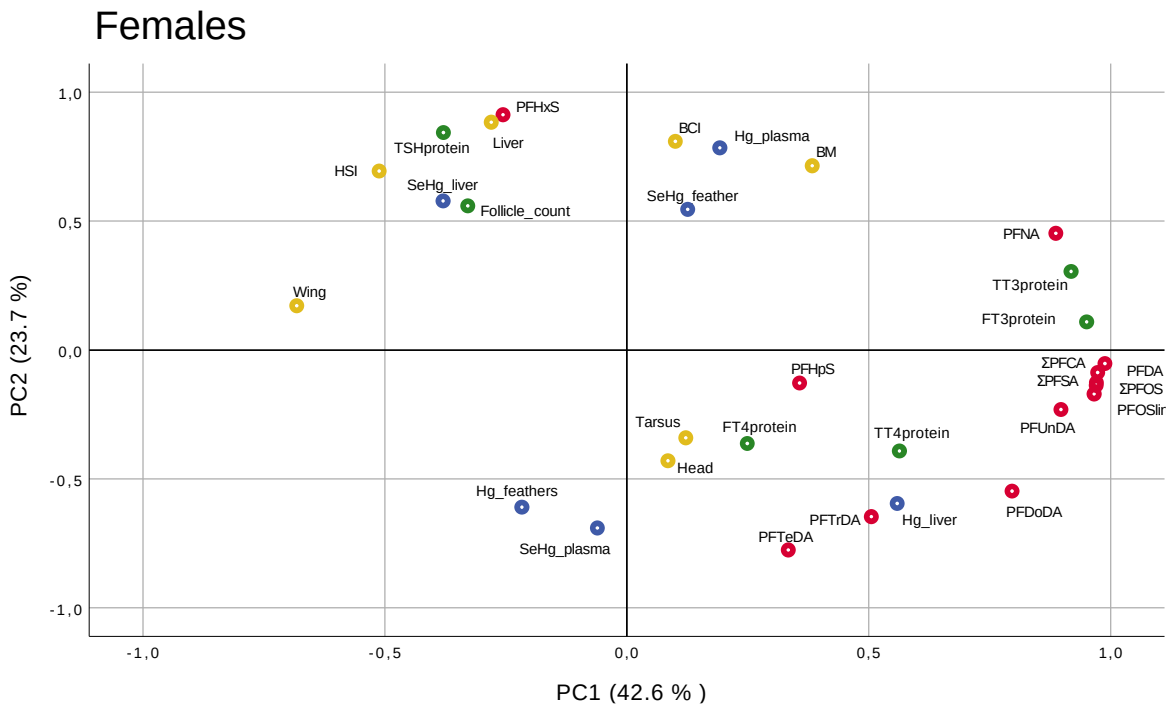

Figure 10. Loading plot of biometric variables, contaminant levels, and thyroid related variables in glaucous gull (*Larus hyperboreus*) females captured in Sassendalen and Adventdalen, Svalbard, in April and May 2017. Component 1 explains 42.6 % of the variation in the data set; component 2 explains 23.7 % of the variation in the data set. The different colours highlight the subgroups in the plot: PFASs (red), thyroid hormone related variables (green), mercury related variables (blue), and biometric variables (yellow).

Table 6. Significant correlations between thyroid response variables (TT3:protein, TT4:protein, FT3:protein, FT4:protein, TSH:protein, and follicle count) and contaminants (hepatic PFASs, and Hg and Se:Hg in plasma, feather and liver) in male (n=7) and female (n=8) glaucous gulls (*Larus hyperboreus*) captured in Sassendalen and Adventdalen, Svalbard, in April and May 2017, as tested by Pearson correlations and Spearman rank correlation (italic). Correlation coefficients (r) and significance levels (p) are included.

	TT3:protein		TT4:protein		FT3:protein		FT4:protein		TSH:protein		Follicle count	
Compound	*r*	*p*	*r*	*p*	*r*	*p*	*r*	*p*	*r*	*p*	*r*	*p*
PFOSlin all	-	-	-	-	-	-	-	-	*-0.546*	*0.035*	-	-
PFOSlin m	-	-	-	-	-	-	-	-	-	-	-	-
PFOSlin f	-	-	-	-			-	-	-	-	-	-
SumPFOS all	-	-	-	-	-	-	-	-	*-0.521*	*0.046*	-	-
SumPFOS m	-	-	-	-	-	-	-	-	-	-	-	-
SumPFOS f	-	-	-	-			-	-	-	-	-	-
PFNA all	0.561	0.030	-	-	-	-	-	-	-	-	-	-
PFNA m	-	-	-	-	-	-	-	-	-	-	-	-
PFNA f	*0.714*	*0.047*	-	-	-	-	-	-	-	-	-	-
PFDA all	0.686	0.005	-	-	0.570	0.027	-	-	-	-	-	-
PFDA m	-	-	-	-	-	-	-	-	-	-	-	-
PFDA f	-	-	-	-			-	-	-	-	-	-
PFUnDA all	0.567	0.028	-	-	0.538	0.039	-	-	-	-	-	-
PFUnDA m	-	-	-	-	-	-	-	-	-	-	-	-
PFUnDA f	-	-	-	-	-	-	-	-	-	-	-	-
PFDoDA all	0.548	0.034	-	-	0.555	0.032	-	-			-	-
PFDoDA m	-	-	-	-	-	-	-	-	-	-	-	-
PFDoDA f	-	-	0.730	0.040	-	-	-	-	-	-	-	-
PFTeDA all	-	-	-	-	-	-	-	-	*-0.639*	*0.01*	-	-
PFTeDA m	-	-	-	-	-	-	-	-	-	-	-	-
PFTeDA f	-	-	-	-	-	-	-	-	*-0.714*	*0.047*	-	-
∑PFSAs all	-	-	-	-	-	-	-	-	*-0.521*	*0.046*	-	-
∑PFSAs m	-	-	-	-	-	-	-	-	-	-	-	-
∑PFSAs f	-	-	-	-	0.728	0.041	-	-	-	-	-	-
∑PFCAs all	0.640	0.010	-	-	0.563	0.039	-	-	-	-	-	-
∑PFCAs m	-	-	-	-	-	-	-	-	-	-	-	-
∑PFCAs f	-	-	-	-	-	-	-	-	-	-	-	-
Hg plasma all	-	-	-	-	-	-	-	-	-	-	0.686	0.007
Hg plasma m	-	-	-	-	-	-	-	-	-	-	-	-
Hg plasma f	-	-	-	-	-	-	-	-	-	-	-	-
Hg feather all	-	-	-	-	-	-	-	-	-	-	-	-
Hg feather m	-	-	-	-	-	-	-0.914	0.004	-	-	0.831	0.021
Hg feather f	-	-	-	-	-	-	-	-	-	-	-	-
Se:Hg plasma all	-	-	-	-	-	-	-	-	-	-	-	-
Se:Hg plasma m	-	-	-	-	-	-	-	-	0.833	0.020	-	-
Se:Hg plasma f	-	-	-	-	-	-	-	-	-	-	-	-
Se:Hg feathers all	-	-	-	-	-	-	-	-	-	-	-	-
Se:Hg feathers m	-	-	-	-	-	-	-	-	-	-	-	-
Se:Hg feathers f	-	-	-	-	-	-	-	-	*0.714*	*0.047*	-	-
Se:Hg liver all	-	-	-	-	-	-	-	-	*0.564*	*0.028*	-	-
Se:Hg liver m	-	-	-	-	-	-	-	-	-	-	-	-
Se:Hg liver f	-	-	-	-	-	-	-	-	-	-	-	-

3.5.2 O-PLS

O-PLS models were made for each of the five hormone fractions (TT3, TT4, FT3 FT4, and TSH), and one model, describing the TSH:protein ratios, was significant according to Lundstedt's criteria (Lundstedt et al., 1998). The TSH model (R^2X=0.521, R^2Y=1, Q^2=0.414, CV-ANOVA: p=0.041) consisted of seven PFASs, Hg and Se:Hg ratio in liver, follicle count mean, and HSI. PFDoDA was the *X*-variable with the highest importance in the model (highest VIP value), followed by (in descending order) PFDA, PFUnDA, Hg_{liver}, PFTrDA, PFOSlin, $Se:Hg_{liver}$, PFTeDA, PFNA, follicle count, HSI, and PFHxS. The eight most important variables had VIP > 1, and the remaining four had VIP > 0.5. The coefficient plot (Figure 11) shows that $Se:Hg_{liver}$ ratio was positively associated with TSH:protein ratio, whereas most PFASs and Hg_{liver} were negatively associated with TSH:protein, PFTeDA being the most important.

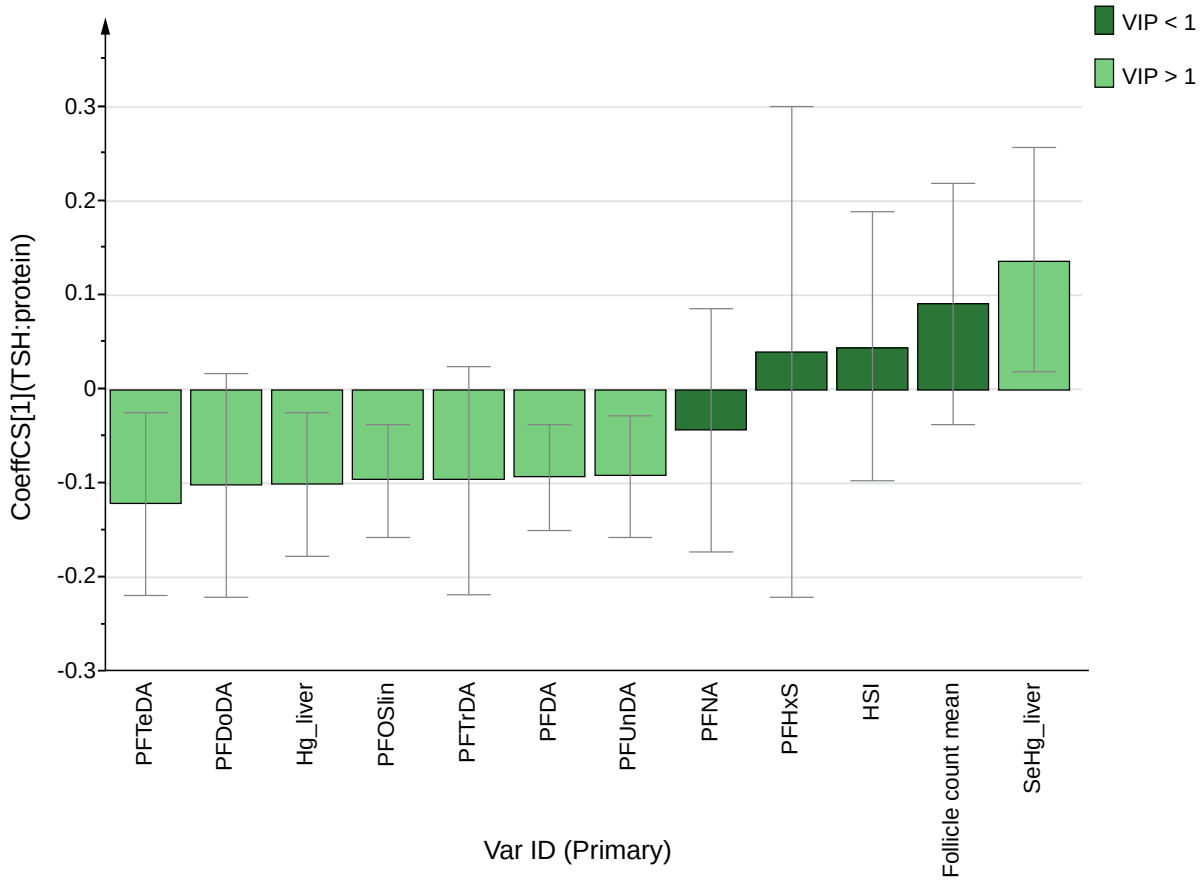

Figure 11. Orthogonal projections to latent structures (O-PLS) regression coefficient plot visualizing the importance of PFDoDA, PFDA, PFUnDA, Hg_{liver}, PFTrDA, PFOSlin, $Se:Hg_{liver}$, PFTeDA, PFNA, follicle count, HSI, and PFHxS (X-variables) in modelling the TSH:protein ratio (Y-variable) in the plasma of the 15 glaucous gulls (*Larus hyperboreus*) captured in Sassendalen and Adventfjorden, Svalbard, in April and May 2017. Variables with VIP > 1 are presented in bright green.

The positive relationship between TSH:protein and $Se:Hg_{liver}$ was confirmed by Spearman correlation testing, as well as the negative relationship between TSH:protein and $PFOS_{lin}$ and PFTeDA (Table 6; Figure 12 A, B, and C). The negative relationship between TSH:protein and Hg_{liver} was only close to significant (p=0.052, r_S=-0.511). The correlations between the remaining variables in the model and TSH:protein were not statistically significant.

3.5.3 Linear regression

Significant linear regressions between TSH:protein and individual explanatory variables ($PFOS_{lin}$, PFTeDA, and $Se:Hg_{liver}$) are presented in Figure 11 A, B, and C.

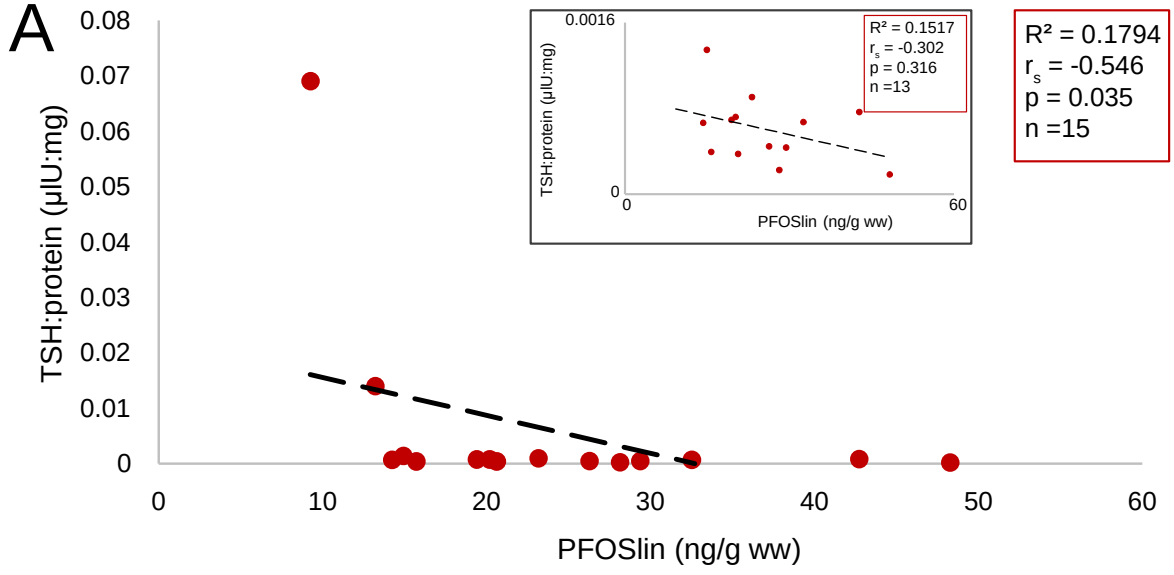

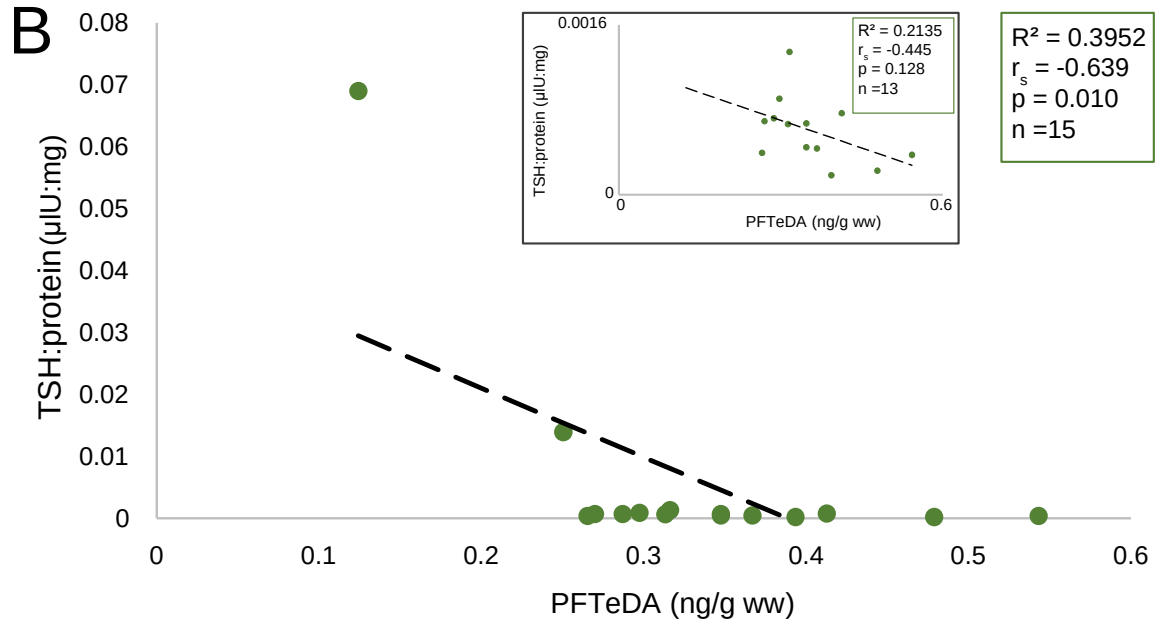

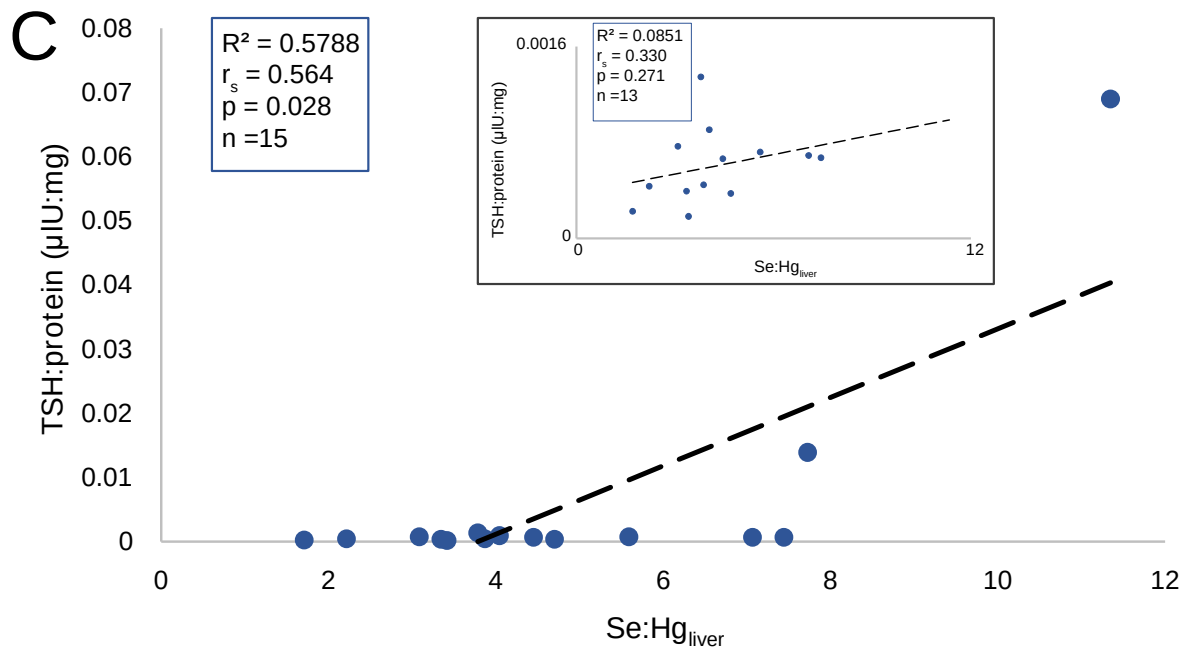

Figure 12. TSH:protein ratios in relation to $PFOS_{lin}$ (A), PFTeDA (B), and $Se:Hg_{liver}$ in glaucous gulls (*Larus hyperboreus*) from Svalbard. LH9 and LH14, which have TSH concentrations two orders of magnitude higher than the other individuals, are excluded in the small figures embedded in A, B, and C to display the spread of the remaining data. A: TSH:protein vs. $PFOS_{lin}$: r_S=-0.546, p=0.035. B: TSH:protein vs. PFTeDA: r_S=-0.639, p=0.010. C: TSH:protein vs. $Se:Hg_{liver}$: r_S=0.564, p=0.028.

4 DISCUSSION

In the present study, PFAS concentrations in liver, and Hg and Se concentrations in liver, plasma and feather, were analysed in 15 glaucous gulls from Svalbard. The Se:Hg molar ratio was calculated in the same three tissue types. Contaminant levels were related to thyroid related responses (TH:protein ratios TSH:protein ratios in plasma, and thyroid gland histology). The major findings were significant negative correlations between PFASs and Hg and TSH:protein, significant positive correlations between other PFASs and free and total T3:protein, and a significant positive association between Hg in plasma and follicle count.

The reader should keep in mind that protein concentration in plasma is not a constant variable, and the hormone:protein ratios used for the correlation analyses cannot be translated directly to correlations with pure hormone concentrations. Nevertheless, hormone:protein ratios in the present study seem to be a sensitive response variable when investigating thyroid disruption. However, it is proposed that future studies use a sampling method for plasma that does not involve a risk of diluting the samples with body fluids.

It is important to note that the present study is a correlative study. Correlation does not imply causation, and the relationships need to be further investigated in order to fully understand the possible disruptive effects of PFAS and Hg on the thyroid function in birds.

4.1 Contaminant levels and patterns

4.1.1 PFAS

The levels of PFASs detected in this study are somewhat different, but in the same order of magnitude, as those reported in Svalbard glaucous gull liver (Haukås et al., 2007) and plasma (Haugerud, 2011, Melnes et al., 2017, Verreault et al., 2005 b) (Table 7). However, PFASs accumulate differently in different tissue compartments (here plasma and liver). Verreault et al. (2005 b) found that plasma concentrations of PFOS were lower than liver concentrations in glaucous gulls. The present liver concentrations can therefore be properly compared only to those of Haukås et al. (2007), which were approximately twice as high as in the present study (Table 7).

Table 7. ∑PFOS and ∑PFAS concentrations reported in plasma and liver in glaucous gulls (*Larus hyperboreus*) Svalbard: Sassendalen and Adventfjorden (present study), Kongsfjorden (Melnes et al. 2017, Haugerud 2011), Barents Sea East of Svalbard (Haukås et al. 2007), and Bjørnøya (Verreault et al. 2005 b).

Study (Author, year)			Males		Females		Males + females	
	Contaminant	Tissue	n	Mean ± SD	n	Mean ± SD	n	Mean ± SD
Present study	∑PFOS (ng/g ww)	Liver	7	25.89 ± 11.10	8	26.83 ± 13.26	15	26.39 ± 11.87
	∑PFAS (ng/g ww)	Liver	7	37,68 ± 15.01	8	31.16 ± 17.15	15	37.40 ± 15.0
Melnes et al 2017	∑PFOS (ng/g ww)	Plasma	15	14.26 ± 8.01	24	47.22 ± 110.60		-
	∑PFAS (ng/g ww)	Plasma	15	29.79 ± 12.68	24	60.58 ± 113.86		-
Haugerud 2011	∑PFOS (ng/g ww)	Plasma		-	19	31.12 ± 96.78		-
	∑PFAS (ng/g ww)	Plasma		-	19	40.80 ±102.62		-
Haukås et al 2007	∑PFOS (ng/g ww)	Liver		-		-	9	65.8 ± 22.4
	∑PFAS (ng/g ww)	Liver		-		-	9	69.6 ± 23.7
Verreault et al 2005 b	∑PFOS (ng/g ww)	Pasma		-		-	20	134 ± 16.6

PFOS dominated the hepatic PFAS profile in all gulls (n=15), accounting for 71 % of the PFAS load (ng/g ww), followed by PFUnDA (10 %), PFNA (6 %), and PFDA (5 %) (Figure 3). The dominance of PFOS is in line with findings in previous studies on PFAS levels in glaucous gulls (Melnes et al., 2017, Verreault et al., 2005 b), ringed seal (Routti et al., 2016), and in Arctic wildlife and environment in general (Butt et al., 2010, Kelly et al., 2009, Martin et al., 2004). PFUnDA, PFNA, and PFDA are all long-chained (C_8-C_{14}) PFCAs (11, 9, and 10 carbons, respectively), which, in addition to PFOS, is the group of PFASs that are the most bioaccumulative in the Arctic marine food web (Kelly et al., 2009, Martin et al., 2004).

Concentrations of PFSAs were higher in females than males, but PFHpS was the only compound that was significantly higher (Table 3). This could support the finding of Jones et al. (2003), that sulfonic acids are more potent to bind to plasma proteins than carboxylates. Circulating protein levels are namely thought to reflect the total protein reserves in an animal (Dawson and Bortolotti, 1997) and circulating protein concentrations in this study were on average higher in female glaucous gulls than in males (p=0.18) (Table 4A). Therefore, the higher hepatic ∑PFSA levels in females may result from a higher circulating protein level. However, neither the difference in protein levels, nor the difference in ∑PFSA levels between the sexes was significant. Further, the circulating protein concentrations in this study must be treated with great caution since some blood samples were diluted in the field. Hence, the suggestion that PFSAs are more potent to bind PFCAs (Jones et al., 2003) cannot be stated by the present study. The different levels of PFSA in males and females can also be a result of differences in elimination between sexes. All PFCAs were higher in males than females, but not significantly.

Melnes et al. (2017) reported significantly lower concentrations of PFDoDA, PFTrDA, and PFTeDA in females than males, whereas PFOA concentrations were significantly higher in females than males. Melnes et al. ascribe these opposite concentrations patterns to differences in maternal transfer between PFSAs and PFCAs. However, no big differences in PFAS levels between males and females were detected in the present study, which is also what was expected since the birds were collected before the breeding season, and females had not yet laid their eggs.

In summary, hepatic PFAS concentrations were in accordance with what is previously reported in glaucous gulls. In line with previous findings, PFOS dominated the PFAS profile. Lastly, there were no major differences between sexes regarding PFAS levels or profiles.

4.1.2 Mercury

In the present study, Hg concentrations in liver (3.26 ± 1.22 μg/g dw) were slightly higher than reported in glaucous gull liver from Kongsfjorden, Svalbard (Jæger et al., 2009) (1.17 ± 0.16 μg/g ww) and glaucous gull eggs in the Canadian Arctic (Braune et al., 2016) (2.8 μg/g dw). However, comparison is challenging since the present results are presented in dry weight (dw) and not wet weight (ww). Since wet weight samples also contain the weight of the moisture in the wet tissue, dw concentrations would correspond to a higher wet weight concentration. Hence, the present Hg concentrations are probably lower than the reported Hg concentrations reported by Jæger et al.

Males in the present study had significantly higher concentrations of Hg in feathers than females, reflecting the maternal transfer of Hg (mainly in the form of MeHg) to eggs (Wolfe et al., 1998, Ackerman et al., 2016). There were no significant differences in liver and plasma concentrations of Hg between sexes.

Hg showed dissimilar concentrations in plasma, feather, and liver (Figure 8A, 9, and 10). This is probably because the concentrations represent different exposure periods in the three tissues. While plasma levels represent the present exposure at the time when the birds were euthanized, the liver concentrations most probable reflect the exposure during the last month (Martin et al., 2003). Feather concentrations, on the other hand, reflect the concentrations the bird was exposed to during the last molt (Svendsen et al., 2018), which for glaucous gulls is

from the breeding season (April-May) until August/September (Løvenskiold, 1964). Feather concentrations of contaminants may not be correlated to the plasma concentrations (Svendsen et al., 2018). Since feather does not represent the present exposure levels, $Hg_{feather}$ and $Se:Hg_{feather}$ are not included in the discussion about thyroid related responses.

As the PCA plots indicate, Hg levels in the liver are the most correlated to PFAS concentrations, which were also analysed in the liver, and thereby represent the same exposure period (n=15: Hg_{liver} and ∑PFSA: p=0.022, r_P=0.586. Hg_{liver} and ∑PFCA: p=0.022, r_P=0.586. See Appendix X for all correlations).

Out of feathers, liver, and plasma, a Se:Hg ratio which was < 1 was only evident in feathers from male glaucous gulls. Hence, Hg concentrations were on average higher than the Se concentrations in feathers from males. This could represent an actual excess of Hg over Se in the males when the feathers were grown, but also give information about uptake mechanisms of different elements into feathers. However, evaluation of the components of feathers was not within the scope of this study.

In summary, Hg levels in plasma and liver of female gulls did not seem to be affected by maternal transfer, while feather concentrations were significantly higher in males than females. Hg levels in feathers are excluded from the remaining discussion. There was a molar surplus of Se compared to Hg in all three tissue types (plasma, liver, and feather) for n=15.

4.2 Thyroid hormones and thyroid stimulating hormone

Circulating TH levels in glaucous gulls in the present study (Table 4) were similar to those reported in glaucous gulls by Melnes et al. (2017) and Verreault et al. (2007) (Table 8). The TH concentrations are also comparable to those reported in kittiwakes (Ask, 2015, Nøst et al., 2012) and fulmars (Nøst et al., 2012) (Table 8). However, due to the dilution of an unknown number of blood samples, the reported concentrations in this study should be considered with great caution. The TH:protein ratios were calculated to correct for this mistake. The author did not succeed to find avian protein corrected TH levels in the literature for comparison.

Table 8. Overview of TT3, TT4, FT3, and FT4 concentrations reported in plasma from Artic birds from Svalbard. All birds were collected in Kongsfjorden, Svalbard, except for those in the present study, which were collected in Sassendalen and Adventfjorden, Svalbard. Concentrations reported by Ask (2015) were converted from ng/mL to nmol/L using the online unit converter calculator unitslab.com. LH: Larus hyperboreus. RT: Rissa tridactyla. FG: Fulmaris glacialis.

Study (Author, year)	Species		Males			Females			Males + females		
			n	Mean ± SD	Range	n	Mean ± SD	Range	n	Mean ± SD	Range
Present study	LH	TT3 (nmol/L)	7	3.30 ± 1.50	0.66 - 4.75	8	3.24 ± 1.74	1.89 - 7.32	15	3.27 ± 1.57	0.66 - 7.32
		TT4 (nmol/L)	7	28.51 ± 5.60	18.43 - 34.15	8	35.34 ± 14.31	17.12 - 57.57	15	32.15 ± 11.33	17.12 - 57.57
		FT3 (pmol/L)	7	8.43 ± 4.41	1.00 - 13.10	8	6.99 ± 4.34	2.26 - 16.63	15	7.66 ± 4.28	1.00 - 16.62
		FT4 (pmol/L)	7	14.16 ± 2.44	10.61 - 17.74	8	17.14 ± 8.90	7.56 - 33.54	15	15.75 ± 6.67	7.56 - 33.53
Melnes et al 2017	LH	TT3 (nmol/L)	15	2.21 ± 1.02	1.72 - 4.38	24	2.38 ± 0.97	0.82 - 4.59		-	-
		TT4 (nmol/L)	15	24.52 ± 11.53	13.16 - 43.71	24	30.69 ± 9.59	10.62 - 50.90		-	-
		FT3 (pmol/L)	15	3.23 ± 1.83	0.80 - 6.12	24	2.97 ± 1.61	0.55 - 6.57		-	-
		FT4 (pmol/L)	15	30.32 ± 41.35	4.94 - 133.15	24	22.64 ± 9.37	6.26 - 41.47		-	-
Ask 2015	RT	TT3 (nmol/L)	8	4.27 ± 1.10	2.69 - 7.05	5	4.54 ± 1.66	2.47 - 4.92		-	-
		TT4 (nmol/L)	9	46.90 ± 14.42	23.95 - 90.17	5	47.86 ± 19.18	14.43 - 60.10		-	-
Nøst et al 2012	RT	TT3 (nmol/L)		-	-		-	-	13	4.27 ± 0.37	2.33 - 6.8
		TT4 (nmol/L)		-	-		-	-	13	22.3 ± 11.3	3.05 - 40.3
		FT3 (pmol/L)		-	-		-	-	13	7.45 ± 0.14	3.74 - 11.8
		FT4 (pmol/L)		-	-		-	-	13	26.9 ± 2.66	3.92 - 49.5
Nøst et al 2012	FG	TT3 (nmol/L)		-	-		-	-	15	5.51 ± 1.11	1.5 - 8.64
		TT4 (nmol/L)		-	-		-	-	15	95.5 ± 37.6	36.3 - 181
		FT3 (pmol/L)		-	-		-	-	15	6.65 ± 0.77	0.4 - 12.3
		FT4 (pmol/L)		-	-		-	-	15	60.1 ± 3.18	11.3 - 124
Verreault et al 2007	LH	TT3 (nmol/L)	11	4.02 ± 0.41	1.80 - 6.60	12	2.69 ± 0.31	0.90 - 5.10		-	-
		TT4 (nmol/L)	11	22.4 ± 1.67	15.1 - 36.6	12	22.7 ± 1.37	13.9 - 31.0		-	-
		FT3 (pmol/L)	11	4.71 ± 0.57	2.30 - 7.90	12	2.96 ± 0.42	0.80 - 6.70		-	-
		FT4 (pmol/L)	11	24.3 ± 2.16	16.0 - 44.2	12	25.3 ± 1.55	16.7 - 34.3		-	-

In this study mean ± SD for circulating TSH concentration was 0.17 ± 0.53 μIU/ml. There are very few studies available on avian TSH levels due to the lack of a bird-specific antibody. In an experimental study by Pandey and Mohanty (2017), TSH was analysed in pesticide exposed wild birds (red munia, *Amandava amandava*) and control birds. They used an ELISA kit developed for human serum (SmarTest Diagnostics, Israel), and TSH concentrations were reported in μIU/ml, as in the present study. TSH levels in controls were between 10 – 15 μIU/ml, while most exposure groups had decreased TSH levels (5-10 μIU/ml) (Pandey and Mohanty, 2017).

In a study by Troisi et al. (2016), TSH levels in stranded, oil contaminated guillemots (*Uria aalge*) were found to be 0.13 ± 0.02 ng/ml. In this study, they used an immunoassay kit was used based on an antibody raised against mammalian TSH from *IBL International* (Troisi et al., 2016). The concentrations in the present study and that of Troisi were reported in different units, and conversion between the two (μIU/ml and ng/ml) is not straight forward (Donadio-Andréi et al., 2017). Therefore, comparison between TSH levels in these two studies is challenging. However, homology of TSH antibody binding domains are highly conserved in vertebrate species. There is 70.4 – 69.6 % homology in the amino acid sequences in avian and mammalian TSH-beta (Gregory and Porter, 1997), which is the TSH sub unit that is unique to

TSH. Therefore, if the EIA kit used in the present study succeeded in catching, albeit not the absolute values, but at least the variation of TSH concentrations in the glaucous gulls, the correlation analysis with TSH is valid.

Altogether, TH concentrations in the present study were similar to previous reported levels. TH:protein ratios for comparison were not found in the literature, nor avian TSH levels or TSH:protein ratios. Yet, the TSH concentrations measured, as well as the TSH:protein ratios, are considered sufficient for correlation purposes.

4.3 Relationships between contaminant levels and hormone levels

4.3.1 PFASs and thyroid response

PFTeDA and linear PFOS were negatively correlated to circulating TSH:protein ratios (Table 6, Figure 8). Interestingly, these were not significantly correlated to circulating TH levels, which could be expected since TSH and THs are theoretically closely related. Rather, PFNA, PFDA, PFUnDA, and PFDoDA were all positively correlated to TT3 and FT3 levels (except PFNA, which was correlated only to TT3) (Table 6, Figure 8). As long-chained PFCAs, PFTeDA, PFDA, PFUnDA, and PFDoDA are strongly proteinophilic (Kelly et al., 2009). PFOS is also recognized as highly proteinophilic and binds mainly to albumin (Jones et al., 2003). These compounds therefore have the chemical properties necessary to potentially displace T4, which by far dominates the TH fraction in plasma, from their main transport protein. This could lead to less T4 available to the target tissues, i.e. less substrate for deiodinase enzymes at the target tissue, and hence decreased availability of T3 to the thyroid receptors (Ucán-Marin et al., 2009). This could stimulate to TSH release, and hence T4 release from the thyroid gland, as an attempt to restore T3 in target tissues. However, this explanation does not support the *negative* correlation between PFTeDA and PFOS and TSH:protein, nor the *positive* relationship between PFNA, PFDA, PFUnDA, and PFDoDA and circulating T3 levels. This could indicate that thyroid disruption by PFASs occurs at another level of the HPT axis than the transport level. However, the effect on the T3 and THS levels could also be an effect of exposure to unstable precursor PFASs that are already metabolized by the glaucous gulls, or effects caused by thyroid disruptive OCs (Melnes et al., 2017).

Modelling studies have shown that PFSAs with medium chain length can be optimal for transthyretin (TTR) binding (Ren et al., 2016). In a study by Weiss et al. (2009), competitive binding of PFASs with T4 on human TTR was investigated. PFHxS had the highest binding potency, closely followed by PFOS, with binding potencies 12.5 times lower than T4. TTR is, however, not as important as albumin for the transportation of THs in birds. PFOS levels in this study were orders of magnitude less than the vitro-based effect threshold for displacement of corticosteroid from globulins in bald eagle (*Halieetus leucocephalus*) (257 μg/ml) (Jones et al., 2003). Although displacement thresholds for globulin may not directly represent displacement thresholds for albumin, the current PFOS levels (26 ng/g ww) should not be expected to cause measurable effects on TH binding to transport proteins. Nevertheless, the present positive correlations between PFASs and THs are supported by recent findings of Melnes et al. (2017) and Nøst et al. (2012), who found positive associations between PFOS and FT3 and TT3 in female glaucous gulls, and PFHpS, PFOS, PFNA and TT4 in northern fulmar and kittiwakes, respectively. Altogether, the present findings indicate that PFASs have a positive relationship to circulating TT3 and FT3 levels in glaucous gulls.

However, when interpreting these results, it is important to keep in mind that OC contaminants were not analysed in the present study. As this group of contaminants are also known to have thyroid disruptive effects, reducing circulating T3 in birds, it is highly probable that they also contribute to the present thyroid economy (Melnes et al., 2017).

Altogether, PFTeDA and linear PFOS seem to decrease TSH levels, whereas several PFCAs seem to increase T3 levels. The mechanisms behind this disruption are not clear in the present study, but TH displacement by PFASs from albumin may be a contributing factor.

4.3.2 Mercury and thyroid response

Hg concentrations were not correlated to TSH:protein ratio in glaucous gulls. However, Se:Hg ratio in liver (p=0.028, r_S=0.564) was positively correlated to TSH:protein ratios (Table 6). The $Se:Hg_{liver}$ ratio was >1, indicating that the more Se per Hg, the higher the levels of circulating TSH. Or contrary; the less Se per Hg, the lower the levels of circulating TSH. This can be interpreted as a result of the feedback mechanism of the HPT axis; when Se:Hg in the liver is >1, deiodinase enzymes in the liver are undisturbed by Hg, and convert T4 to T3. This lowers the circulating T4 levels, which, through the feedback mechanism of the HPT axis, stimulates an increase in TSH release to restore the T4 levels. This explanation is also in

line with the negative relationship, albeit not significant, between Hg_{liver} and TSH:protein (p=0.052, r_S=-0.511), which underlines the toxic effect of Hg on deiodinase (Mulder et al., 2012), and hence lower TSH levels (Table 6). The positive relationship between the $Se:Hg_{liver}$ ratios and circulating TSH:protein ratios is also supported by the O-PLS model, in which $Se:Hg_{liver}$ is one of the *X*-variables that contributes positively to the significant model explaining TSH:protein (Figure 11). The linear relationship (R^2=0.58) between $Se:Hg_{liver}$ and TSH:protein is also visualized in Figure 12.

However, this explanation is contrary to the findings of Rosene et al. (2010), which indicated that inhibition of deiodinase enzyme 5´D II increases TSH levels in mice. 5´D II is, however, is only found in the brain of chicks and herring gulls (McNabb, 2007), and it is assumed that it is deiodinase enzyme 5´D1, which is present in the liver, that plays the major role in supplying most of the T3 for circulation in birds (McNabb, 2007). It may be that inhibition of 5´D1 affects TSH levels in a different manner than inhibition of 5´D II. However, the author did not succeed in finding literature on the inhibitory effects of 5´DI on TSH levels in birds. There was no significant correlation between TSH:protein and Se:Hg ratios in the plasma, but as 5´D I is present in the liver, and not the plasma, Se:Hg ratio in plasma may not be a relevant measure.

Altogether, although several factors must be taken into account, Hg seem to have a negative effect on circulating TSH levels in the present study.

4.4 Follicle count and histology

4.4.1 Follicle count

No significant differences were found between follicle counts in Class A (normal thyroid tissue), Class B (moderate histological changes), and Class C (pronounced histological changes) thyroid glands (20.12 ± 4.1; 25.2 ± 6.5; 21.9 follicles in the 326 x 244 μm fields, respectively) (Appendix H). Follicle count was not significantly correlated to PFAS levels (Table 6). Follicle count was, however, positively correlated to Hg_{plasma} (p=0.007, r_P=0.686, n=15). Hg accumulates in thyroid glands in mammals (Nylander and Weiner, 1991), and fish studies have indicated that Hg inhibits iodine uptake to the thyroids, damages thyroid follicles and thereby decreases T4 synthesis (Kirubagaran and Joy, 1994). In the present study, the significant positive correlations between Hg levels in plasma and follicle count might

therefore be due to initial damage of thyroid follicles caused by Hg, followed by regeneration and maturation of new follicles. Since new follicles are smaller than mature follicles, the follicle count also increased, hence the positive correlations.

Follicle count was not significantly correlated to TSH:protein (Table 6). A measure of follicle size, rather than count, would probably be a more sensitive measure of TSH effects on thyroid gland morphology. Follicle size is known to decrease under sustained TSH secretion because of increased endocytosis of the colloid (Ness et al., 1993). A rapid assessment of the appearance of the glands revealed that small follicle size did not necessarily imply a high follicle count, since proliferation of the epithelial cells, rather than multiple small follicles, took up much of the area. A measure of follicle size would probably better reflect the TSH responses than what was achieved in the present study. A more comprehensive study of the thyroid histopathology could also include thyroid weigh, thyroid volume, density of colloid-filled follicles, cell height and nucleus size of epithelial cells, and a cell height to nucleus size ratio (Pandey and Mohanty, 2017).

Altogether, Hg might have a damaging effect on the thyroid glands, possibly resulting in generation of new follicles. Follicle size would, however, probably be a better measure of the state of the thyroid gland.

4.4.2 Thyroid gland histology

Neither PFAS concentration, Hg concentration, nor Se:Hg ratio were significantly different between histology classes. This is probably because the classification methodology of thyroid glands was subjective, and there are subtle differences in the degrees of histological damages. The main purpose of classification was, however, not for correlation purposes, but to present the state of thyroid glands in contaminated glaucous gulls. Quantitative measures of histology are preferable to reveal possible underlying mechanisms of contaminated-induced thyroid disruption.

In mammalian studies, alterations in thyroid histology is regularly used as indicators of altered thyroid function (McNabb, 2007). In birds, this approach has been less common. Sonne et al. (2010) studied blood OC concentrations and thyroid gland histology in 10 adult female glaucous gulls from Bjørnøya, Svalbard, but could not attribute the histological changes observed to the OC concentrations. Morphological changes in thyroid glands were

also seen in OC-contaminated glaucous gulls from Grumantbyen, Svalbard, but there were no differences in hepatic OC-concentrations in individuals with (n=5) and without (n=5) lesions in the thyroids (Sonne et al., 2013). An experimental study on Japanese quail (*Coturnix japonica*) did, however, show proliferations in the thyroid follicular cells and a large variation in follicle size in the thyroid glands of one quail exposed to a mixture of two organohalogen flame retardants (Jacobsen et al., 2017). Furthermore, in a field study from Japan, they found that great cormorants (*Phalacrocorax carbo*) from a dioxin- and furan contaminated site in Tokyo Bay (n= 18) had a higher occurrence of increased density of small follicles and increased number of epithelial cells in the thyroids than great cormorants from a reference site (n=11) (Saita et al., 2004). McNabb & Fox (2003) reported decreased follicular size in free-ranging herring gulls living in OHC-contaminated areas in the Great Lakes, Canada.

The presence of epithelial cell proliferation in nine of 14 glaucous gulls, including one with nodular hyperplasia, indicates that PFAS- and Hg exposure may be a co-factor in the development of thyroid gland alterations in glaucous gulls. However, natural variation, age (Sonne et al., 2013), and food availability cannot be ruled out as additional explanatory variables, and further research with larger sample sizes and more sensitive measures of thyroid gland alterations are required.

4.5 Thyroid response: Comparison between males and females

Melnes et al. (2017) reported a significant positive relationship between PFOS and FT3 in female glaucous gulls (p=0.008, r_P= 0.525), which was not evident in males. The correlation between PFOS and FT3 in females was not significant in the present study (females: p=0.233, r_P=0.476); however, the correlation between ∑PFSA and FT3 was significant (p=0.041, r_P=0.728) (Table 6, Figure 10). In females, and not males, there was also a significant correlation between TT4 and PFDoDA (p=0.040, r_P=0.730).

It was suggested by Melnes et al. (2017) that the sex differences revealed in her study regarding the “lack of associations” between T3 and PFOS in males could be ascribed to BCI, which might have confounded the PFAS levels in males. Since BCI and plasma protein levels could be interconnected, Melnes et al. suggested that whether BCI was confounding or not would be clarified if the protein concentrations were known (Melnes et al., 2017). In the

present study, protein normalized TH concentrations were applied, and yet, relationships between individual PFASs and THs were not significant in male glaucous gulls (Table 6). Protein levels in plasma therefore do not seem to confound the relationships between PFASs and THs. Hence, there are probably other sex dependent mechanisms that cause the difference in TH responses between sexes.

4.6 Considerations

Since the PFAS and Hg concentrations measured in this study represent chronic exposure, the hormone levels in the glaucous gulls may already be tuned into a state of homeostasis that compensates for the potential disruption by contaminants. The relationships seen between hormone levels and contaminants therefore probably indicate only parts of the underlying mechanisms of disruption, which are hidden by the maintenance of constant circulating TH levels controlled by the HPT axis. Thyroid disruption could may also occur at other levels of the HPT axis than those discussed here.

5 CONCLUSION

In the present study, high levels of persistent PFASs and Hg were quantified in liver from glaucous gulls captured in Sassendalen and Adventfjorden, Svalbard, spring 2017. Hg was also quantified in feather and plasma. The Se:Hg ratio revealed that there was more Se than Hg available in all three tissue types. The predominant PFAS analysed was PFOS. The contaminant concentrations demonstrate that glaucous gulls, as Arctic top predators, are still highly exposed to anthropogenic emissions of PFASs and Hg.

Relationships between contaminants and TSH levels indicate that Hg and certain PFASs have a negative effect on circulating TSH levels in glaucous gulls, though the mechanisms need to be further investigated. The hypothesized positive correlations between PFASs and THs were confirmed for certain PFCAs and T3, however the expected significant relationship between THs and TSH was not confirmed. The hypothesized correlations between Hg and THs were not significant. Sex differences in thyroid response suggest that females might be more subjected to thyroid disruption by PFASs than males. Histological alterations were reported in nine of fourteen glaucous gulls, but the potential contaminant induced mechanisms underlying these histological changes could not be revealed in the present study. However, there are indications in the present study that Hg may play a role in the development of thyroid gland pathology. Altogether, this study adds to the weight of evidence that PFASs and Hg have adverse effects on the thyroid hormone homeostasis in glaucous gulls in Svalbard. Future studies should include experimental studies in order to confirm or disprove the mechanisms of disruption proposed here.

7 References

ACKERMAN, J. T., EAGLES-SMITH, C. A., HERZOG, M. P. & HARTMAN, C. A. 2016. Maternal transfer of contaminants in birds: mercury and selenium concentrations in parents and their eggs. *Environmental pollution,* 210**,** 145-154.

ALAVA, J. J., CHEUNG, W. W., ROSS, P. S. & SUMAILA, U. R. 2017. Climate change–contaminant interactions in marine food webs: Toward a conceptual framework. *Global change biology,* 23**,** 3984-4001.

ALLEN-ROWLANDS, C., CASTRACANE, V. D., HAMILTON, M. & SEIFTER, J. 1981. Effect of polybrominated biphenyls (PBB) on the pituitary-thyroid axis of the rat. *Proceedings of the Society for Experimental Biology and Medicine,* 166**,** 506-514.

AMAP 2004. AMAP Assessment 2002: Persistent Organic Pollutants in the Arctic. Oslo, Norway.

ANKER-NILSSEN, T., BAKKEN, V. & TERTIKSKI, G. M. 2000. *The status of marine birds breeding in the Barents Sea region,* Tromsø, Norsk polarinstitutt.

ARMITAGE, J. M., SCHENKER, U., SCHERINGER, M., MARTIN, J. W., MACLEOD, M. & COUSINS, I. T. 2009. Modeling the global fate and transport of perfluorooctane sulfonate (PFOS) and precursor compounds in relation to temporal trends in wildlife exposure. *Environmental science & technology,* 43**,** 9274-9280.

ARTSDATABANKEN. *Larus hyperboreus Gunnerus, 1767* [Online]. Available: https://artsdatabanken.no/Rodliste2015/rodliste2015/Svalbard/3692 [Accessed 15.04.2018].

ASK, A. V. 2015. *Perfluoroalkyl and Polyfluoroalkyl Substances (PFASs) Affect the Thyroid Hormone System, Body Condition, and Body Mass in Two Arctic Seabird Species.* Master Master, Norwegian University for Science and Technology, NTNU.

BARRY, S. J. & BARRY, T. W. 1990. Food habits of glaucous gulls in the Beaufort Sea. *Arctic***,** 43-49.

BIRDLIFE INTERNATIONAL. 2016. *Larus hyperboreus* [Online]. The IUCN Red List of Threatened Species Available: http://dx.doi.org/10.2305/IUCN.UK.2016-3.RLTS.T22694343A86730550.en. [Accessed 26.04.2018].

BORGÅ, K., GABRIELSEN, G. & SKAARE, J. 2001. Biomagnification of organochlorines along a Barents Sea food chain. *Environmental Pollution,* 113**,** 187-198.

BOULANGER, B., VARGO, J. D., SCHNOOR, J. L. & HORNBUCKLE, K. C. 2005. Evaluation of perfluorooctane surfactants in a wastewater treatment system and in a commercial surface protection product. *Environmental Science & Technology,* 39**,** 5524-5530.

BOURNE, W. & BOGAN, J. 1972. Polychlorinated biphenyls in North Atlantic seabirds. *Marine Pollution Bulletin,* 3**,** 171-175.

BRADFORD, M. M. 1976. A Rapid and Sensitive Method for the Quantification of Microgram Quantities of Protein Utilizing the Principle of Protein-Dye Binding. *Analytical Biochemistry,* 72**,** 7.

BRAUNE, B., CHÉTELAT, J., AMYOT, M., BROWN, T., CLAYDEN, M., EVANS, M., FISK, A., GADEN, A., GIRARD, C. & HARE, A. 2015. Mercury in the marine environment of the Canadian Arctic: Review of recent findings. *Science of the Total Environment,* 509**,** 67-90.

BRAUNE, B. M., GASTON, A. J. & MALLORY, M. L. 2016. Temporal trends of mercury in eggs of five sympatrically breeding seabird species in the Canadian Arctic. *Environmental Pollution,* 214**,** 124-131.

BUSTNES, J. O., GABRIELSEN, G. W. & VERREAULT, J. 2010. Climate variability and temporal trends of persistent organic pollutants in the Arctic: A study of glaucous gulls. *Environmental science & technology,* 44**,** 3155-3161.
BUTT, C. M., BERGER, U., BOSSI, R. & TOMY, G. T. 2010. Levels and trends of poly-and perfluorinated compounds in the arctic environment. *Science of the total environment,* 408**,** 2936-2965.
CHANG, L., MUNRO, S. L., RICHARDSON, S. J. & SCHREIBER, G. 1999. Evolution of thyroid hormone binding by transthyretins in birds and mammals. *The FEBS Journal,* 259**,** 534-542.
COGBURN, L. A. & FREEMAN, R. M. 1987. Response surface of daily thyroid hormone rhythms in young chickens exposed to constant ambient temperature. *General and comparative endocrinology,* 68**,** 113-123.
COLLINS, W. T. & CAPEN, C. C. 1980. Ultrastructural and functional alterations of the rat thyroid gland produced by polychlorinated biphenyls compared with iodide excess and deficiency, and thyrotropin and thyroxine administration. *Virchows Archiv B,* 33**,** 213.
DAWSON, A. 2000. Mechanisms of endocrine disruption with particular reference to occurrence in avian wildlife: a review. *Ecotoxicology,* 9**,** 59-69.
DAWSON, R. D. & BORTOLOTTI, G. R. 1997. Total plasma protein level as an indicator of condition in wild American kestrels (Falco sparverius). *Canadian Journal of Zoology,* 75**,** 680-686.
DE WIT, C., FISK, A. T. & MUIR, D. C. 2005. Effects of persistent organic pollutants (POPs) in arctic wildlife. *Organohalogen Compounds,* 67.
DECUYPERE, E., VAN AS, P., VAN DER GEYTEN, S. & DARRAS, V. 2005. Thyroid hormone availability and activity in avian species: a review. *Domestic animal endocrinology,* 29**,** 63-77.
DENTICE, M., MARSILI, A., ZAVACKI, A., LARSEN, P. R. & SALVATORE, D. 2013. The deiodinases and the control of intracellular thyroid hormone signaling during cellular differentiation. *Biochimica et Biophysica Acta (BBA)-General Subjects,* 1830**,** 3937-3945.
DIETZ, R., BORN, E., RIGET, F., AUBAIL, A., SONNE, C., DRIMMIE, R. & BASU, N. 2011. Temporal trends and future predictions of mercury concentrations in Northwest Greenland polar bear (Ursus maritimus) hair. *Environmental science & technology,* 45**,** 1458-1465.
DIETZ, R., GUSTAVSON, K., SONNE, C., DESFORGES, J.-P., RIGÉT, F. F., PAVLOVA, V., MCKINNEY, M. A. & LETCHER, R. J. 2015. Physiologically-based pharmacokinetic modelling of immune, reproductive and carcinogenic effects from contaminant exposure in polar bears (Ursus maritimus) across the Arctic. *Environmental research,* 140**,** 45-55.
DONADIO-ANDRÉI, S., CHIKH, K., HEUCLIN, C., KUCZEWSKI, E., CHARRIÉ, A., GAUCHEZ, A. S. & RONIN, C. 2017. Variability among TSH Measurements Can Be Reduced by Combining a Glycoengineered Calibrator to Epitope-Defined Immunoassays. *European Thyroid Journal,* 6**,** 3-11.
EALES, J. G. 1988. The influence of nutritional state on thyroid function in various vertebrates. *American Zoologist,* 28**,** 351-362.
EMBRYOLOGY. 2012. *HPT axis* [Online]. Available: https://embryology.med.unsw.edu.au/embryology/index.php/File:HPT_axis.jpg [Accessed].
ERIKSSON, L., BYRNE, T., JOHANSSON, E., TRYGG, J. & VIKSTRÖM, C. 2013. *Multi- and megavariate data analysis basic principles and applications,* Umetrics Academy.

ERIKSTAD, K. E., SANDVIK, H., REIERTSEN, T. K., BUSTNES, J. O. & STRØM, H. 2013. Persistent organic pollution in a high-Arctic top predator: sex-dependent thresholds in adult survival. *Proceedings of the Royal Society of London B: Biological Sciences,* 280**,** 20131483.

FAUCHALD, P., ANKER-NILSSEN, T., BARRETT, R., BUSTNES, J. O., BÅRDSEN, B.-J., CHRISTENSEN-DALSGAARD, S., DESCAMPS, S., ENGEN, S., ERIKSTAD, K. E. & HANSSEN, S. A. 2015. The status and trends of seabirds breeding in Norway and Svalbard.

FISK, A. T., HOBSON, K. A. & NORSTROM, R. J. 2001. Influence of chemical and biological factors on trophic transfer of persistent organic pollutants in the Northwater Polynya marine food web. *Environmental Science & Technology,* 35**,** 732-738.

GABRIELSEN, G. W. 2007. Levels and effects of persistent organic pollutants in arctic animals. *Arctic alpine ecosystems and people in a changing environment.* Springer.

GABRIELSEN, G. W., SKAARE, J. U., POLDER, A. & BAKKEN, V. 1995. Chlorinated hydrocarbons in glaucous gulls (Larus hyperboreus) in the southern part of Svalbard. *Science of the Total Environment,* 160**,** 337-346.

GREGORY, C. C. & PORTER, T. E. 1997. Cloning and sequence analysis of a cDNA for the β subunit of chicken thyroid-stimulating hormone. *General and comparative endocrinology,* 107**,** 182-190.

HALLGREN, S., SINJARI, T., HÅKANSSON, H. & DARNERUD, P. 2001. Effects of polybrominated diphenyl ethers (PBDEs) and polychlorinated biphenyls (PCBs) on thyroid hormone and vitamin A levels in rats and mice. *Archives of toxicology,* 75**,** 200-208.

HANSSEN, L., DUDAREV, A. A., HUBER, S., ODLAND, J. Ø., NIEBOER, E. & SANDANGER, T. M. 2013. Partition of perfluoroalkyl substances (PFASs) in whole blood and plasma, assessed in maternal and umbilical cord samples from inhabitants of arctic Russia and Uzbekistan. *Science of the Total Environment,* 447**,** 430-437.

HAUGERUD, A. J. 2011. *Levels and Effects of Organohalogenated Contaminants on Thyroid Hormone Levels in Glaucous Gulls (Larus hyperboreus) from Kongsfjorden, Svalbard.* Master's, Norwegian University of Science and Technology.

HAUKÅS, M., BERGER, U., HOP, H., GULLIKSEN, B. & GABRIELSEN, G. W. 2007. Bioaccumulation of per-and polyfluorinated alkyl substances (PFAS) in selected species from the Barents Sea food web. *Environmental Pollution,* 148**,** 360-371.

HENRIKSEN, E., GABRIELSEN, G., TRUDEAU, S., WOLKERS, J., SAGERUP, K. & SKAARE, J. 2000. Organochlorines and possible biochemical effects in glaucous gulls (Larus hyperboreus) from Bjørnøya, the Barents Sea. *Archives of Environmental Contamination and Toxicology,* 38**,** 234-243.

HULBERT, A. 2000. Thyroid hormones and their effects: a new perspective. *Biological Reviews,* 75**,** 519-631.

HUNG, H., KATSOYIANNIS, A. A., BRORSTRÖM-LUNDÉN, E., OLAFSDOTTIR, K., AAS, W., BREIVIK, K., BOHLIN-NIZZETTO, P., SIGURDSSON, A., HAKOLA, H. & BOSSI, R. 2016. Temporal trends of Persistent Organic Pollutants (POPs) in arctic air: 20 years of monitoring under the Arctic Monitoring and Assessment Programme (AMAP). *Environmental Pollution,* 217**,** 52-61.

ISHIHARA, A., NISHIYAMA, N., SUGIYAMA, S.-I. & YAMAUCHI, K. 2003. The effect of endocrine disrupting chemicals on thyroid hormone binding to Japanese quail transthyretin and thyroid hormone receptor. *General and comparative endocrinology,* 134**,** 36-43.

JACOBSEN, M. L., JASPERS, V. L., CIESIELSKI, T. M., JENSSEN, B. M., LØSETH, M. E., BRIELS, N., EULAERS, I., LEIFSSON, P. S., RIGÉT, F. F. & GOMEZ-

RAMIREZ, P. 2017. Japanese quail (Coturnix japonica) liver and thyroid gland histopathology as a result of in ovo exposure to the flame retardants tris (1, 3-dichloro-2-propyl) phosphate and Dechlorane Plus. *Journal of Toxicology and Environmental Health, Part A,* 80**,** 525-531.
JAKOB, E. M., MARSHALL, S. D. & UETZ, G. W. 1996. Estimating fitness: a comparison of body condition indices. *Oikos***,** 61-67.
JOLICOEUR, P. & MOSIMANN, J. E. 1960. Size and shape variation in the painted turtle. A principal component analysis. *Growth,* 24**,** 339-354.
JONES, P. D., HU, W., DE COEN, W., NEWSTED, J. L. & GIESY, J. P. 2003. Binding of perfluorinated fatty acids to serum proteins. *Environmental toxicology and chemistry,* 22**,** 2639-2649.
JÆGER, I., HOP, H. & GABRIELSEN, G. W. 2009. Biomagnification of mercury in selected species from an Arctic marine food web in Svalbard. *Science of the Total Environment,* 407**,** 4744-4751.
KELLY, B. C., IKONOMOU, M. G., BLAIR, J. D., SURRIDGE, B., HOOVER, D., GRACE, R. & GOBAS, F. A. 2009. Perfluoroalkyl contaminants in an Arctic marine food web: trophic magnification and wildlife exposure. *Environmental science & technology,* 43**,** 4037-4043.
KEMI 2015. Occurrence and use of highly fluorinated substances and alternatives. Report from a government assignment.
KHAN, M. A. & WANG, F. 2009. Mercury-selenium compounds and their toxicological significance: Toward a molecular understanding of the mercury-selenium antagonism. *Environmental Toxicology and Chemistry,* 28**,** 1567-1577.
KIRUBAGARAN, R. & JOY, K. 1994. Effects of short-term exposure to methylmercury chloride and its withdrawal on serum levels of thyroid hormones in the catfish Clarias batrachus. *Bulletin of environmental contamination and toxicology,* 53**,** 166-170.
LETCHER, R. J., BUSTNES, J. O., DIETZ, R., JENSSEN, B. M., JØRGENSEN, E. H., SONNE, C., VERREAULT, J., VIJAYAN, M. M. & GABRIELSEN, G. W. 2010. Exposure and effects assessment of persistent organohalogen contaminants in arctic wildlife and fish. *Science of the Total Environment,* 408**,** 2995-3043.
LUNDSTEDT, T., SEIFERT, E., ABRAMO, L., THELIN, B., NYSTRÖM, Å., PETTERSEN, J. & BERGMAN, R. 1998. Experimental design and optimization. *Chemometrics and intelligent laboratory systems,* 42**,** 3-40.
LYDERSEN, C., GIERTZ, I. & WESLAWSKI, J. M. 1985. Aspects of vertebrate feeding in the marine ecosystem in Hornsund, Svalbard.
LØVENSKIOLD, H. L. 1964. Avifauna Svalbardensis: with a discussion on the geographical distribution of the birds in Spitsbergen and adjacent islands.
MAQBOOL, F., MOSTAFALOU, S., BAHADAR, H. & ABDOLLAHI, M. 2016. Review of endocrine disorders associated with environmental toxicants and possible involved mechanisms. *Life sciences,* 145**,** 265-273.
MARTIN, J. W., MABURY, S. A., SOLOMON, K. R. & MUIR, D. C. 2003. Dietary accumulation of perfluorinated acids in juvenile rainbow trout (Oncorhynchus mykiss). *Environmental Toxicology and Chemistry,* 22**,** 189-195.
MARTIN, J. W., SMITHWICK, M. M., BRAUNE, B. M., HOEKSTRA, P. F., MUIR, D. C. & MABURY, S. A. 2004. Identification of long-chain perfluorinated acids in biota from the Canadian Arctic. *Environmental Science & Technology,* 38**,** 373-380.
MCNABB, F. & FOX, G. A. 2003. Avian thyroid development in chemically contaminated environments: is there evidence of alterations in thyroid function and development? *Evolution & development,* 5**,** 76-82.

MCNABB, F. A. 2007. The hypothalamic-pituitary-thyroid (HPT) axis in birds and its role in bird development and reproduction. *Critical reviews in toxicology,* 37**,** 163-193.
MELNES, M., GABRIELSEN, G. W., HERZKE, D., SAGERUP, K. & JENSSEN, B. M. 2017. Dissimilar effects of organohalogenated compounds on thyroid hormones in glaucous gulls. *Environmental research,* 158**,** 350-357.
MENDEL, C. M. 1989. The free hormone hypothesis: a physiologically based mathematical model. *Endocrine reviews,* 10**,** 232-274.
MORAN, M. D. 2003. Arguments for rejecting the sequential Bonferroni in ecological studies. *Oikos,* 100**,** 403-405.
MORSE, D., KOETER, H., VAN PROOIJEN, A. S. & BROUWER, A. 1992. Interference of polychlorinated biphenyls in thyroid hormone metabolism: possible neurotoxic consequences in fetal and neonatal rats. *Chemosphere,* 25**,** 165-168.
MORTENSEN, Å.-K. 2015. *Competitive Binding of Persistent Organic Pollutants to the Thyroid Hormone Transport Protein Transthyretin in Glaucous Gull (Larus hyperboreus).* Master, Norwegian University for Science and Technology.
MOVASSEGHI, A. R., RODRÍGUEZ-ESTIVAL, J. & SMITS, J. E. 2017. Thyroid pathology in deer mice (Peromyscus maniculata) from a reclaimed mine site on the athabasca oil sands. *Environmental Pollution,* 222**,** 42-49.
MULDER, P. J., LIE, E., EGGEN, G. S., CIESIELSKI, T. M., BERG, T., SKAARE, J. U., JENSSEN, B. M. & SØRMO, E. G. 2012. Mercury in molar excess of selenium interferes with thyroid hormone function in free-ranging freshwater fish. *Environmental science & technology,* 46**,** 9027-9037.
NESS, D. K., SCHANTZ, S. L., MOSHTAGHIAN, J. & HANSEN, L. G. 1993. Effects of perinatal exposure to specific PCB congeners on thyroid hormone concentrations and thyroid histology in the rat. *Toxicology letters,* 68**,** 311-323.
NEWCOMER, W. 1974. Diurnal rhythms of thyroid function in chicks. *General and comparative Endocrinology,* 24**,** 65-73.
NYLANDER, M. & WEINER, J. 1991. Mercury and selenium concentrations and their interrelations in organs from dental staff and the general population. *Occupational and Environmental Medicine,* 48**,** 729-734.
NØST, T. H., HELGASON, L. B., HARJU, M., HEIMSTAD, E. S., GABRIELSEN, G. W. & JENSSEN, B. M. 2012. Halogenated organic contaminants and their correlations with circulating thyroid hormones in developing Arctic seabirds. *Science of the Total Environment,* 414**,** 248-256.
O'SULLIVAN, G. 2013. *Environmental forensics for persistent organic pollutants,* Newnes.
PANDEY, S. P. & MOHANTY, B. 2017. Disruption of the hypothalamic-pituitary-thyroid axis on co-exposures to dithiocarbamate and neonicotinoid pesticides: Study in a wildlife bird, Amandava amandava. *NeuroToxicology,* 60**,** 16-22.
POWLEY, C. R., GEORGE, S. W., RYAN, T. W. & BUCK, R. C. 2005. Matrix Effect-Free Analytical Methods for Determination of Perfluorinated Carboxylic Acids in Environmental Matrixes. *Analytical Chemistry,* 77**,** 6353-6358.
REN, X.-M., QIN, W.-P., CAO, L.-Y., ZHANG, J., YANG, Y., WAN, B. & GUO, L.-H. 2016. Binding interactions of perfluoroalkyl substances with thyroid hormone transport proteins and potential toxicological implications. *Toxicology,* 366**,** 32-42.
REYNS, G., JANSSENS, K., BUYSE, J., KÜHN, E. & DARRAS, V. 2002. Changes in thyroid hormone levels in chicken liver during fasting and refeeding. *Comparative Biochemistry and Physiology Part B: Biochemistry and Molecular Biology,* 132**,** 239-245.

RIGÉT, F., VORKAMP, K., BOSSI, R., SONNE, C., LETCHER, R. & DIETZ, R. 2016. Twenty years of monitoring of persistent organic pollutants in Greenland biota. A review. *Environmental Pollution,* 217**,** 114-123.

ROSENE, M. L., WITTMANN, G. B., ARROJO E DRIGO, R., SINGRU, P. S., LECHAN, R. M. & BIANCO, A. C. 2010. Inhibition of the type 2 iodothyronine deiodinase underlies the elevated plasma TSH associated with amiodarone treatment. *Endocrinology,* 151**,** 5961-5970.

ROSS, M. H. & PAWLINA, W. 2006. *Histology. A Text and Atlas With correlated cell end molecular biology,* Lippincott Williams & Wilkins.

ROTANDER, A., KÄRRMAN, A., VAN BAVEL, B., POLDER, A., RIGÉT, F., AUÐUNSSON, G. A., VÍKINGSSON, G., GABRIELSEN, G. W., BLOCH, D. & DAM, M. 2012. Increasing levels of long-chain perfluorocarboxylic acids (PFCAs) in Arctic and North Atlantic marine mammals, 1984–2009. *Chemosphere,* 86**,** 278-285.

ROUTTI, H., GABRIELSEN, G. W., HERZKE, D., KOVACS, K. M. & LYDERSEN, C. 2016. Spatial and temporal trends in perfluoroalkyl substances (PFASs) in ringed seals (Pusa hispida) from Svalbard. *Environmental Pollution,* 214**,** 230-238.

SAGERUP, K., LARSEN, H. J. R. S., SKAARE, J. U., JOHANSEN, G. M. & GABRIELSEN, G. W. 2009a. The toxic effects of multiple persistent organic pollutant exposures on the post-hatch immunity maturation of glaucous gulls. *Journal of Toxicology and Environmental Health, Part A,* 72**,** 870-883.

SAGERUP, K., HELGASON, L. B., POLDER, A., STRØM, H., JOSEFSEN, T. D., SKÅRE, J. U. & GABRIELSEN, G. W. 2009b. Persistent organic pollutants and mercury in dead and dying glaucous gulls (Larus hyperboreus) at Bjørnøya (Svalbard). *Science of the Total Environment,* 407**,** 6009-6016.

SAGERUP, K., HERZKE, D., HARJU, M., EVENSET, A., CHRISTENSEN, G. N., ROUTTI, H., FUGLEI, E., AARS, J., STRØM, H. & GABRIELSEN, G. W. 2010. New brominated flame retardants in Arctic biota.

SAITA, E., HAYAMA, S., KAJIGAYA, H., YONEDA, K., WATANABE, G. & TAYA, K. 2004. Histologic changes in thyroid glands from great cormorant (Phalacrocorax carbo) in Tokyo Bay, Japan: Possible association with environmental contaminants. *Journal of wildlife diseases,* 40**,** 763-768.

SCHAEFER, J. K., ROCKS, S. S., ZHENG, W., LIANG, L., GU, B. & MOREL, F. M. 2011. Active transport, substrate specificity, and methylation of Hg (II) in anaerobic bacteria. *Proceedings of the National Academy of Sciences,* 108**,** 8714-8719.

SCHROEDER, W. H. & MUNTHE, J. 1998. Atmospheric mercury—an overview. *Atmospheric environment,* 32**,** 809-822.

SOLDIN, O. P., O'MARA, D. M. & ASCHNER, M. 2008. Thyroid hormones and methylmercury toxicity. *Biological trace element research,* 126**,** 1.

SONNE, C., VERREAULT, J., GABRIELSEN, G. W., LETCHER, R. J., LEIFSSON, P. S. & IBURG, T. 2010. Screening of thyroid gland histology in organohalogen-contaminated glaucous gulls (Larus hyperboreus) from the Norwegian Arctic. *Toxicological & Environ Chemistry,* 92**,** 1705-1713.

SONNE, C., IBURG, T., LEIFSSON, P. S., BORN, E. W., LETCHER, R. J. & DIETZ, R. 2011. Thyroid gland lesions in organohalogen contaminated East Greenland polar bears (Ursus maritimus). *Toxicological & Environmental Chemistry,* 93**,** 789-805.

SONNE, C., MÆHRE, S. A., SAGERUP, K., HARJU, M., HEIMSTAD, E. S., LEIFSSON, P. S., DIETZ, R. & GABRIELSEN, G. W. 2013. A screening of liver, kidney, and thyroid gland morphology in organochlorine-contaminated glaucous gulls (Larus hyperboreus) from Svalbard. *Toxicological & Environmental Chemistry,* 95**,** 172-186.

STRØM, H. & DESCAMPS, S. *Polarmåke (Larus hyperboreus)* [Online]. Available: http://www.npolar.no/no/arter/polarmake.html [Accessed 28.04.2018].
STURKIE, P. D. 2012. *Avian physiology*, Springer Science & Business Media.
SVENDSEN, N., HERZKE, D., HARJU, M., BECH, C., GABRIELSEN, G. & JASPERS, V. 2018. Persistent organic pollutants and organophosphate esters in feathers and blood plasma of adult kittiwakes (Rissa tridactyla) from Svalbard–associations with body condition and thyroid hormones. *Environmental research,* 164**,** 158-164.
TROISI, G., BARTON, S. & BEXTON, S. 2016. Impacts of oil spills on seabirds: Unsustainable impacts of non-renewable energy. *international journal of hydrogen energy,* 41**,** 16549-16555.
UCÁN-MARIN, F., ARUKWE, A., MORTENSEN, A. S., GABRIELSEN, G. W. & LETCHER, R. J. 2009. Recombinant albumin and transthyretin transport proteins from two gull species and human: chlorinated and brominated contaminant binding and thyroid hormones. *Environmental science & technology,* 44**,** 497-504.
UNITSLAB.COM. 2018. Available: http://unitslab.com/index.php/ [Accessed].
VERREAULT, J., BECH, C., LETCHER, R. J., ROPSTAD, E., DAHL, E. & GABRIELSEN, G. W. 2007. Organohalogen contamination in breeding glaucous gulls from the Norwegian Arctic: Associations with basal metabolism and circulating thyroid hormones. *Environmental Pollution,* 145**,** 138-145.
VERREAULT, J., GABRIELSEN, G. & BUSTNES, J. 2010. The Svalbard glaucous gull as bioindicator species in the European Arctic: insight from 35 years of contaminants research. *Reviews of Environmental Contamination and Toxicology Volume 205.* Springer.
VERREAULT, J., HOUDE, M., GABRIELSEN, G. W., BERGER, U., HAUKÅS, M., LETCHER, R. J. & MUIR, D. C. 2005. Perfluorinated alkyl substances in plasma, liver, brain, and eggs of glaucous gulls (Larus hyperboreus) from the Norwegian Arctic. *Environmental science & technology,* 39**,** 7439-7445.
WADA, H., CRISTOL, D. A., MCNABB, F. A. & HOPKINS, W. A. 2009. Suppressed adrenocortical responses and thyroid hormone levels in birds near a mercury-contaminated river. *Environmental science & technology,* 43**,** 6031-6038.
WALKER, C. 1992. The ecotoxicology of persistent pollutants in marine fish-eating birds. *Persistent pollutants in marine ecosystems***,** 211-32.
WANG, Z., DEWITT, J. C., HIGGINS, C. P. & COUSINS, I. T. 2017. A never-ending story of per-and polyfluoroalkyl substances (PFASs)? : ACS Publications.
WEISS, J. M., ANDERSSON, P. L., LAMOREE, M. H., LEONARDS, P. E. G., VAN LEEUWEN, S. P. J. & HAMERS, T. 2009. Competitive Binding of Poly- and Perfluorinated Compounds to the Thyroid Hormone Transport Protein Transthyretin. *Toxicological Sciences,* 109**,** 206-216.
WOLFE, M. F., SCHWARZBACH, S. & SULAIMAN, R. A. 1998. Effects of mercury on wildlife: a comprehensive review. *Environmental toxicology and chemistry,* 17**,** 146-160.

APPENDIX A: Individual biometric measures

Table A9 Biological measurements, capture site, sex, and body condition index (BCI) of the individual male (n=7, M) and female (n=8, F) glaucous gulls (*Larus hyperboreus*) captured in Sassendalen and Adventfjorden, Svalbard, in April and May 2017.

ID	Collection site	Sex	Body mass (g)	Head (mm)	Tarsus (mm)	Wing (mm)	Liver (g)	BCI
LH01	Sassendalen	F	1340	145.48	75.96	44.5	34.30	-1.4014
LH02	Sassendalen	M	1685	148.93	75.48	46.1	33.30	-1.3783
LH03	Sassendalen	M	1750	154.26	75.90	47.2	n/a	-0.3977
LH04	Sassendalen	F	1687	132.25	75.86	43.1	39.80	0.9237
LH05	Sassendalen	F	1450	130.92	75.60	44.8	38.15	-0.3081
LH06	Sassendalen	F	1550	135.08	79.90	45.2	41.40	0.9034
LH07	Sassen/Fredheim	F	1425	134.54	77.44	43.5	38.35	-1.2565
LH08	Adventfjorden	M	1875	143.46	78.20	46.3	46.65	-0.0642
LH09	Adventfjorden	F	1589	132.05	73.74	44.9	55.45	1.0429
LH10	Adventfjorden	F	1450	130.57	72.25	44.8	34.95	-0.2805
LH11	Adventfjorden	M	1950	145.53	79.32	46.9	42.80	0.7918
LH12	Adventfjorden	F	1500	128.93	76.54	45.2	35.70	0.3765
LH13	Adventfjorden	M	1820	145.11	78.25	45.7	42.65	-0.2591
LH14	Adventfjorden	M	1920	141.60	78.15	45.7	33.35	0.3904
LH15	Adventfjorden	M	1875	151.61	84.55	46.2	39.75	0.9171

APPENDIX B: Washing procedure for feathers

Feathers were washed prior to elemental analysis according to the following procedure developed by researcher Tomasz Maciej Ciesielski and master student Ingvild Kroglund Buran at NTNU:

Feathers were washed in five main steps, each separated by two water flushes:

1. Acetone 5 minutes
2. Water 5 minutes
3. Acetone 5 minutes
4. 2 % v/v HNO_3 5 minutes
5. Water 5 minutes

APPENDIX C: Recovery standards

Table A10 Mass labelled internal standards (13C labelled PFAS analytes). Recovery is given as % of recovery standards added.

	13C PFHxS	13C PFOS	13C FOSA	13C PFHxA	13C PFHpA	13C PFOA	13C PFNA	13C PFDA	13C PFUnDA	13C PFDoDA	13C PFTeDA
Mean	69	67	51	76	86	96	122	101	101	94	92
SD	20	14	16	21	24	29	33	30	25	20	14

APPENDIX D: Individual PFAS concentrations

Table A11. Individual PFAS concentrations (ng/g ww) detected in liver of male (n=7, M) and female (n=8, F) glaucous gulls (*Larus hyperboreus*) captured in Sassendalen and Adventfjorden, Svalbard, in April and May, 2017.

		No. of carbons in chain				4	6	7		8		9	10		4
ID	Sex	4:2 FTS	6:2 FTS	8:2 FTS	FOSA	PFBS	PFHxS	PFHpS	PFOSlin	∑PFOS	% branched	PFNS	PFDcS	F-53 B	PFBA
LH01	F	<0.15	<0.15	<0.15	<0.10	<0.05	0.18	0.19	32.51	35.74	9.03	<0.10	<0.10	<0.20	<0.05
LH02	M	<0.15	<0.15	<0.15	<0.10	<0.05	0.08	0.14	42.72	47.10	9.31	<0.10	<0.10	<0.20	<0.05
LH03	M	<0.15	<0.15	<0.15	<0.10	<0.05	0.19	<0.10	14.91	16.49	9.61	<0.10	<0.10	<0.20	<0.05
LH04	F	<0.15	<0.15	<0.15	<0.10	<0.05	0.25	0.18	48.25	52.73	8.50	<0.10	0.17	<0.20	<0.05
LH05	F	<0.15	<0.15	<0.15	<0.10	<0.05	0.21	<0.10	23.16	25.96	10.80	<0.10	<0.10	<0.20	<0.05
LH06	F	<0.15	<0.15	<0.15	<0.10	<0.05	0.18	<0.10	15.71	17.21	8.73	<0.10	0.15	<0.20	<0.05
LH07	F	<0.15	<0.15	<0.15	<0.10	<0.05	0.07	0.17	20.61	22.16	6.98	<0.10	<0.10	<0.20	<0.05
LH08	M	<0.15	<0.15	<0.15	<0.10	<0.05	0.17	<0.10	20.16	22.69	11.15	<0.10	<0.10	<0.20	<0.05
LH09	F	<0.15	<0.15	<0.15	<0.10	<0.05	0.58	0.14	9.24	11.84	21.99	<0.10	<0.10	<0.20	<0.05
LH10	F	<0.15	<0.15	<0.15	<0.10	<0.05	0.30	0.12	14.22	16.45	13.51	<0.10	<0.10	<0.20	<0.05
LH11	M	<0.15	<0.15	<0.15	<0.10	<0.05	0.27	<0.10	19.40	22.03	11.95	<0.10	0.28	<0.20	<0.05
LH12	F	<0.15	<0.15	<0.15	<0.10	<0.05	0.24	0.17	29.37	32.53	9.72	<0.10	<0.10	<0.20	<0.05
LH13	M	<0.15	<0.15	<0.15	<0.10	<0.05	0.45	0.10	26.26	28.29	7.20	<0.10	<0.10	<0.20	<0.05
LH14	M	<0.15	<0.15	<0.15	<0.10	<0.05	0.03	<0.10	13.21	13.82	4.42	<0.10	<0.10	<0.20	<0.05
LH15	M	<0.15	<0.15	<0.15	<0.10	<0.05	0.39	<0.10	28.12	30.81	8.74	0.10	<0.10	<0.20	<0.05

No. of carbons in ch:	5	6	7	8	9	10	11	12	13	14	15	16			
ID	Sex	PFPeA	PFHxA	PFHpA	PFOA	PFNA	PFDA	PFUnDA	PFDoDA	PFTrDA	PFTeDA	PFHxDA	PFODcA	∑PFSA	∑PFCA	∑PFAS
LH01	F	<0.05	<0.10	<0.05	<0.05	2.46	2.09	4.93	0.77	1.71	0.35	<0.15	<0.15	36.11	12.31	48.41
LH02	M	<0.05	<0.10	<0.05	<0.05	3.20	2.75	5.56	0.86	2.03	0.41	<0.15	<0.15	47.32	14.82	62.14
LH03	M	<0.05	<0.10	<0.05	<0.05	2.43	1.87	4.63	0.85	2.08	0.32	<0.15	<0.15	16.74	12.18	28.92
LH04	F	<0.05	<0.10	<0.05	<0.05	5.02	3.48	5.38	0.81	1.79	0.39	<0.15	<0.15	53.49	16.87	70.36
LH05	F	<0.05	<0.10	<0.05	<0.05	2.73	1.94	3.58	0.70	1.78	0.30	<0.15	<0.15	26.23	11.03	37.27
LH06	F	<0.05	<0.10	<0.05	<0.05	1.66	1.26	2.87	0.52	1.45	0.27	<0.15	<0.15	17.76	8.02	25.78
LH07	F	<0.05	<0.10	<0.05	<0.05	1.21	1.02	2.54	0.65	2.24	0.54	<0.15	<0.15	22.39	8.21	30.60
LH08	M	<0.05	<0.10	<0.05	<0.05	2.60	2.19	4.67	0.73	2.07	0.29	<0.15	<0.15	22.91	12.56	35.46
LH09	F	<0.05	<0.10	<0.05	<0.05	2.60	0.58	1.49	0.22	0.71	0.12	<0.15	<0.15	12.56	5.73	18.29
LH10	F	<0.05	<0.10	<0.05	<0.05	0.96	0.70	1.54	0.37	0.86	0.31	<0.15	<0.15	16.86	4.74	21.60
LH11	M	<0.05	<0.10	<0.05	<0.05	1.63	1.35	2.98	0.50	1.32	0.27	<0.15	<0.15	22.93	8.05	30.98
LH12	F	<0.05	<0.10	<0.05	<0.05	3.88	2.14	3.50	0.63	1.84	0.37	<0.15	<0.15	32.94	12.36	45.29
LH13	M	<0.05	<0.10	<0.05	<0.05	1.59	1.73	4.10	0.66	1.83	0.35	<0.15	<0.15	28.84	10.27	39.11
LH14	M	<0.05	<0.10	<0.05	<0.05	0.91	1.20	2.42	0.54	1.56	0.25	<0.15	<0.15	13.93	6.88	20.81
LH15	M	<0.05	<0.10	<0.05	<0.05	2.77	2.71	5.88	0.98	2.50	0.48	<0.15	<0.15	31.40	15.32	46.61

APPENDIX E: Individual Hg and Se concentrations, and Se:Hg ratios

Table A12. Individual Hg and Se concentrations (µg/g dw) and molar Hg:Se ratio detected in plasma, feather, and liver of male (n=7, M) and female (n=8, F) glaucous gulls (*Larus hyperboreus*) captured in Sassendalen and Adventfjorden, Svalbard, in April and May, 2017.

ID	Sex	Hg plasma	Hg feathers	Hg liver	Se plasma	Se feathers	Se liver	Se:Hg plasma	Se:Hg feather	Se:Hg liver
LH01	F	0.007	1.062	2.482	0.391	0.906	7.271	145.84	2.17	7.44
LH02	M	0.015	5.155	4.595	0.261	1.298	5.583	45.32	0.64	3.09
LH03	M	0.015	6.084	2.017	0.308	0.946	3.006	52.69	0.40	3.79
LH04	F	0.016	1.898	3.613	0.293	0.999	4.857	47.95	1.34	3.42
LH05	F	0.017	1.949	3.718	0.383	1.096	5.921	55.72	1.43	4.05
LH06	F	0.011	3.060	2.109	0.217	0.960	2.779	50.12	0.80	3.35
LH07	F	0.010	4.152	3.574	0.429	0.869	6.613	104.09	0.53	4.70
LH08	M	0.012	6.574	2.873	0.361	1.121	6.323	76.30	0.43	5.59
LH09	F	0.018	0.852	1.075	0.334	0.754	4.802	46.88	2.26	11.35
LH10	F	0.010	2.582	2.945	0.303	0.931	5.158	76.29	0.92	4.45
LH11	M	0.012	1.402	2.823	0.183	0.858	7.854	37.99	1.55	7.07
LH12	F	0.008	1.950	5.322	0.168	0.896	4.640	50.69	1.17	2.21
LH13	M	0.009	4.393	3.479	0.243	1.221	5.300	71.25	0.71	3.87
LH14	M	0.011	5.652	2.747	0.471	1.955	8.358	112.866	0.88	7.73
LH15	M	0.012	3.070	5.547	0.187	0.769	3.729	40.950	0.64	1.71

APPENDIX F: Class wise contaminant levels

Table A13. Class wise mean, SD, median, and range of hepatic PFAS concentrations, and Hg, and Se concentrations, and Se:Hg ratio in plasma, feather, and liver in Class A (normal thyroid tissue, n=5), Class B (moderate histological changes, n=8), and Class C (pronounced histological changes, n=1) of glaucous gulls (*Larus hyperboreus*) captured in Sassendalen and Adventfjorden, Svalbard, in April and May 2017.

	Class A				Class B				Class C	
Compound	N	Mean ± SD	Median	Range	N	Mean ± SD	Median	Range	N	Concentration
PFHxS (ng/g)	5	0.25 ± 0.14	0.25	0.08 - 0.45	8	0.24 ± 1.78	0.20	0.03 - 0.58	1	0.18
PFHpS (ng/g)	5	0.15 ± 0.04	0.14	0.10 - 0.19	8	0.09 ± 0.04	0.08	0.05 - 0.17	1	0.07
PFOSlin (ng/g)	5	32.79 ± 13.46	32.51	14.44 - 48.25	8	18.60 ± 5.96	19.78	9.24 - 28.12	1	15.71
∑PFOS (ng/g)	5	36.06 ± 14.5	35.74	16.45 - 52.73	8	20.73 ± 6.34	22.09	11.84 - 30.81	1	17.21
PFNA (ng/g)	5	2.65 ± 1.58	2.46	0.96 - 5.02	8	2.11 ± 0.74	2.52	0.91 - 2.77	1	1.66
PFDA (ng/g)	5	2.15 ± 1.05	2.09	0.70 - 3.48	8	1.61 ± 0.69	1.61	0.59 - 2.71	1	1.26
PFUnDA (ng/g)	5	4.30 ± 1.65	4.93	1.54 - 5.56	8	3.52 ± 1.45	3.78	1.49 - 5.88	1	2.98
PFDoDA(ng/g)	5	0.69 ± 0.20	0.77	0.37 - 0.86	8	0.65 ± 0.23	0.67	0.22 - 0.98	1	0.52
PFTrDA (ng/g)	5	1.65 ± 0.45	1.77	0.86 - 2.03	8	1.78 ± 0.58	1.93	0.71 - 2.50	1	1.45
PFTeDA (ng/g)	5	0.32 ± 0.04	0.35	0.31 - 0.41	8	0.32 ± 0.13	0.29	0.12 - 0.54	1	0.27
∑PFSA (ng/g)	5	36.49 ± 14.53	36.11	16.86 - 53.33	8	21.09 ± 6.33	22.52	12.56 - 31.30	1	17.61
∑PFCA (ng/g)	5	11.80 ± 4.67	12.31	4.74 - 16.87	8	9.99 ± 3.29	9.62	5.73 - 15.32	1	8.02
∑PFAS (ng/g)	5	48.29 ± 19.16	48.41	21.60 - 70.20	8	31.08 ± 9.05	30.65	18.29 - 46.61	1	25.63
Hg plasma (µg/g)	5	0.01 ± 0.00	0.01	0.01 - 0.02	8	0.01 ± 0.00	0.01	0.01 - 0.02	1	0.01
Hg feathers (µg/g)	5	3.02 ± 1.71	2.58	1.06 - 5.15	8	3.72 ± 2.23	3.61	0.85 - 6.57	1	3.06
Hg liver (µg/g)	5	3.42 ± 0.79	3.48	2.48 - 4.59	8	3.05 ± 1.31	2.85	1.08 - 5.55	1	2.12
Se plasma (µg/g)	5	0.30 ± 0.06	0.29	0.24 - 0.39	8	0.33 ± 0.10	0.35	0.18 - 0.47	1	0.22
Se feathers (µg/g)	5	1.07 ± 0.18	1.00	0.90 - 1.30	8	1.05 ± 0.39	0.91	0.75 - 1.95	1	0.96
Se liver (µg/g)	5	5.63 ± 0.95	5.30	4.86 - 7.27	8	5.83 ± 1.88	6.12	3.01 - 8.36	1	2.78
Se:Hg ratio plasma	5	77.33 ± 40.68	71.25	45.32 - 145.84	8	65.93 ± 28.82	54.20	37.99 - 112.87	1	50.12
Se:Hg ratio feather	5	1.15 ± 0.63	0.92	0.64 - 2.17	8	1.01 ± 0.67	0.76	0.40 - 2.45	1	0.80
Se:Hg ratio liver	5	4.45 ± 1.75	3.87	3.09 - 7.44	8	5.75 ± 2.96	5.15	1.71 - 11.35	1	3.35

APPENDIX G: Individual TH, TSH, and protein concentrations, TH:protein and TSH:protein ratios

Table A14. Individual levels of FT4 (pmol/L), FT3 (pmol/L), TT4 (nmol/L), TT3 (nmol/L), TSH (µIU/ml), and protein (mg/ml), as well as FT4:protein (nmol/mg), FT3:protein (nmol/mg), TT4:protein (µmol/mg), TT3:protein (µmol/L), and TSH:protein (mIU:mg) ratios in plasma of male (n=7, M) and female (n=8, F) glaucous gulls (*Larus hyperboreus*) captured in Sassendalen and Adventfjorden, Svalbard, in April and May, 2017.

ID	FT4	TT4	FT3	TT3	TSH	Protein	FT4:protein	TT4:protein	FT3:protein	TT3:protein	TSH:protein
LH01	23.47	46.82	5.70	2.24	0.02	23.80	0.99	1.97	0.24	0.09	0.67
LH02	14.60	25.01	4.21	2.36	0.02	22.80	0.64	1.10	0.18	0.10	0.77
LH03	10.61	32.56	11.30	4.56	0.04	32.30	0.33	1.01	0.35	0.14	1.35
LH04	14.88	44.72	16.62	7.32	0.01	30.00	0.50	1.49	0.55	0.24	0.18
LH05	33.54	57.57	8.84	3.75	0.02	24.30	1.38	2.37	0.36	0.15	0.91
LH06	7.56	21.04	4.41	2.70	0.01	27.90	0.27	0.75	0.16	0.10	0.39
LH07	19.14	40.79	6.90	2.69	0.01	36.00	0.53	1.13	0.19	0.07	0.38
LH08	12.80	29.94	13.05	4.53	0.02	27.10	0.47	1.10	0.48	0.17	0.72
LH09	9.60	17.12	4.90	2.90	2.06	29.90	0.32	0.57	0.16	0.10	69.00
LH10	20.50	30.84	6.32	2.41	0.02	30.10	0.68	1.02	0.21	0.08	0.66
LH11	13.70	34.15	1.00	0.66	0.01	13.00	1.05	2.63	0.08	0.05	0.69
LH12	8.42	23.80	2.26	1.89	0.01	20.70	0.41	1.15	0.11	0.09	0.43
LH13	17.74	32.99	8.25	2.74	0.01	25.80	0.69	1.28	0.32	0.11	0.45
LH14	12.95	18.43	9.12	3.51	0.31	22.60	0.57	0.82	0.40	0.16	13.92
LH15	16.70	26.48	12.09	4.75	0.01	24.40	0.68	1.09	0.50	0.19	0.23

APPENDIX H: Class wise TH, TSH, and protein concentrations, TH:protein ratios, TSH:protein ratios, and follicle count

Table A15 Class wise mean, SD, median, and range of FT4 (pmol/L), FT3 (pmol/L), TT4 (nmol/L), TT3 (nmol/L), TSH (μIU/ml), and protein (mg/ml), as well as FT4:protein (nmol/mg), FT3:protein (nmol/mg), TT4:protein (μmol/mg), TT3:protein (μmol/L), and TSH:protein (mIU:mg) ratios, as well as follicle count in Class A (normal thyroid tissue, n=5), Class B (moderate histological changes, n=8), and Class C (pronounced histological changes, n=1) of glaucous gulls (*Larus hyperboreus*) captured in Sassendalen and Adventfjorden, Svalbard, in April and May 2017.

	Class A (n=5)			Class B (n=8)			Class C (n=1)
	Mean ± SD	Median	Range	Mean ± SD	Median	Range	Mean
TT3 (nmol/L)	3.41 ± 2.19	2.41	2.2 - 7.3	3.41 ± 1.36	3.63	0.7 - 4.8	2.70
TT4 (nmol/L)	36.07 ± 9.35	32.99	25.0 - 46.8	32.13 ± 12.96	31.25	17.1 - 57.6	21.04
FT3 (pmol/L)	8.22 ± 4.92	6.32	4.2 - 16.6	8.40 ± 4.03	8.98	1.0 - 13.1	4.41
FT4 (pmol/L)	18.24 ± 3.78	17.74	14.6 - 23.5	16.13 ± 7.68	13.32	9.6 - 33.5	7.56
TSH (μIU/ml)	0.01 ± 0.01	0.02	0.0 - 0.0	0.31 ± 0.71	0.02	0.0 - 2.1	0.01
Protein (mg/ml)	26.5 ± 3.42	25.80	22.8 - 31.10	26.2 - 6.99	25.75	13.0 - 36.0	27.9
TT3:protein (μmol:mg)	0.13 ± 0.07	0.10	0.10 - 0.20	0.13 ± 0.05	0.15	0.1 - 0.2	0.10
TT4:protein (μmol:mg)	1.37 ± 0.39	1.28	1.0 - 2.0	1.34 ± 0.74	1.10	0.6 - 2.6	0.75
FT3:protein (nmol:mg)	0.30 ± 0.15	0.24	0.2 - 0.6	0.32 ± 0.15	0.36	0.1 - 0.5	0.16
FT4:protein (nmol:mg)	0.70 ± 0.18	0.68	0.5 - 1.0	0.67 ± 0.37	0.55	0.3 - 1.4	0.27
TSH:protein (mIU:mg)	0.55 ± 0.23	0.66	0.2 - 0.8	10.90 ± 23.93	0.81	0.2 - 69.0	0.39
Follicle count	20.12 ± 4.08	18.80	16.6 - 27.0	25.17 ± 6.54	26.35	16.2 - 35.6	21.85

APPENDIX I: Score plot (PCA), sampling area

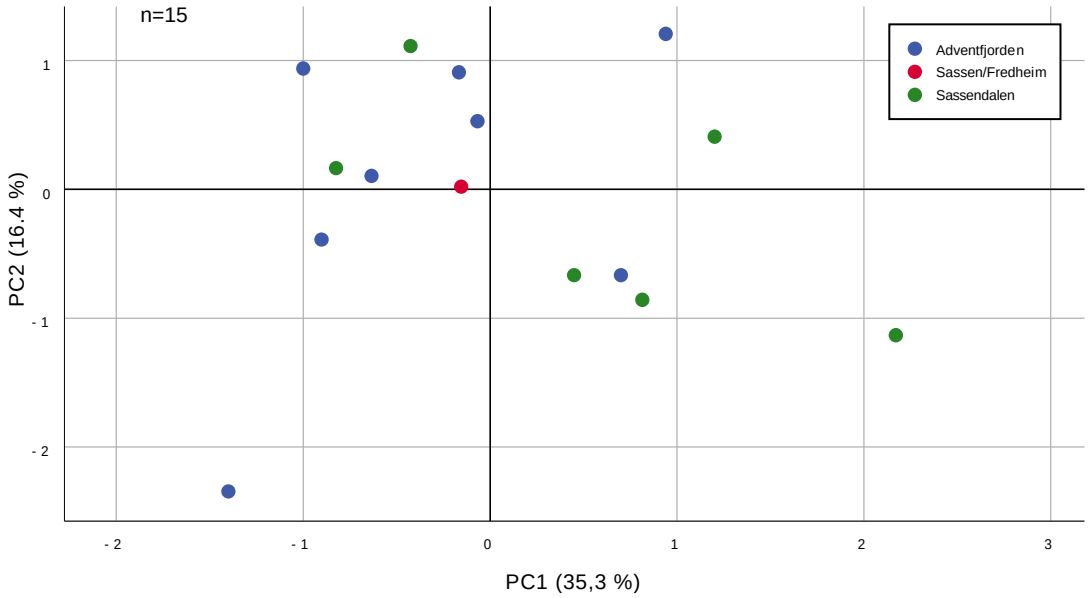

Figure A13. Principal component score plot showing where the 15 glaucous gulls (*Larus hyperboreus*) were captured (Sassendalen (green), Fredheim in Sassendalen (red), and Adventfjorden (blue)), Svalbard, in April and May 2017. Component 1 explains 35.3 % of the variation in the data set; component 2 explains 16.4 % of the variation in the data set.

APPENDIX J: Shapiro-Wilk's test of normality

Table A16. Biometric, PFAS, Hg, Se, Hg:Se, TH, and follicle count variables in n=15, male, and female glaucous gulls (*Larus hyperboreus*) as tested for normality using Shapiro-Wilk's normality test. Significance level is set at $p<0.05$. H_0: Data are normally distributed, H_1: Data are normally distributed.

Tests of Normality									
Shapiro-Wilk	n=15			Males			Females		
	Statistic	df	Sig.				Statistic	df	Sig.
BCl	0,87	13	0,052	0,92	6	0,505	0,859	7	0,149
BM	0,922	13	0,264	0,892	6	0,327	0,961	7	0,827
Head	0,896	13	0,118	0,959	6	0,813	0,742	7	0,01
Tarsus	0,947	13	0,549	0,841	6	0,132	0,969	7	0,888
Wing	0,961	13	0,77	0,91	6	0,434	0,852	7	0,129
Liver	0,891	13	0,101	0,893	6	0,335	0,777	7	0,024
HSI	0,927	13	0,311	0,989	6	0,986	0,765	7	0,018
Follicle count mean	0,915	13	0,217	0,928	6	0,565	0,934	7	0,588
Log_follicle_count	0,943	13	0,501	0,937	6	0,636			
PFHxS	0,944	13	0,513	0,942	6	0,672	0,851	7	0,125
PFHpS	0,942	13	0,484	0,969	6	0,889	0,91	7	0,396
PFOSlin	0,922	13	0,267	0,929	6	0,573	0,907	7	0,378
∑PFOS	0,909	13	0,176	0,933	6	0,603	0,889	7	0,267
PFNA	0,896	13	0,119	0,938	6	0,645	0,883	7	0,24
PFDA	0,961	13	0,764	0,9	6	0,372	0,897	7	0,316
PFUnDA	0,938	13	0,428	0,943	6	0,686	0,917	7	0,448
PFDoDA	0,982	13	0,988	0,96	6	0,817	0,927	7	0,524
PFTrDA	0,963	13	0,799	0,981	6	0,957	0,918	7	0,452
PFTeDA	0,969	13	0,878	0,916	6	0,476	0,966	7	0,867
∑PFSA	0,907	13	0,165	0,936	6	0,626	0,881	7	0,231
∑PFCA	0,957	13	0,709	0,925	6	0,54	0,946	7	0,69
LogPFHxS	0,935	13	0,397	0,916	6	0,475	0,939	7	0,632
LogPFHpS	0,96	13	0,76	0,968	6	0,879	0,873	7	0,196
LogPFOSlin	0,986	13	0,997	0,981	6	0,955	0,991	7	0,994
LogSum PFOS	0,976	13	0,955	0,977	6	0,933	0,976	7	0,935
LogPFNA	0,947	13	0,553	0,914	6	0,462	0,961	7	0,829
LogPFDA	0,965	13	0,824	0,906	6	0,411	0,967	7	0,875
LogPFUnDA	0,917	13	0,228	0,926	6	0,55	0,919	7	0,461
LogPFDoDA	0,888	13	0,091	0,966	6	0,868	0,863	7	0,161
LogPFTrDA	0,884	13	0,08	0,976	6	0,931	0,868	7	0,178
LogPFTeDA	0,911	13	0,188	0,934	6	0,611	0,906	7	0,368
Log∑PFSA	0,972	13	0,919	0,972	6	0,907	0,969	7	0,894
Log∑PFCA	0,961	13	0,771	0,922	6	0,519	0,976	7	0,941
FT4:protein	0,914	13	0,21	0,858	6	0,184	0,903	7	0,35
TT4:protein	0,874	13	0,058	0,704	6	0,007	0,946	7	0,693
FT3:protein	0,93	13	0,345	0,919	6	0,497	0,796	7	0,037
TT3:protein	0,919	13	0,241	0,958	6	0,801	0,752	7	0,013
TSH:protein	0,399	13	0	0,532	6	0	0,462	7	0
LogFT4:protein	0,97	13	0,892	0,926	6	0,552	0,969	7	0,893
LogTT4:protein	0,954	13	0,666	0,812	6	0,075	0,976	7	0,94
LogFT3:protein	0,944	13	0,516	0,847	6	0,15	0,882	7	0,236
LogTT3:protein	0,968	13	0,866	0,897	6	0,357	0,838	7	0,096
LogTSH:protein	0,736	13	0,001	0,784	6	0,042	0,71	7	0,005
Hg_plasma	0,95	13	0,605	0,971	6	0,9	0,914	7	0,422
Hg_feathers	0,946	13	0,535	0,962	6	0,838	0,956	7	0,782
Hg_liver	0,964	13	0,817	0,835	6	0,118	0,897	7	0,315
LogHg_plasma	0,965	13	0,83	0,962	6	0,838	0,918	7	0,456
LogHg_feathers	0,955	13	0,668	0,865	6	0,209	0,956	7	0,786
LogHg_liver	0,906	13	0,161	0,854	6	0,17	0,828	7	0,076
SeHg_plasma	0,855	13	0,033	0,878	6	0,26	0,81	7	0,051
SeHg_feather	0,872	13	0,056	0,819	6	0,087	0,916	7	0,441
SeHg_liver	0,912	13	0,196	0,954	6	0,773	0,781	7	0,026
LogSeHg_plasma	0,923	13	0,273	0,91	6	0,439	0,858	7	0,145
LogSeHg_feather	0,948	13	0,564	0,928	6	0,568	0,946	7	0,694
LogSeHg_liver	0,975	13	0,944	0,935	6	0,619	0,865	7	0,167

Correlations n=15		BCI	BM	Follicle count mean	PFHxS	PFHpS	PFOSlin	∑PFOS	PFNA	PFDA	PFUnDA	PFDoDA	PFTrDA	PFTeDA
BCI	Pearson Correlation	1	0,437	-0,099	0,497	-0,276	-0,225	-0,216	0,182	-0,035	-0,197	-0,317	-0,327	-0,44
	Sig. (2-tailed)		0,103	0,737	0,059	0,32	0,421	0,44	0,516	0,901	0,481	0,25	0,234	0,1
	N	15	15	14	15	15	15	15	15	15	15	15	15	15
BM	Pearson Correlation	0,437	1	-0,21	0,084	-,564*	-0,065	-0,074	-0,065	0,193	0,253	0,187	0,202	-0,14
	Sig. (2-tailed)	0,103		0,471	0,765	0,028	0,818	0,792	0,819	0,491	0,362	0,503	0,47	0,619
	N	15	15	14	15	15	15	15	15	15	15	15	15	15
Follicle count mean	Pearson Correlation	-0,099	-0,21	1	0,046	-0,042	-0,278	-0,264	0,129	-0,243	-0,254	-0,216	-0,068	-0,231
	Sig. (2-tailed)	0,737	0,471		0,876	0,886	0,335	0,362	0,659	0,403	0,38	0,458	0,817	0,428
	N	14	14	14	14	14	14	14	14	14	14	14	14	14
PFHxS	Pearson Correlation	0,497	0,084	0,046	1	0,007	-0,178	-0,154	0,116	-0,166	-0,155	-0,352	-0,403	-0,358
	Sig. (2-tailed)	0,059	0,765	0,876		0,98	0,525	0,584	0,68	0,555	0,581	0,199	0,136	0,19
	N	15	15	14	15	15	15	15	15	15	15	15	15	15
PFHpS	Pearson Correlation	-0,276	-,564*	-0,042	0,007	1	,543*	,547*	0,373	0,187	0,053	0,001	-0,047	0,39
	Sig. (2-tailed)	0,32	0,028	0,886	0,98		0,036	0,035	0,171	0,504	0,851	0,998	0,868	0,151
	N	15	15	14	15	15	15	15	15	15	15	15	15	15
PFOSlin	Pearson Correlation	-0,225	-0,065	-0,278	-0,178	,543*	1	,999**	,733**	,876**	,752**	,649**	0,459	,557*
	Sig. (2-tailed)	0,421	0,818	0,335	0,525	0,036		0	0,002	0	0,001	0,009	0,085	0,031
	N	15	15	14	15	15	15	15	15	15	15	15	15	15
∑PFOS	Pearson Correlation	-0,216	-0,074	-0,264	-0,154	,547*	,999**	1	,750**	,873**	,745**	,631*	0,435	,535*
	Sig. (2-tailed)	0,44	0,792	0,362	0,584	0,035	0		0,001	0	0,001	0,012	0,105	0,04
	N	15	15	14	15	15	15	15	15	15	15	15	15	15
PFNA	Pearson Correlation	0,182	-0,065	0,129	0,116	0,373	,733**	,750**	1	,801**	,604*	0,449	0,272	0,161
	Sig. (2-tailed)	0,516	0,819	0,659	0,68	0,171	0,002	0,001		0	0,017	0,093	0,327	0,566
	N	15	15	14	15	15	15	15	15	15	15	15	15	15
PFDA	Pearson Correlation	-0,035	0,193	-0,243	-0,166	0,187	,876**	,873**	,801**	1	,921**	,835**	,642**	0,467
	Sig. (2-tailed)	0,901	0,491	0,403	0,555	0,504	0	0	0		0	0	0,01	0,079
	N	15	15	14	15	15	15	15	15	15	15	15	15	15
PFUnDA	Pearson Correlation	-0,197	0,253	-0,254	-0,155	0,053	,752**	,745**	,604*	,921**	1	,931**	,755**	0,5
	Sig. (2-tailed)	0,481	0,362	0,38	0,581	0,851	0,001	0,001	0,017	0		0	0,001	0,058
	N	15	15	14	15	15	15	15	15	15	15	15	15	15
PFDoDA	Pearson Correlation	-0,317	0,187	-0,216	-0,352	0,001	,649**	,631*	0,449	,835**	,931**	1	,905**	,679**
	Sig. (2-tailed)	0,25	0,503	0,458	0,199	0,998	0,009	0,012	0,093	0	0		0	0,005
	N	15	15	14	15	15	15	15	15	15	15	15	15	15
PFTrDA	Pearson Correlation	-0,327	0,202	-0,068	-0,403	-0,047	0,459	0,435	0,272	,642**	,755**	,905**	1	,764**
	Sig. (2-tailed)	0,234	0,47	0,817	0,136	0,868	0,085	0,105	0,327	0,01	0,001	0		0,001
	N	15	15	14	15	15	15	15	15	15	15	15	15	15
PFTeDA	Pearson Correlation	-0,44	-0,14	-0,231	-0,358	0,39	,557*	,535*	0,161	0,467	0,5	,679**	,764**	1
	Sig. (2-tailed)	0,1	0,619	0,428	0,19	0,151	0,031	0,04	0,566	0,079	0,058	0,005	0,001	
	N	15	15	14	15	15	15	15	15	15	15	15	15	15

Table A17. Pearson (for normally distributed variables) and Spearman (for non-normal distributed variables) correlation between BM, BCI, PFAS, Hg, Se:Hg, TH:protein, TSH:protein, and follicle count in n=15 glaucous gulls (*Larus hyperboreus*) captured in Sassendalen and Adventfjorden, Svalbard, in April and May 2017.

Correlations n=15		BCI	BM	Follicle count mean	PFHxS	PFHpS	PFOSlin	∑PFOS	PFNA	PFDA	PFUnDA	PFDoDA	PFTrDA	PFTeDA
∑PFSA	Pearson Correlation	-0,207	-0,074	-0,266	-0,141	,550*	,998**	1,000**	,753**	,871**	,742**	,625*	0,427	,530*
	Sig. (2-tailed)	0,459	0,794	0,358	0,615	0,034	0	0	0,001	0	0,002	0,013	0,112	0,042
	N	15	15	14	15	15	15	15	15	15	15	15	15	15
∑PFCA	Pearson Correlation	-0,103	0,156	-0,145	-0,146	0,183	,831**	,828**	,792**	,979**	,953**	,888**	,730**	,519*
	Sig. (2-tailed)	0,716	0,578	0,62	0,605	0,515	0	0	0	0	0	0	0,002	0,048
	N	15	15	14	15	15	15	15	15	15	15	15	15	15
FT4:protein	Pearson Correlation	-0,276	-0,113	-0,352	-0,064	-0,08	0,168	0,174	-0,097	0,092	0,106	0,135	0,025	0,07
	Sig. (2-tailed)	0,32	0,688	0,217	0,821	0,776	0,549	0,535	0,73	0,745	0,707	0,632	0,928	0,805
	N	15	15	14	15	15	15	15	15	15	15	15	15	15
TT4:protein	Pearson Correlation	-0,146	-0,039	-0,39	-0,088	-0,034	0,277	0,285	0,104	0,217	0,193	0,175	0,058	0,073
	Sig. (2-tailed)	0,603	0,891	0,168	0,754	0,905	0,318	0,304	0,712	0,436	0,492	0,532	0,836	0,797
	N	15	15	14	15	15	15	15	15	15	15	15	15	15
FT3:protein	Pearson Correlation	0,158	0,382	-0,119	-0,042	-0,22	0,28	0,266	0,321	,570*	,538*	,555*	0,462	0,186
	Sig. (2-tailed)	0,573	0,16	0,686	0,881	0,43	0,313	0,339	0,244	0,027	0,039	0,032	0,083	0,506
	N	15	15	14	15	15	15	15	15	15	15	15	15	15
TT3:protein	Pearson Correlation	0,313	0,322	-0,03	-0,023	-0,112	0,406	0,398	,561*	,686**	,567*	,548*	0,415	0,15
	Sig. (2-tailed)	0,256	0,241	0,918	0,936	0,692	0,133	0,142	0,03	0,005	0,028	0,034	0,124	0,593
	N	15	15	14	15	15	15	15	15	15	15	15	15	15
TSH:protein	Spearman Correlation	-0,171	0,174	0,437	-0,139	-0,407	-,546*	-,521*	-0,182	-0,314	-0,304	-0,207	-0,329	-,639*
	Sig. (2-tailed)	0,541	0,536	0,118	0,621	0,132	0,035	0,046	0,516	0,254	0,271	0,459	0,232	0,01
	N	15	15	14	15	15	15	15	15	15	15	15	15	15
Hg_plasma	Pearson Correlation	0,27	0,112	,686**	0,212	-0,254	-0,024	0,001	0,359	0,098	-0,004	-0,066	-0,159	-0,327
	Sig. (2-tailed)	0,33	0,692	0,007	0,448	0,361	0,934	0,997	0,189	0,73	0,988	0,814	0,571	0,234
	N	15	15	14	15	15	15	15	15	15	15	15	15	15
Hg_feathers	Pearson Correlation	-0,3	0,472	0,18	-0,478	-0,478	-0,121	-0,145	-0,247	0,092	0,239	0,368	0,494	0,175
	Sig. (2-tailed)	0,277	0,076	0,537	0,071	0,071	0,668	0,606	0,374	0,746	0,391	0,177	0,062	0,533
	N	15	15	14	15	15	15	15	15	15	15	15	15	15
Hg_liver	Pearson Correlation	-0,096	0,062	-0,345	-0,147	0,231	,597*	,588*	0,383	,592*	0,506	,589*	,626*	,718**
	Sig. (2-tailed)	0,735	0,828	0,227	0,601	0,408	0,019	0,021	0,159	0,02	0,054	0,021	0,013	0,003
	N	15	15	14	15	15	15	15	15	15	15	15	15	15
SeHg_plasma	Spearman Correlation	-,532*	-0,376	0,064	-0,475	0,079	-0,143	-0,146	-,518*	-0,264	-0,229	-0,079	0,032	-0,061
	Sig. (2-tailed)	0,041	0,168	0,829	0,074	0,781	0,612	0,603	0,048	0,341	0,413	0,781	0,909	0,83
	N	15	15	14	15	15	15	15	15	15	15	15	15	15
SeHg_feather	Pearson Correlation	0,176	-0,362	0,015	0,406	0,419	0,022	0,049	0,205	-0,153	-0,25	-0,437	-,593*	-0,476
	Sig. (2-tailed)	0,531	0,184	0,958	0,134	0,12	0,937	0,863	0,464	0,586	0,37	0,103	0,02	0,073
	N	15	15	14	15	15	15	15	15	15	15	15	15	15
SeHg_liver	Pearson Correlation	0,101	0,018	0,312	0,243	0,038	-0,482	-0,465	-0,308	-,567*	-,531*	-,652**	-,637*	-,676**
	Sig. (2-tailed)	0,721	0,95	0,278	0,382	0,892	0,069	0,08	0,264	0,028	0,041	0,008	0,011	0,006
	N	15	15	14	15	15	15	15	15	15	15	15	15	15

Table A18. Pearson (for normally distributed variables) and Spearman (for non-normal distributed variables) correlation between BM, BCI, PFAS, Hg, Se:Hg, TH:protein, TSH:protein, and follicle count in n=15 glaucous gulls (*Larus hyperboreus*) captured in Sassendalen and Adventfjorden, Svalbard, in April and May 2017.

Correlations n=15		∑PFSA	∑PFCA	FT4:protein	TT4:protein	FT3:protein	TT3:protein	TSH:protein	Hg_plasma	Hg_feathers	Hg_liver	SeHg_plasma	SeHg_feather	SeHg_liver
BCI	Pearson Correlation	-0,207	-0,103	-0,276	-0,146	0,158	0,313	-0,171	0,27	-0,3	-0,096	-,532*	0,176	0,101
	Sig. (2-tailed)	0,459	0,716	0,32	0,603	0,573	0,256	0,541	0,33	0,277	0,735	0,041	0,531	0,721
	N	15	15	15	15	15	15	15	15	15	15	15	15	15
BM	Pearson Correlation	-0,074	0,156	-0,113	-0,039	0,382	0,322	0,174	0,112	0,472	0,062	-0,376	-0,362	0,018
	Sig. (2-tailed)	0,794	0,578	0,688	0,891	0,16	0,241	0,536	0,692	0,076	0,828	0,168	0,184	0,95
	N	15	15	15	15	15	15	15	15	15	15	15	15	15
Follicle count mean	Pearson Correlation	-0,266	-0,145	-0,352	-0,39	-0,119	-0,03	0,437	,686**	0,18	-0,345	0,064	0,015	0,312
	Sig. (2-tailed)	0,358	0,62	0,217	0,168	0,686	0,918	0,118	0,007	0,537	0,227	0,829	0,958	0,278
	N	14	14	14	14	14	14	14	14	14	14	14	14	14
PFHxS	Pearson Correlation	-0,141	-0,146	-0,064	-0,088	-0,042	-0,023	-0,139	0,212	-0,478	-0,147	-0,475	0,406	0,243
	Sig. (2-tailed)	0,615	0,605	0,821	0,754	0,881	0,936	0,621	0,448	0,071	0,601	0,074	0,134	0,382
	N	15	15	15	15	15	15	15	15	15	15	15	15	15
PFHpS	Pearson Correlation	,550*	0,183	-0,08	-0,034	-0,22	-0,112	-0,407	-0,254	-0,478	0,231	0,079	0,419	0,038
	Sig. (2-tailed)	0,034	0,515	0,776	0,905	0,43	0,692	0,132	0,361	0,071	0,408	0,781	0,12	0,892
	N	15	15	15	15	15	15	15	15	15	15	15	15	15
PFOSlin	Pearson Correlation	,998**	,831**	0,168	0,277	0,28	0,406	-,546*	-0,024	-0,121	,597*	-0,143	0,022	-0,482
	Sig. (2-tailed)	0	0	0,549	0,318	0,313	0,133	0,035	0,934	0,668	0,019	0,612	0,937	0,069
	N	15	15	15	15	15	15	15	15	15	15	15	15	15
∑PFOS	Pearson Correlation	1,000**	,828**	0,174	0,285	0,266	0,398	-,521*	0,001	-0,145	,588*	-0,146	0,049	-0,465
	Sig. (2-tailed)	0	0	0,535	0,304	0,339	0,142	0,046	0,997	0,606	0,021	0,603	0,863	0,08
	N	15	15	15	15	15	15	15	15	15	15	15	15	15
PFNA	Pearson Correlation	,753**	,792**	-0,097	0,104	0,321	,561*	-0,182	0,359	-0,247	0,383	-,518*	0,205	-0,308
	Sig. (2-tailed)	0,001	0	0,73	0,712	0,244	0,03	0,516	0,189	0,374	0,159	0,048	0,464	0,264
	N	15	15	15	15	15	15	15	15	15	15	15	15	15
PFDA	Pearson Correlation	,871**	,979**	0,092	0,217	,570*	,686**	-0,314	0,098	0,092	,592*	-0,264	-0,153	-,567*
	Sig. (2-tailed)	0	0	0,745	0,436	0,027	0,005	0,254	0,73	0,746	0,02	0,341	0,586	0,028
	N	15	15	15	15	15	15	15	15	15	15	15	15	15
PFUnDA	Pearson Correlation	,742**	,953**	0,106	0,193	,538*	,567*	-0,304	-0,004	0,239	0,506	-0,229	-0,25	-,531*
	Sig. (2-tailed)	0,002	0	0,707	0,492	0,039	0,028	0,271	0,988	0,391	0,054	0,413	0,37	0,041
	N	15	15	15	15	15	15	15	15	15	15	15	15	15
PFDoDA	Pearson Correlation	,625*	,888**	0,135	0,175	,555*	,548*	-0,207	-0,066	0,368	,589*	-0,079	-0,437	-,652**
	Sig. (2-tailed)	0,013	0	0,632	0,532	0,032	0,034	0,459	0,814	0,177	0,021	0,781	0,103	0,008
	N	15	15	15	15	15	15	15	15	15	15	15	15	15
PFTrDA	Pearson Correlation	0,427	,730**	0,025	0,058	0,462	0,415	-0,329	-0,159	0,494	,626*	0,032	-,593*	-,637*
	Sig. (2-tailed)	0,112	0,002	0,928	0,836	0,083	0,124	0,232	0,571	0,062	0,013	0,909	0,02	0,011
	N	15	15	15	15	15	15	15	15	15	15	15	15	15
PFTeDA	Pearson Correlation	,530*	,519*	0,07	0,073	0,186	0,15	-,639*	-0,327	0,175	,718**	-0,061	-0,476	-,676**
	Sig. (2-tailed)	0,042	0,048	0,805	0,797	0,506	0,593	0,01	0,234	0,533	0,003	0,83	0,073	0,006
	N	15	15	15	15	15	15	15	15	15	15	15	15	15

Table A19. Pearson (for normally distributed variables) and Spearman (for non-normal distributed variables) correlation between BM, BCI, PFAS, Hg, Se:Hg, TH:protein, TSH:protein, and follicle count in n=15 glaucous gulls (*Larus hyperboreus*) captured in Sassendalen and Adventfjorden, Svalbard, in April and May 2017.

Correlations n=15		∑PFSA	∑PFCA	FT4:protein	TT4:protein	FT3:protein	TT3:protein	TSH:protein	Hg_plasma	Hg_feathers	Hg_liver	SeHg_plasma	SeHg_feather	SeHg_liver
∑PFSA	Pearson Correlation	1	,826**	0,173	0,286	0,262	0,396	-,521*	0,003	-0,155	,586*	-0,179	0,057	-0,461
	Sig. (2-tailed)		0	0,537	0,301	0,345	0,144	0,046	0,991	0,58	0,022	0,524	0,84	0,083
	N	15	15	15	15	15	15	15	15	15	15	15	15	15
∑PFCA	Pearson Correlation	,826**	1	0,045	0,176	,536*	,640*	-0,379	0,097	0,129	,586*	-0,232	-0,186	-,571*
	Sig. (2-tailed)	0		0,874	0,53	0,039	0,01	0,164	0,731	0,646	0,022	0,405	0,507	0,026
	N	15	15	15	15	15	15	15	15	15	15	15	15	15
FT4:protein	Pearson Correlation	0,173	0,045	1	,868**	0,002	-0,083	-0,018	0,016	-0,35	0,199	0,079	0,341	0,033
	Sig. (2-tailed)	0,537	0,874		0	0,994	0,768	0,95	0,955	0,201	0,477	0,781	0,213	0,907
	N	15	15	15	15	15	15	15	15	15	15	15	15	15
TT4:protein	Pearson Correlation	0,286	0,176	,868**	1	-0,074	-0,099	-0,275	0,011	-0,419	0,133	0,025	0,38	0
	Sig. (2-tailed)	0,301	0,53	0		0,793	0,725	0,321	0,97	0,12	0,637	0,93	0,163	0,999
	N	15	15	15	15	15	15	15	15	15	15	15	15	15
FT3:protein	Pearson Correlation	0,262	,536*	0,002	-0,074	1	,938**	-0,093	0,203	0,368	0,172	0,268	-0,298	-0,231
	Sig. (2-tailed)	0,345	0,039	0,994	0,793		0	0,742	0,467	0,177	0,539	0,334	0,281	0,408
	N	15	15	15	15	15	15	15	15	15	15	15	15	15
TT3:protein	Pearson Correlation	0,396	,640*	-0,083	-0,099	,938**	1	0,036	0,352	0,214	0,239	-0,046	-0,189	-0,287
	Sig. (2-tailed)	0,144	0,01	0,768	0,725	0		0,899	0,199	0,443	0,391	0,869	0,499	0,3
	N	15	15	15	15	15	15	15	15	15	15	15	15	15
TSH:protein	Spearman Correlation	-,521*	-0,379	-0,018	-0,275	-0,093	0,036	1	0,393	0,118	-0,511	0,121	0,154	,564*
	Sig. (2-tailed)	0,046	0,164	0,95	0,321	0,742	0,899	.	0,147	0,676	0,052	0,666	0,585	0,028
	N	15	15	15	15	15	15	15	15	15	15	15	15	15
Hg_plasma	Pearson Correlation	0,003	0,097	0,016	0,011	0,203	0,352	0,393	1	-0,056	-0,226	-,543*	0,152	0,186
	Sig. (2-tailed)	0,991	0,731	0,955	0,97	0,467	0,199	0,147		0,842	0,418	0,037	0,588	0,506
	N	15	15	15	15	15	15	15	15	15	15	15	15	15
Hg_feathers	Pearson Correlation	-0,155	0,129	-0,35	-0,419	0,368	0,214	0,118	-0,056	1	0,032	0,275	-,838**	-0,24
	Sig. (2-tailed)	0,58	0,646	0,201	0,12	0,177	0,443	0,676	0,842		0,909	0,321	0	0,388
	N	15	15	15	15	15	15	15	15	15	15	15	15	15
Hg_liver	Pearson Correlation	,586*	,586*	0,199	0,133	0,172	0,239	-0,511	-0,226	0,032	1	-0,229	-0,345	-,739**
	Sig. (2-tailed)	0,022	0,022	0,477	0,637	0,539	0,391	0,052	0,418	0,909		0,413	0,209	0,002
	N	15	15	15	15	15	15	15	15	15	15	15	15	15
SeHg_plasma	Spearman Correlation	-0,179	-0,232	0,079	0,025	0,268	-0,046	0,121	-,543*	0,275	-0,229	1	-0,132	0,457
	Sig. (2-tailed)	0,524	0,405	0,781	0,93	0,334	0,869	0,666	0,037	0,321	0,413	.	0,639	0,087
	N	15	15	15	15	15	15	15	15	15	15	15	15	15
SeHg_feather	Pearson Correlation	0,057	-0,186	0,341	0,38	-0,298	-0,189	0,154	0,152	-,838**	-0,345	-0,132	1	,643**
	Sig. (2-tailed)	0,84	0,507	0,213	0,163	0,281	0,499	0,585	0,588	0	0,209	0,639		0,01
	N	15	15	15	15	15	15	15	15	15	15	15	15	15
SeHg_liver	Pearson Correlation	-0,461	-,571*	0,033	0	-0,231	-0,287	,564*	0,186	-0,24	-,739**	0,457	,643**	1
	Sig. (2-tailed)	0,083	0,026	0,907	0,999	0,408	0,3	0,028	0,506	0,388	0,002	0,087	0,01	

Table A20. Pearson (for normally distributed variables) and Spearman (for non-normal distributed variables) correlation between BM, BCI, PFAS, Hg, Se:Hg, TH:protein, TSH:protein, and follicle count in n=15 glaucous gulls (*Larus hyperboreus)* captured in Sassendalen and Adventfjorden, Svalbard, in April and May 2017.

Correlations Males		BCI	BM	Follicle_count	PFHxS	PFHpS	PFOSlin	∑PFOS	PFNA	PFDA	PFUnDA	PFDoDA	PFTrDA	PFTeDA
BCI	Pearson Correlation	1	,900**	-,768*	0,377	-0,437	-0,558	-0,554	-0,464	-0,38	-0,362	-0,279	-0,159	-0,134
	Sig. (2-tailed)		0,006	0,044	0,404	0,327	0,193	0,197	0,294	0,401	0,425	0,544	0,734	0,775
	N	7	7	7	7	7	7	7	7	7	7	7	7	7
BM	Pearson Correlation	,900**	1	-0,727	0,173	-0,458	-0,613	-0,608	-0,649	-0,587	-0,625	-0,61	-0,454	-0,453
	Sig. (2-tailed)	0,006		0,064	0,71	0,302	0,143	0,148	0,115	0,166	0,133	0,145	0,306	0,308
	N	7	7	7	7	7	7	7	7	7	7	7	7	7
Follicle_count	Pearson Correlation	-,768*	-0,727	1	-0,623	-0,096	0,079	0,083	0,451	0,274	0,293	0,361	0,281	-0,087
	Sig. (2-tailed)	0,044	0,064		0,135	0,838	0,866	0,859	0,31	0,552	0,523	0,426	0,541	0,854
	N	7	7	7	7	7	7	7	7	7	7	7	7	7
PFHxS	Pearson Correlation	0,377	0,173	-0,623	1	-0,019	0,082	0,079	-0,001	0,109	0,25	0,163	0,24	0,407
	Sig. (2-tailed)	0,404	0,71	0,135		0,967	0,861	0,867	0,999	0,816	0,588	0,727	0,604	0,364
	N	7	7	7	7	7	7	7	7	7	7	7	7	7
PFHpS	Pearson Correlation	-0,437	-0,458	-0,096	-0,019	1	,849*	,830*	0,241	0,426	0,306	0,214	0,087	0,579
	Sig. (2-tailed)	0,327	0,302	0,838	0,967		0,016	0,021	0,603	0,34	0,505	0,645	0,853	0,174
	N	7	7	7	7	7	7	7	7	7	7	7	7	7
PFOSlin	Pearson Correlation	-0,558	-0,613	0,079	0,082	,849*	1	,999**	0,669	,768*	0,676	0,494	0,384	0,734
	Sig. (2-tailed)	0,193	0,143	0,866	0,861	0,016		0	0,1	0,044	0,096	0,26	0,395	0,061
	N	7	7	7	7	7	7	7	7	7	7	7	7	7
∑PFOS	Pearson Correlation	-0,554	-0,608	0,083	0,079	,830*	,999**	1	0,688	,773*	0,682	0,493	0,38	0,726
	Sig. (2-tailed)	0,197	0,148	0,859	0,867	0,021	0		0,087	0,041	0,092	0,261	0,401	0,065
	N	7	7	7	7	7	7	7	7	7	7	7	7	7
PFNA	Pearson Correlation	-0,464	-0,649	0,451	-0,001	0,241	0,669	0,688	1	,932**	,929**	,837*	0,751	0,69
	Sig. (2-tailed)	0,294	0,115	0,31	0,999	0,603	0,1	0,087		0,002	0,002	0,019	0,052	0,086
	N	7	7	7	7	7	7	7	7	7	7	7	7	7
PFDA	Pearson Correlation	-0,38	-0,587	0,274	0,109	0,426	,768*	,773*	,932**	1	,969**	,890**	,852*	,861*
	Sig. (2-tailed)	0,401	0,166	0,552	0,816	0,34	0,044	0,041	0,002		0	0,007	0,015	0,013
	N	7	7	7	7	7	7	7	7	7	7	7	7	7
PFUnDA	Pearson Correlation	-0,362	-0,625	0,293	0,25	0,306	0,676	0,682	,929**	,969**	1	,943**	,905**	,864*
	Sig. (2-tailed)	0,425	0,133	0,523	0,588	0,505	0,096	0,092	0,002	0		0,001	0,005	0,012
	N	7	7	7	7	7	7	7	7	7	7	7	7	7
PFDoDA	Pearson Correlation	-0,279	-0,61	0,361	0,163	0,214	0,494	0,493	,837*	,890**	,943**	1	,956**	,842*
	Sig. (2-tailed)	0,544	0,145	0,426	0,727	0,645	0,26	0,261	0,019	0,007	0,001		0,001	0,017
	N	7	7	7	7	7	7	7	7	7	7	7	7	7
PFTrDA	Pearson Correlation	-0,159	-0,454	0,281	0,24	0,087	0,384	0,38	0,751	,852*	,905**	,956**	1	,786*
	Sig. (2-tailed)	0,734	0,306	0,541	0,604	0,853	0,395	0,401	0,052	0,015	0,005	0,001		0,036
	N	7	7	7	7	7	7	7	7	7	7	7	7	7
PFTeDA	Pearson Correlation	-0,134	-0,453	-0,087	0,407	0,579	0,734	0,726	0,69	,861*	,864*	,842*	,786*	1
	Sig. (2-tailed)	0,775	0,308	0,854	0,364	0,174	0,061	0,065	0,086	0,013	0,012	0,017	0,036	
	N	7	7	7	7	7	7	7	7	7	7	7	7	7

Table A21. Pearson (for normally distributed variables) and Spearman (for non-normal distributed variables) correlation between BM, BCI, PFAS, Hg, Se:Hg, TH:protein, TSH:protein, and follicle count in male glaucous gulls (*Larus hyperboreus*) (n=7) captured in Sassendalen and Adventfjorden, Svalbard, in April and May 2017.

Correlations Males		BCI	BM	Follicle_count	PFHxS	PFHpS	PFOSlin	∑PFOS	PFNA	PFDA	PFUnDA	PFDoDA	PFTrDA	PFTeDA
∑PFSA	Pearson Correlation	-0,545	-0,6	0,069	0,094	,829*	,999**	1,000**	0,684	,770*	0,68	0,489	0,376	0,728
	Sig. (2-tailed)	0,206	0,154	0,883	0,842	0,021	0	0	0,09	0,043	0,093	0,265	0,406	0,064
	N	7	7	7	7	7	7	7	7	7	7	7	7	7
∑PFCA	Pearson Correlation	-0,37	-0,621	0,332	0,168	0,299	0,673	0,68	,949**	,981**	,995**	,943**	,901**	,845*
	Sig. (2-tailed)	0,414	0,136	0,466	0,719	0,514	0,097	0,092	0,001	0	0	0,001	0,006	0,017
	N	7	7	7	7	7	7	7	7	7	7	7	7	7
FT4:protein	Pearson Correlation	0,434	0,492	-,802*	0,336	0,309	0,189	0,201	-0,269	-0,229	-0,305	-0,474	-0,53	-0,002
	Sig. (2-tailed)	0,33	0,262	0,03	0,462	0,5	0,684	0,666	0,56	0,621	0,505	0,283	0,221	0,997
	N	7	7	7	7	7	7	7	7	7	7	7	7	7
TT4:protein	Spearman correlation	0,071	0,18	-0,5	0,536	0,036	0,357	0,357	0,036	0	-0,036	-0,357	-0,393	0,036
	Sig. (2-tailed)	0,879	0,699	0,253	0,215	0,939	0,432	0,432	0,939	1	0,939	0,432	0,383	0,939
	N	7	7	7	7	7	7	7	7	7	7	7	7	7
FT3:protein	Pearson Correlation	0,227	0,116	0,126	0,078	-0,353	-0,265	-0,281	0,094	0,256	0,289	0,435	0,651	0,197
	Sig. (2-tailed)	0,624	0,804	0,787	0,868	0,438	0,566	0,542	0,841	0,58	0,529	0,329	0,113	0,672
	N	7	7	7	7	7	7	7	7	7	7	7	7	7
TT3:protein	Pearson Correlation	0,183	0,015	0,197	-0,043	-0,233	-0,147	-0,161	0,239	0,397	0,405	0,58	0,741	0,335
	Sig. (2-tailed)	0,694	0,975	0,671	0,927	0,616	0,754	0,73	0,606	0,377	0,367	0,173	0,057	0,462
	N	7	7	7	7	7	7	7	7	7	7	7	7	7
TSH:protein	Spearman correlation	-0,464	-0,126	0,679	-,857*	-0,25	-0,607	-0,607	-0,25	-0,286	-0,429	-0,214	-0,214	-0,571
	Sig. (2-tailed)	0,294	0,788	0,094	0,014	0,589	0,148	0,148	0,589	0,535	0,337	0,645	0,645	0,18
	N	7	7	7	7	7	7	7	7	7	7	7	7	7
Hg_plasma	Pearson Correlation	-0,449	-0,564	0,681	-0,51	-0,01	0,217	0,242	0,646	0,396	0,396	0,439	0,228	0,137
	Sig. (2-tailed)	0,312	0,188	0,092	0,242	0,984	0,641	0,601	0,117	0,379	0,379	0,325	0,623	0,77
	N	7	7	7	7	7	7	7	7	7	7	7	7	7
Hg_feathers	Pearson Correlation	-0,57	-0,451	,831*	-0,526	-0,215	-0,127	-0,138	0,16	0,122	0,129	0,22	0,299	-0,202
	Sig. (2-tailed)	0,181	0,31	0,021	0,225	0,643	0,786	0,767	0,732	0,795	0,783	0,635	0,515	0,664
	N	7	7	7	7	7	7	7	7	7	7	7	7	7
Hg_liver	Pearson Correlation	0,03	-0,175	-0,329	0,32	0,69	,757*	0,747	0,51	0,753	0,666	0,596	0,585	,901**
	Sig. (2-tailed)	0,949	0,708	0,471	0,484	0,086	0,049	0,054	0,242	0,051	0,102	0,157	0,168	0,006
	N	7	7	7	7	7	7	7	7	7	7	7	7	7
SeHg_plasma	Pearson Correlation	0,039	0,294	0,118	-0,418	-0,197	-0,489	-0,516	-0,641	-0,52	-0,582	-0,464	-0,295	-0,566
	Sig. (2-tailed)	0,934	0,523	0,801	0,351	0,672	0,266	0,236	0,12	0,232	0,17	0,294	0,521	0,186
	N	7	7	7	7	7	7	7	7	7	7	7	7	7
SeHg_feather	Pearson Correlation	0,49	0,603	-0,686	0,085	0,09	-0,139	-0,127	-0,519	-0,553	-0,621	-0,706	-,781*	-0,345
	Sig. (2-tailed)	0,265	0,151	0,089	0,857	0,847	0,766	0,786	0,232	0,198	0,136	0,076	0,038	0,449
	N	7	7	7	7	7	7	7	7	7	7	7	7	7
SeHg_liver	Pearson Correlation	0,295	0,629	-0,141	-0,457	-0,39	-0,631	-0,625	-0,75	-,846*	-,925**	-,916**	-,863*	-,925**
	Sig. (2-tailed)	0,521	0,131	0,762	0,302	0,387	0,129	0,134	0,052	0,016	0,003	0,004	0,012	0,003
	N	7	7	7	7	7	7	7	7	7	7	7	7	7

Table A22. Pearson (for normally distributed variables) and Spearman (for non-normal distributed variables) correlation between BM, BCI, PFAS, Hg, Se:Hg, TH:protein, TSH:protein, and follicle count in male glaucous gulls (*Larus hyperboreus*) (n=7) captured in Sassendalen and Adventfjorden, Svalbard, in April and May 2017.

Correlations Males		∑PFSA	∑PFCA	FT4:protein	TT4:protein	FT3:protein	TT3:protein	TSH:protein	Hg_plasma	Hg_feathers	Hg_liver	SeHg_plasma	SeHg_feather	SeHg_liver
BCI	Pearson Correlation	-0,545	-0,37	0,434	0,071	0,227	0,183	-0,464	-0,449	-0,57	0,03	0,039	0,49	0,295
	Sig. (2-tailed)	0,206	0,414	0,33	0,879	0,624	0,694	0,294	0,312	0,181	0,949	0,934	0,265	0,521
	N	7	7	7	7	7	7	7	7	7	7	7	7	7
BM	Pearson Correlation	-0,6	-0,621	0,492	0,18	0,116	0,015	-0,126	-0,564	-0,451	-0,175	0,294	0,603	0,629
	Sig. (2-tailed)	0,154	0,136	0,262	0,699	0,804	0,975	0,788	0,188	0,31	0,708	0,523	0,151	0,131
	N	7	7	7	7	7	7	7	7	7	7	7	7	7
Follicle_count	Pearson Correlation	0,069	0,332	-,802*	-0,5	0,126	0,197	0,679	0,681	,831*	-0,329	0,118	-0,686	-0,141
	Sig. (2-tailed)	0,883	0,466	0,03	0,253	0,787	0,671	0,094	0,092	0,021	0,471	0,801	0,089	0,762
	N	7	7	7	7	7	7	7	7	7	7	7	7	7
PFHxS	Pearson Correlation	0,094	0,168	0,336	0,536	0,078	-0,043	-,857*	-0,51	-0,526	0,32	-0,418	0,085	-0,457
	Sig. (2-tailed)	0,842	0,719	0,462	0,215	0,868	0,927	0,014	0,242	0,225	0,484	0,351	0,857	0,302
	N	7	7	7	7	7	7	7	7	7	7	7	7	7
PFHpS	Pearson Correlation	,829*	0,299	0,309	0,036	-0,353	-0,233	-0,25	-0,01	-0,215	0,69	-0,197	0,09	-0,39
	Sig. (2-tailed)	0,021	0,514	0,5	0,939	0,438	0,616	0,589	0,984	0,643	0,086	0,672	0,847	0,387
	N	7	7	7	7	7	7	7	7	7	7	7	7	7
PFOSlin	Pearson Correlation	,999**	0,673	0,189	0,357	-0,265	-0,147	-0,607	0,217	-0,127	,757*	-0,489	-0,139	-0,631
	Sig. (2-tailed)	0	0,097	0,684	0,432	0,566	0,754	0,148	0,641	0,786	0,049	0,266	0,766	0,129
	N	7	7	7	7	7	7	7	7	7	7	7	7	7
∑PFOS	Pearson Correlation	1,000**	0,68	0,201	0,357	-0,281	-0,161	-0,607	0,242	-0,138	0,747	-0,516	-0,127	-0,625
	Sig. (2-tailed)	0	0,092	0,666	0,432	0,542	0,73	0,148	0,601	0,767	0,054	0,236	0,786	0,134
	N	7	7	7	7	7	7	7	7	7	7	7	7	7
PFNA	Pearson Correlation	0,684	,949**	-0,269	0,036	0,094	0,239	-0,25	0,646	0,16	0,51	-0,641	-0,519	-0,75
	Sig. (2-tailed)	0,09	0,001	0,56	0,939	0,841	0,606	0,589	0,117	0,732	0,242	0,12	0,232	0,052
	N	7	7	7	7	7	7	7	7	7	7	7	7	7
PFDA	Pearson Correlation	,770*	,981**	-0,229	0	0,256	0,397	-0,286	0,396	0,122	0,753	-0,52	-0,553	-,846*
	Sig. (2-tailed)	0,043	0	0,621	1	0,58	0,377	0,535	0,379	0,795	0,051	0,232	0,198	0,016
	N	7	7	7	7	7	7	7	7	7	7	7	7	7
PFUnDA	Pearson Correlation	0,68	,995**	-0,305	-0,036	0,289	0,405	-0,429	0,396	0,129	0,666	-0,582	-0,621	-,925**
	Sig. (2-tailed)	0,093	0	0,505	0,939	0,529	0,367	0,337	0,379	0,783	0,102	0,17	0,136	0,003
	N	7	7	7	7	7	7	7	7	7	7	7	7	7
PFDoDA	Pearson Correlation	0,489	,943**	-0,474	-0,357	0,435	0,58	-0,214	0,439	0,22	0,596	-0,464	-0,706	-,916**
	Sig. (2-tailed)	0,265	0,001	0,283	0,432	0,329	0,173	0,645	0,325	0,635	0,157	0,294	0,076	0,004
	N	7	7	7	7	7	7	7	7	7	7	7	7	7
PFTrDA	Pearson Correlation	0,376	,901**	-0,53	-0,393	0,651	0,741	-0,214	0,228	0,299	0,585	-0,295	-,781*	-,863*
	Sig. (2-tailed)	0,406	0,006	0,221	0,383	0,113	0,057	0,645	0,623	0,515	0,168	0,521	0,038	0,012
	N	7	7	7	7	7	7	7	7	7	7	7	7	7
PFTeDA	Pearson Correlation	0,728	,845*	-0,002	0,036	0,197	0,335	-0,571	0,137	-0,202	,901**	-0,566	-0,345	-,925**
	Sig. (2-tailed)	0,064	0,017	0,997	0,939	0,672	0,462	0,18	0,77	0,664	0,006	0,186	0,449	0,003
	N	7	7	7	7	7	7	7	7	7	7	7	7	7

Table A23. Pearson (for normally distributed variables) and Spearman (for non-normal distributed variables) correlation between BM, BCI, PFAS, Hg, Se:Hg, TH:protein, TSH:protein, and follicle count in male glaucous gulls (*Larus hyperboreus)* (n=7) captured in Sassendalen and Adventfjorden, Svalbard, in April and May 2017.

Correlations Males														
		∑PFSA	∑PFCA	FT4:protein	TT4:protein	FT3:protein	TT3:protein	TSH:protein	Hg_plasma	Hg_feathers	Hg_liver	SeHg_plasma	SeHg_feather	SeHg_liver
∑PFSA	Pearson Correlation	1	0,678	0,214	0,357	-0,287	-0,169	-0,607	0,235	-0,153	0,75	-0,525	-0,117	-0,626
	Sig. (2-tailed)		0,094	0,645	0,432	0,533	0,717	0,148	0,613	0,743	0,052	0,227	0,803	0,132
	N	7	7	7	7	7	7	7	7	7	7	7	7	7
∑PFCA	Pearson Correlation	0,678	1	-0,322	-0,036	0,294	0,425	-0,429	0,449	0,157	0,661	-0,565	-0,623	-,893**
	Sig. (2-tailed)	0,094		0,482	0,939	0,522	0,341	0,337	0,313	0,737	0,106	0,186	0,135	0,007
	N	7	7	7	7	7	7	7	7	7	7	7	7	7
FT4:protein	Pearson Correlation	0,214	-0,322	1	0,679	-0,647	-0,653	-0,679	-0,292	-,914**	0,257	-0,37	,909**	0,25
	Sig. (2-tailed)	0,645	0,482		0,094	0,116	0,112	0,094	0,525	0,004	0,578	0,414	0,005	0,589
	N	7	7	7	7	7	7	7	7	7	7	7	7	7
TT4:protein	Spearman correlation	0,357	-0,036	0,679	1	-0,536	-0,536	-0,607	-0,071	-0,464	0,286	-0,429	0,357	0,107
	Sig. (2-tailed)	0,432	0,939	0,094	.	0,215	0,215	0,148	0,879	0,294	0,535	0,337	0,432	0,819
	N	7	7	7	7	7	7	7	7	7	7	7	7	7
FT3:protein	Pearson Correlation	-0,287	0,294	-0,647	-0,536	1	,961**	-0,107	-0,264	0,523	0,153	0,433	-0,698	-0,254
	Sig. (2-tailed)	0,533	0,522	0,116	0,215		0,001	0,819	0,567	0,228	0,744	0,332	0,081	0,582
	N	7	7	7	7	7	7	7	7	7	7	7	7	7
TT3:protein	Pearson Correlation	-0,169	0,425	-0,653	-0,536	,961**	1	-0,107	-0,067	0,495	0,282	0,32	-0,707	-0,349
	Sig. (2-tailed)	0,717	0,341	0,112	0,215	0,001		0,819	0,887	0,259	0,54	0,483	0,075	0,442
	N	7	7	7	7	7	7	7	7	7	7	7	7	7
TSH:protein	Spearman correlation	-0,607	-0,429	-0,679	-0,607	-0,107	-0,107	1	0,357	0,643	-0,714	0,536	-0,071	0,429
	Sig. (2-tailed)	0,148	0,337	0,094	0,148	0,819	0,819	.	0,432	0,119	0,071	0,215	0,879	0,337
	N	7	7	7	7	7	7	7	7	7	7	7	7	7
Hg_plasma	Pearson Correlation	0,235	0,449	-0,292	-0,071	-0,264	-0,067	0,357	1	0,199	-0,077	-0,489	-0,211	-0,224
	Sig. (2-tailed)	0,613	0,313	0,525	0,879	0,567	0,887	0,432		0,669	0,87	0,266	0,65	0,63
	N	7	7	7	7	7	7	7	7	7	7	7	7	7
Hg_feathers	Pearson Correlation	-0,153	0,157	-,914**	-0,464	0,523	0,495	0,643	0,199	1	-0,34	0,566	-,807*	-0,005
	Sig. (2-tailed)	0,743	0,737	0,004	0,294	0,228	0,259	0,119	0,669		0,455	0,185	0,028	0,991
	N	7	7	7	7	7	7	7	7	7	7	7	7	7
Hg_liver	Pearson Correlation	0,75	0,661	0,257	0,286	0,153	0,282	-0,714	-0,077	-0,34	1	-0,401	-0,094	-0,683
	Sig. (2-tailed)	0,052	0,106	0,578	0,535	0,744	0,54	0,071	0,87	0,455		0,372	0,842	0,091
	N	7	7	7	7	7	7	7	7	7	7	7	7	7
SeHg_plasma	Pearson Correlation	-0,525	-0,565	-0,37	-0,429	0,433	0,32	0,536	-0,489	0,566	-0,401	1	-0,163	0,574
	Sig. (2-tailed)	0,227	0,186	0,414	0,337	0,332	0,483	0,215	0,266	0,185	0,372		0,727	0,177
	N	7	7	7	7	7	7	7	7	7	7	7	7	7
SeHg_feather	Pearson Correlation	-0,117	-0,623	,909**	0,357	-0,698	-0,707	-0,071	-0,211	-,807*	-0,094	-0,163	1	0,564
	Sig. (2-tailed)	0,803	0,135	0,005	0,432	0,081	0,075	0,879	0,65	0,028	0,842	0,727		0,187
	N	7	7	7	7	7	7	7	7	7	7	7	7	7
SeHg_liver	Pearson Correlation	-0,626	-,893**	0,25	0,107	-0,254	-0,349	0,429	-0,224	-0,005	-0,683	0,574	0,564	1
	Sig. (2-tailed)	0,132	0,007	0,589	0,819	0,582	0,442	0,337	0,63	0,991	0,091	0,177	0,187	
	N	7	7	7	7	7	7	7	7	7	7	7	7	7

Table A24. Pearson (for normally distributed variables) and Spearman (for non-normal distributed variables) correlation between BM, BCI, PFAS, Hg, Se:Hg, TH:protein, TSH:protein, and follicle count in male glaucous gulls (*Larus hyperboreus*) (n=7) captured in Sassendalen and Adventfjorden, Svalbard, in April and May 2017.

Correlations Females		BCI	BM	Follicle_count	PFHxS	PFHpS	PFOSlin	∑PFOS	PFNA	PFDA	PFUnDA	PFDoDA	PFTrDA	PFTeDA
BCI	Pearson Correlation	1	,896**	0,271	0,592	-0,287	-0,037	-0,019	0,455	0,117	-0,124	-0,382	-0,458	-0,591
	Sig. (2-tailed)		0,003	0,557	0,122	0,491	0,931	0,965	0,257	0,783	0,77	0,35	0,254	0,123
	N	8	8	7	8	8	8	8	8	8	8	8	8	8
BM	Pearson Correlation	,896**	1	0,251	0,442	-0,045	0,237	0,251	0,588	0,327	0,071	-0,147	-0,232	-0,289
	Sig. (2-tailed)	0,003		0,588	0,273	0,915	0,572	0,549	0,125	0,429	0,867	0,728	0,581	0,488
	N	8	8	7	8	8	8	8	8	8	8	8	8	8
Follicle_count	Pearson Correlation	0,271	0,251	1	0,474	-0,197	-0,477	-0,467	-0,029	-0,416	-0,494	-0,462	-0,127	-0,288
	Sig. (2-tailed)	0,557	0,588		0,283	0,672	0,279	0,29	0,951	0,353	0,259	0,297	0,786	0,531
	N	7	7	7	7	7	7	7	7	7	7	7	7	7
PFHxS	Pearson Correlation	0,592	0,442	0,474	1	-0,067	-0,37	-0,333	0,161	-0,305	-0,433	-,739*	-,832*	-,832*
	Sig. (2-tailed)	0,122	0,273	0,283		0,874	0,367	0,42	0,703	0,463	0,284	0,036	0,01	0,01
	N	8	8	7	8	8	8	8	8	8	8	8	8	8
PFHpS	Pearson Correlation	-0,287	-0,045	-0,197	-0,067	1	0,544	0,545	0,361	0,353	0,399	0,323	0,287	0,459
	Sig. (2-tailed)	0,491	0,915	0,672	0,874		0,164	0,162	0,379	0,391	0,328	0,435	0,49	0,253
	N	8	8	7	8	8	8	8	8	8	8	8	8	8
PFOSlin	Pearson Correlation	-0,037	0,237	-0,477	-0,37	0,544	1	,999**	,781*	,967**	,929**	,849**	0,577	0,476
	Sig. (2-tailed)	0,931	0,572	0,279	0,367	0,164		0	0,022	0	0,001	0,008	0,134	0,233
	N	8	8	7	8	8	8	8	8	8	8	8	8	8
∑PFOS	Pearson Correlation	-0,019	0,251	-0,467	-0,333	0,545	,999**	1	,799*	,969**	,926**	,833*	0,55	0,446
	Sig. (2-tailed)	0,965	0,549	0,29	0,42	0,162	0		0,017	0	0,001	0,01	0,158	0,268
	N	8	8	7	8	8	8	8	8	8	8	8	8	8
PFNA	Pearson Correlation	0,455	0,588	-0,029	0,161	0,361	,781*	,799*	1	,854**	0,693	0,472	0,245	-0,012
	Sig. (2-tailed)	0,257	0,125	0,951	0,703	0,379	0,022	0,017		0,007	0,057	0,237	0,559	0,978
	N	8	8	7	8	8	8	8	8	8	8	8	8	8
PFDA	Pearson Correlation	0,117	0,327	-0,416	-0,305	0,353	,967**	,969**	,854**	1	,935**	,826*	0,534	0,323
	Sig. (2-tailed)	0,783	0,429	0,353	0,463	0,391	0	0	0,007		0,001	0,011	0,173	0,435
	N	8	8	7	8	8	8	8	8	8	8	8	8	8
PFUnDA	Pearson Correlation	-0,124	0,071	-0,494	-0,433	0,399	,929**	,926**	0,693	,935**	1	,903**	0,604	0,361
	Sig. (2-tailed)	0,77	0,867	0,259	0,284	0,328	0,001	0,001	0,057	0,001		0,002	0,113	0,38
	N	8	8	7	8	8	8	8	8	8	8	8	8	8
PFDoDA	Pearson Correlation	-0,382	-0,147	-0,462	-,739*	0,323	,849**	,833*	0,472	,826*	,903**	1	,855**	0,668
	Sig. (2-tailed)	0,35	0,728	0,297	0,036	0,435	0,008	0,01	0,237	0,011	0,002		0,007	0,07
	N	8	8	7	8	8	8	8	8	8	8	8	8	8
PFTrDA	Pearson Correlation	-0,458	-0,232	-0,127	-,832*	0,287	0,577	0,55	0,245	0,534	0,604	,855**	1	,832*
	Sig. (2-tailed)	0,254	0,581	0,786	0,01	0,49	0,134	0,158	0,559	0,173	0,113	0,007		0,01
	N	8	8	7	8	8	8	8	8	8	8	8	8	8
PFTeDA	Pearson Correlation	-0,591	-0,289	-0,288	-,832*	0,459	0,476	0,446	-0,012	0,323	0,361	0,668	,832*	1
	Sig. (2-tailed)	0,123	0,488	0,531	0,01	0,253	0,233	0,268	0,978	0,435	0,38	0,07	0,01	
	N	8	8	7	8	8	8	8	8	8	8	8	8	8

Table A25. Pearson (for normally distributed variables) and Spearman (for non-normal distributed variables) correlation between BM, BCI, PFAS, Hg, Se:Hg, TH:protein, TSH:protein, and follicle count in female glaucous gulls (*Larus hyperboreus*) (n=8) captured in Sassendalen and Adventfjorden, Svalbard, in April and May 2017.

Correlations Females		BCI	BM	Follicle_count	PFHxS	PFHpS	PFOSlin	∑PFOS	PFNA	PFDA	PFUnDA	PFDoDA	PFTrDA	PFTeDA
∑PFSA	Pearson Correlation	-0,01	0,26	-0,464	-0,323	0,547	,999**	1,000**	,804*	,969**	,924**	,826*	0,542	0,438
	Sig. (2-tailed)	0,982	0,535	0,295	0,435	0,16	0	0	0,016	0	0,001	0,011	0,166	0,278
	N	8	8	7	8	8	8	8	8	8	8	8	8	8
∑PFCA	Pearson Correlation	0,043	0,258	-0,341	-0,343	0,417	,961**	,961**	,848**	,985**	,952**	,862**	0,625	0,373
	Sig. (2-tailed)	0,92	0,537	0,454	0,406	0,304	0	0	0,008	0	0	0,006	0,098	0,362
	N	8	8	7	8	8	8	8	8	8	8	8	8	8
Protein	Pearson Correlation	-0,081	0,191	0,354	-0,044	0,088	-0,235	-0,249	-0,414	-0,37	-0,386	-0,246	-0,039	0,299
	Sig. (2-tailed)	0,85	0,65	0,436	0,917	0,836	0,575	0,552	0,308	0,368	0,345	0,557	0,927	0,471
	N	8	8	7	8	8	8	8	8	8	8	8	8	8
FT4:protein	Pearson Correlation	-0,575	-0,562	-0,194	-0,277	-0,238	0,162	0,166	-0,048	0,199	0,311	0,426	0,241	0,095
	Sig. (2-tailed)	0,136	0,147	0,676	0,507	0,571	0,701	0,695	0,911	0,636	0,454	0,292	0,566	0,822
	N	8	8	7	8	8	8	8	8	8	8	8	8	8
TT4:protein	Pearson Correlation	-0,511	-0,414	-0,307	-0,43	-0,031	0,513	0,513	0,261	0,548	0,648	,730*	0,499	0,272
	Sig. (2-tailed)	0,196	0,307	0,504	0,287	0,942	0,194	0,193	0,532	0,159	0,082	0,04	0,208	0,515
	N	8	8	7	8	8	8	8	8	8	8	8	8	8
FT3:protein	Spearman Correlatio	-0,238	-0,096	-0,429	0,095	0,214	0,476	0,476	0,214	0,31	0,571	0,69	0,071	0,238
	Sig. (2-tailed)	0,57	0,821	0,337	0,823	0,61	0,233	0,233	0,61	0,456	0,139	0,058	0,867	0,57
	N	8	8	7	8	8	8	8	8	8	8	8	8	8
TT3:protein	Spearman Correlatio	0,524	0,635	0,107	0,333	-0,143	0,286	0,286	,714*	0,357	0,476	0,333	-0,214	-0,357
	Sig. (2-tailed)	0,183	0,091	0,819	0,42	0,736	0,493	0,493	0,047	0,385	0,233	0,42	0,61	0,385
	N	8	8	7	8	8	8	8	8	8	8	8	8	8
TSH:protein	Spearman Correlatio	-0,048	-0,192	0,25	0,405	-0,357	-0,429	-0,429	-0,048	-0,452	-0,333	-0,405	-0,619	-,714*
	Sig. (2-tailed)	0,911	0,649	0,589	0,32	0,385	0,289	0,289	0,911	0,26	0,42	0,32	0,102	0,047
	N	8	8	7	8	8	8	8	8	8	8	8	8	8
Hg_plasma	Pearson Correlation	0,535	0,601	0,693	0,551	-0,418	-0,111	-0,089	0,288	0,023	-0,148	-0,257	-0,294	-0,472
	Sig. (2-tailed)	0,172	0,115	0,085	0,157	0,303	0,794	0,834	0,49	0,957	0,727	0,539	0,48	0,238
	N	8	8	7	8	8	8	8	8	8	8	8	8	8
Hg_feathers	Pearson Correlation	-0,259	-0,129	-0,026	-0,671	-0,165	-0,169	-0,205	-0,497	-0,243	-0,252	0,111	0,447	0,664
	Sig. (2-tailed)	0,535	0,761	0,955	0,069	0,697	0,69	0,627	0,21	0,562	0,547	0,794	0,266	0,073
	N	8	8	7	8	8	8	8	8	8	8	8	8	8
Hg_liver	Pearson Correlation	-0,182	-0,098	-0,315	-0,524	0,216	0,512	0,502	0,394	0,507	0,37	0,578	0,66	0,632
	Sig. (2-tailed)	0,666	0,817	0,492	0,183	0,607	0,195	0,205	0,334	0,199	0,368	0,134	0,075	0,093
	N	8	8	7	8	8	8	8	8	8	8	8	8	8
SeHg_plasma	Pearson Correlation	-,891**	-,795*	-0,41	-0,447	0,481	0,111	0,097	-0,378	-0,066	0,238	0,337	0,301	0,433
	Sig. (2-tailed)	0,003	0,018	0,36	0,266	0,228	0,793	0,82	0,356	0,877	0,571	0,414	0,469	0,284
	N	8	8	7	8	8	8	8	8	8	8	8	8	8
SeHg_feather	Pearson Correlation	0,079	-0,005	0,158	0,627	0,224	0,075	0,106	0,339	0,111	0,208	-0,12	-0,386	-0,606
	Sig. (2-tailed)	0,852	0,991	0,735	0,096	0,594	0,861	0,803	0,412	0,793	0,621	0,777	0,345	0,112
	N	8	8	7	8	8	8	8	8	8	8	8	8	8
SeHg_liver	Spearman Correlatio	-0,214	-0,347	0,214	0,167	0,262	-0,357	-0,357	-0,381	-0,595	-0,381	-0,167	-0,405	-0,19
	Sig. (2-tailed)	0,61	0,399	0,645	0,693	0,531	0,385	0,385	0,352	0,12	0,352	0,693	0,32	0,651
	N	8	8	7	8	8	8	8	8	8	8	8	8	8

Table 26. Pearson (for normally distributed variables) and Spearman (for non-normal distributed variables) correlation between BM, BCI, PFAS, Hg, Se:Hg, TH:protein, TSH:protein, and follicle count in female glaucous gulls (*Larus hyperboreus*) (n=8) captured in Sassendalen and Adventfjorden, Svalbard, in April and May 2017.

Correlations Females		∑PFSA	∑PFCA	Protein	FT4:protein	TT4:protein	FT3:protein	TT3:protein	TSH:protein	Hg_plasma	Hg_feathers	Hg_liver	SeHg_plasma	SeHg_feather	SeHg_liver
BCI	Pearson Correlation	-0,01	0,043	-0,081	-0,575	-0,511	-0,238	0,524	-0,048	0,535	-0,259	-0,182	-,891**	0,079	-0,214
	Sig. (2-tailed)	0,982	0,92	0,85	0,136	0,196	0,57	0,183	0,911	0,172	0,535	0,666	0,003	0,852	0,61
	N	8	8	8	8	8	8	8	8	8	8	8	8	8	8
BM	Pearson Correlation	0,26	0,258	0,191	-0,562	-0,414	-0,096	0,635	-0,192	0,601	-0,129	-0,098	-,795*	-0,005	-0,347
	Sig. (2-tailed)	0,535	0,537	0,65	0,147	0,307	0,821	0,091	0,649	0,115	0,761	0,817	0,018	0,991	0,399
	N	8	8	8	8	8	8	8	8	8	8	8	8	8	8
Follicle_count	Pearson Correlation	-0,464	-0,341	0,354	-0,194	-0,307	-0,429	0,107	0,25	0,693	-0,026	-0,315	-0,41	0,158	0,214
	Sig. (2-tailed)	0,295	0,454	0,436	0,676	0,504	0,337	0,819	0,589	0,085	0,955	0,492	0,36	0,735	0,645
	N	7	7	7	7	7	7	7	7	7	7	7	7	7	7
PFHxS	Pearson Correlation	-0,323	-0,343	-0,044	-0,277	-0,43	0,095	0,333	0,405	0,551	-0,671	-0,524	-0,447	0,627	0,167
	Sig. (2-tailed)	0,435	0,406	0,917	0,507	0,287	0,823	0,42	0,32	0,157	0,069	0,183	0,266	0,096	0,693
	N	8	8	8	8	8	8	8	8	8	8	8	8	8	8
PFHpS	Pearson Correlation	0,547	0,417	0,088	-0,238	-0,031	0,214	-0,143	-0,357	-0,418	-0,165	0,216	0,481	0,224	0,262
	Sig. (2-tailed)	0,16	0,304	0,836	0,571	0,942	0,61	0,736	0,385	0,303	0,697	0,607	0,228	0,594	0,531
	N	8	8	8	8	8	8	8	8	8	8	8	8	8	8
PFOSlin	Pearson Correlation	,999**	,961**	-0,235	0,162	0,513	0,476	0,286	-0,429	-0,111	-0,169	0,512	0,111	0,075	-0,357
	Sig. (2-tailed)	0	0	0,575	0,701	0,194	0,233	0,493	0,289	0,794	0,69	0,195	0,793	0,861	0,385
	N	8	8	8	8	8	8	8	8	8	8	8	8	8	8
∑PFOS	Pearson Correlation	1,000**	,961**	-0,249	0,166	0,513	0,476	0,286	-0,429	-0,089	-0,205	0,502	0,097	0,106	-0,357
	Sig. (2-tailed)	0	0	0,552	0,695	0,193	0,233	0,493	0,289	0,834	0,627	0,205	0,82	0,803	0,385
	N	8	8	8	8	8	8	8	8	8	8	8	8	8	8
PFNA	Pearson Correlation	,804*	,848**	-0,414	-0,048	0,261	0,214	,714*	-0,048	0,288	-0,497	0,394	-0,378	0,339	-0,381
	Sig. (2-tailed)	0,016	0,008	0,308	0,911	0,532	0,61	0,047	0,911	0,49	0,21	0,334	0,356	0,412	0,352
	N	8	8	8	8	8	8	8	8	8	8	8	8	8	8
PFDA	Pearson Correlation	,969**	,985**	-0,37	0,199	0,548	0,31	0,357	-0,452	0,023	-0,243	0,507	-0,066	0,111	-0,595
	Sig. (2-tailed)	0	0	0,368	0,636	0,159	0,456	0,385	0,26	0,957	0,562	0,199	0,877	0,793	0,12
	N	8	8	8	8	8	8	8	8	8	8	8	8	8	8
PFUnDA	Pearson Correlation	,924**	,952**	-0,386	0,311	0,648	0,571	0,476	-0,333	-0,148	-0,252	0,37	0,238	0,208	-0,381
	Sig. (2-tailed)	0,001	0	0,345	0,454	0,082	0,139	0,233	0,42	0,727	0,547	0,368	0,571	0,621	0,352
	N	8	8	8	8	8	8	8	8	8	8	8	8	8	8
PFDoDA	Pearson Correlation	,826*	,862**	-0,246	0,426	,730*	0,69	0,333	-0,405	-0,257	0,111	0,578	0,337	-0,12	-0,167
	Sig. (2-tailed)	0,011	0,006	0,557	0,292	0,04	0,058	0,42	0,32	0,539	0,794	0,134	0,414	0,777	0,693
	N	8	8	8	8	8	8	8	8	8	8	8	8	8	8
PFTrDA	Pearson Correlation	0,542	0,625	-0,039	0,241	0,499	0,071	-0,214	-0,619	-0,294	0,447	0,66	0,301	-0,386	-0,405
	Sig. (2-tailed)	0,166	0,098	0,927	0,566	0,208	0,867	0,61	0,102	0,48	0,266	0,075	0,469	0,345	0,32
	N	8	8	8	8	8	8	8	8	8	8	8	8	8	8
PFTeDA	Pearson Correlation	0,438	0,373	0,299	0,095	0,272	0,238	-0,357	-,714*	-0,472	0,664	0,632	0,433	-0,606	-0,19
	Sig. (2-tailed)	0,278	0,362	0,471	0,822	0,515	0,57	0,385	0,047	0,238	0,073	0,093	0,284	0,112	0,651
	N	8	8	8	8	8	8	8	8	8	8	8	8	8	8

Table A27. Pearson (for normally distributed variables) and Spearman (for non-normal distributed variables) correlation between BM, BCI, PFAS, Hg, Se:Hg, TH:protein, TSH:protein, and follicle count in female glaucous gulls (*Larus hyperboreus*) (n=8) captured in Sassendalen and Adventfjorden, Svalbard, in April and May 2017.

Correlations Females															
		∑PFSA	∑PFCA	Protein	FT4:protein	TT4:protein	FT3:protein	TT3:protein	TSH:protein	Hg_plasma	Hg_feathers	Hg_liver	SeHg_plasma	SeHg_feather	SeHg_liver
∑PFSA	Pearson Correlation	1	,961**	-0,248	0,159	0,507	0,476	0,286	-0,429	-0,083	-0,212	0,496	0,091	0,113	-0,357
	Sig. (2-tailed)		0	0,553	0,706	0,2	0,233	0,493	0,289	0,844	0,614	0,211	0,83	0,791	0,385
	N	8	8	8	8	8	8	8	8	8	8	8	8	8	8
∑PFCA	Pearson Correlation	,961**	1	-0,376	0,198	0,561	0,31	0,357	-0,405	-0,014	-0,234	0,521	0,009	0,142	-0,429
	Sig. (2-tailed)	0		0,359	0,638	0,148	0,456	0,385	0,32	0,973	0,577	0,185	0,983	0,738	0,289
	N	8	8	8	8	8	8	8	8	8	8	8	8	8	8
Protein	Pearson Correlation	-0,248	-0,376	1	-0,327	-0,418	0,69	-0,071	0,262	0,215	0,577	-0,356	0,065	-0,394	0,286
	Sig. (2-tailed)	0,553	0,359		0,429	0,302	0,058	0,867	0,531	0,609	0,134	0,386	0,878	0,334	0,493
	N	8	8	8	8	8	8	8	8	8	8	8	8	8	8
FT4:protein	Pearson Correlation	0,159	0,198	-0,327	1	,919**	0,643	0,262	-0,024	0,097	-0,199	0,181	0,369	0,229	-0,167
	Sig. (2-tailed)	0,706	0,638	0,429		0,001	0,086	0,531	0,955	0,819	0,637	0,668	0,368	0,585	0,693
	N	8	8	8	8	8	8	8	8	8	8	8	8	8	8
TT4:protein	Pearson Correlation	0,507	0,561	-0,418	,919**	1	1	0,476	-0,048	0,025	-0,213	0,369	0,357	0,215	0,238
	Sig. (2-tailed)	0,2	0,148	0,302	0,001		.	0,233	0,911	0,953	0,613	0,369	0,385	0,61	0,57
	N	8	8	8	8	8	8	8	8	8	8	8	8	8	8
FT3:protein	Spearman Correlatio	0,476	0,31	0,69	0,643	1	0,476	-0,048	0,19	-0,333	0,19	0,19	0,31	0,238	-0,119
	Sig. (2-tailed)	0,233	0,456	0,058	0,086	.	0,233	0,911	0,651	0,42	0,651	0,651	0,456	0,57	0,779
	N	8	8	8	8	8	8	8	8	8	8	8	8	8	8
TT3:protein	Spearman Correlatio	0,286	0,357	-0,071	0,262	0,476	1	0,143	0,667	-0,619	0	-0,643	0,595	-0,119	0,524
	Sig. (2-tailed)	0,493	0,385	0,867	0,531	0,233	.	0,736	0,071	0,102	1	0,086	0,12	0,779	0,183
	N	8	8	8	8	8	8	8	8	8	8	8	8	8	8
TSH:protein	Spearman Correlatio	-0,429	-0,405	0,262	-0,024	-0,048	0,143	1	0,214	-0,571	-0,31	0	,714*	0,524	0,143
	Sig. (2-tailed)	0,289	0,32	0,531	0,955	0,911	0,736	.	0,61	0,139	0,456	1	0,047	0,183	0,736
	N	8	8	8	8	8	8	8	8	8	8	8	8	8	8
Hg_plasma	Pearson Correlation	-0,083	-0,014	0,215	0,097	0,025	-0,333	-0,619	-0,571	1	-0,264	-0,301	-0,634	0,269	-0,429
	Sig. (2-tailed)	0,844	0,973	0,609	0,819	0,953	0,42	0,102	0,139		0,528	0,468	0,092	0,52	0,289
	N	8	8	8	8	8	8	8	8	8	8	8	8	8	8
Hg_feathers	Pearson Correlation	-0,212	-0,234	0,577	-0,199	-0,213	0,19	0	-0,31	-0,264	1	0,271	0,045	-,940**	-0,595
	Sig. (2-tailed)	0,614	0,577	0,134	0,637	0,613	0,651	1	0,456	0,528		0,516	0,916	0,001	0,12
	N	8	8	8	8	8	8	8	8	8	8	8	8	8	8
Hg_liver	Pearson Correlation	0,496	0,521	-0,356	0,181	0,369	0,19	-0,643	0	-0,301	0,271	1	-0,089	-0,447	0,238
	Sig. (2-tailed)	0,211	0,185	0,386	0,668	0,369	0,651	0,086	1	0,468	0,516		0,834	0,267	0,57
	N	8	8	8	8	8	8	8	8	8	8	8	8	8	8
SeHg_plasma	Pearson Correlation	0,091	0,009	0,065	0,369	0,357	0,31	0,595	,714*	-0,634	0,045	-0,089	1	0,161	0,452
	Sig. (2-tailed)	0,83	0,983	0,878	0,368	0,385	0,456	0,12	0,047	0,092	0,916	0,834		0,703	0,26
	N	8	8	8	8	8	8	8	8	8	8	8	8	8	8
SeHg_feather	Pearson Correlation	0,113	0,142	-0,394	0,229	0,215	0,238	-0,119	0,524	0,269	-,940**	-0,447	0,161	1	1
	Sig. (2-tailed)	0,791	0,738	0,334	0,585	0,61	0,57	0,779	0,183	0,52	0,001	0,267	0,703		.
	N	8	8	8	8	8	8	8	8	8	8	8	8	8	8
SeHg_liver	Spearman Correlatio	-0,357	-0,429	0,286	-0,167	0,238	-0,119	0,524	0,143	-0,429	-0,595	0,238	0,452	1	
	Sig. (2-tailed)	0,385	0,289	0,493	0,693	0,57	0,779	0,183	0,736	0,289	0,12	0,57	0,26	.	
	N	8	8	8	8	8	8	8	8	8	8	8	8	8	

Table A28. Pearson (for normally distributed variables) and Spearman (for non-normal distributed variables) correlation between BM, BCI, PFAS, Hg, Se:Hg, TH:protein, TSH:protein, and follicle count in female glaucous gulls (*Larus hyperboreus)* (n=8) captured in Sassendalen and Adventfjorden, Svalbard, in April and May 2017.

APPENDIX L: Histology

Class A

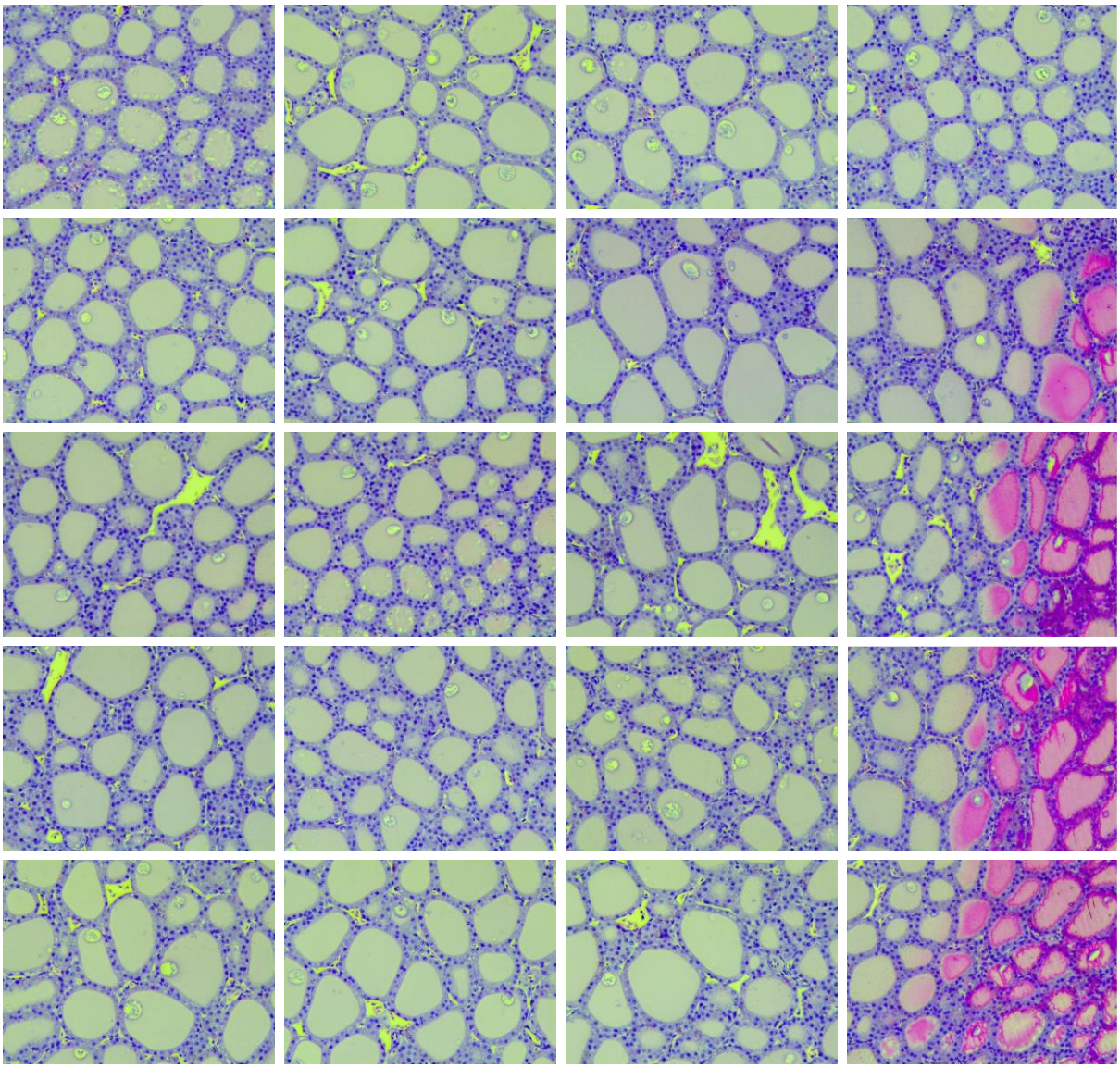

LH1, female
200x, HE stain
326 x 244 µm

Class A

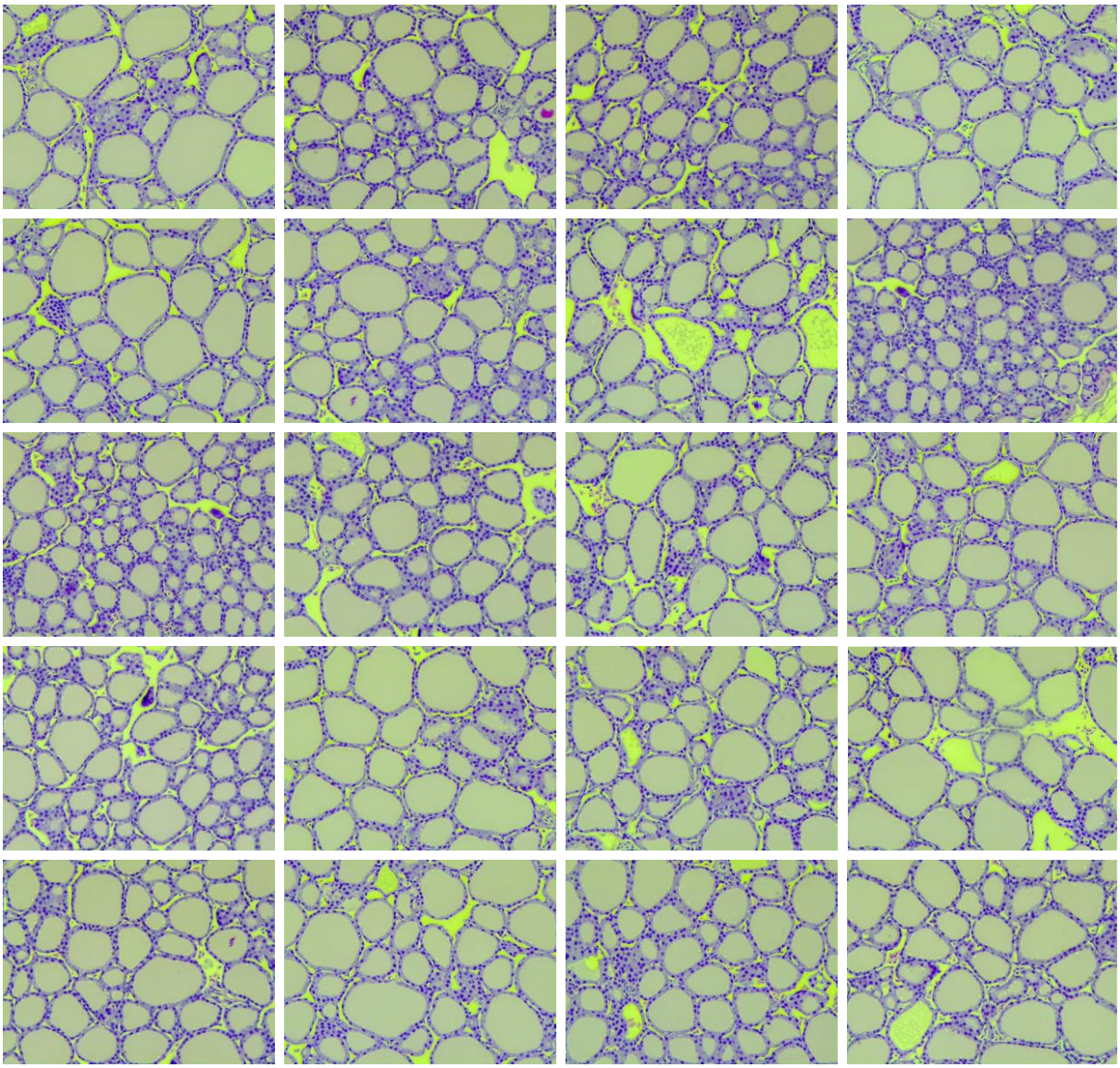

LH2, male
200x, HE stain
326 x 244 µm

Class A

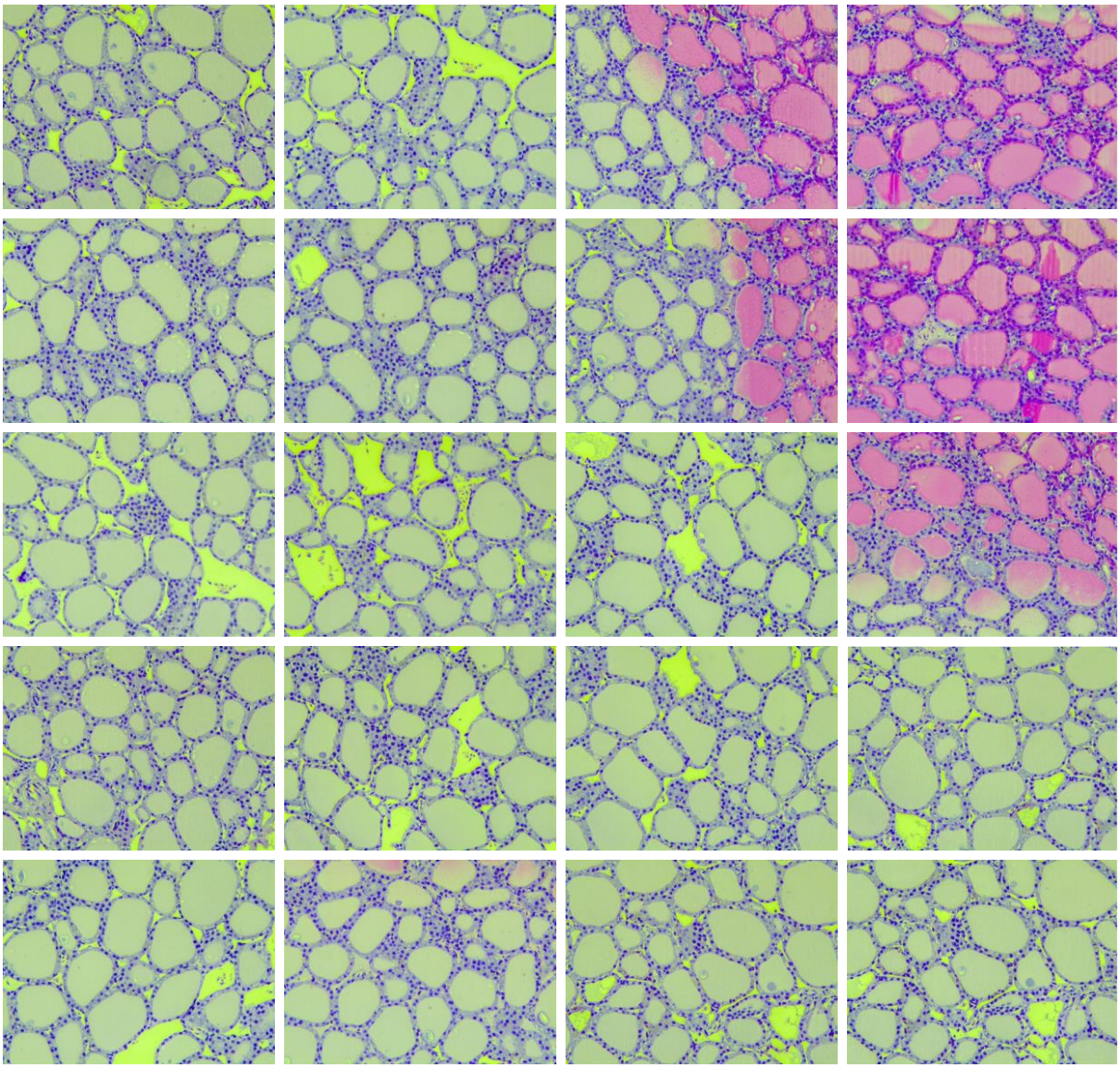

LH4, female
200x, HE stain
326 x 244 µm

Class A

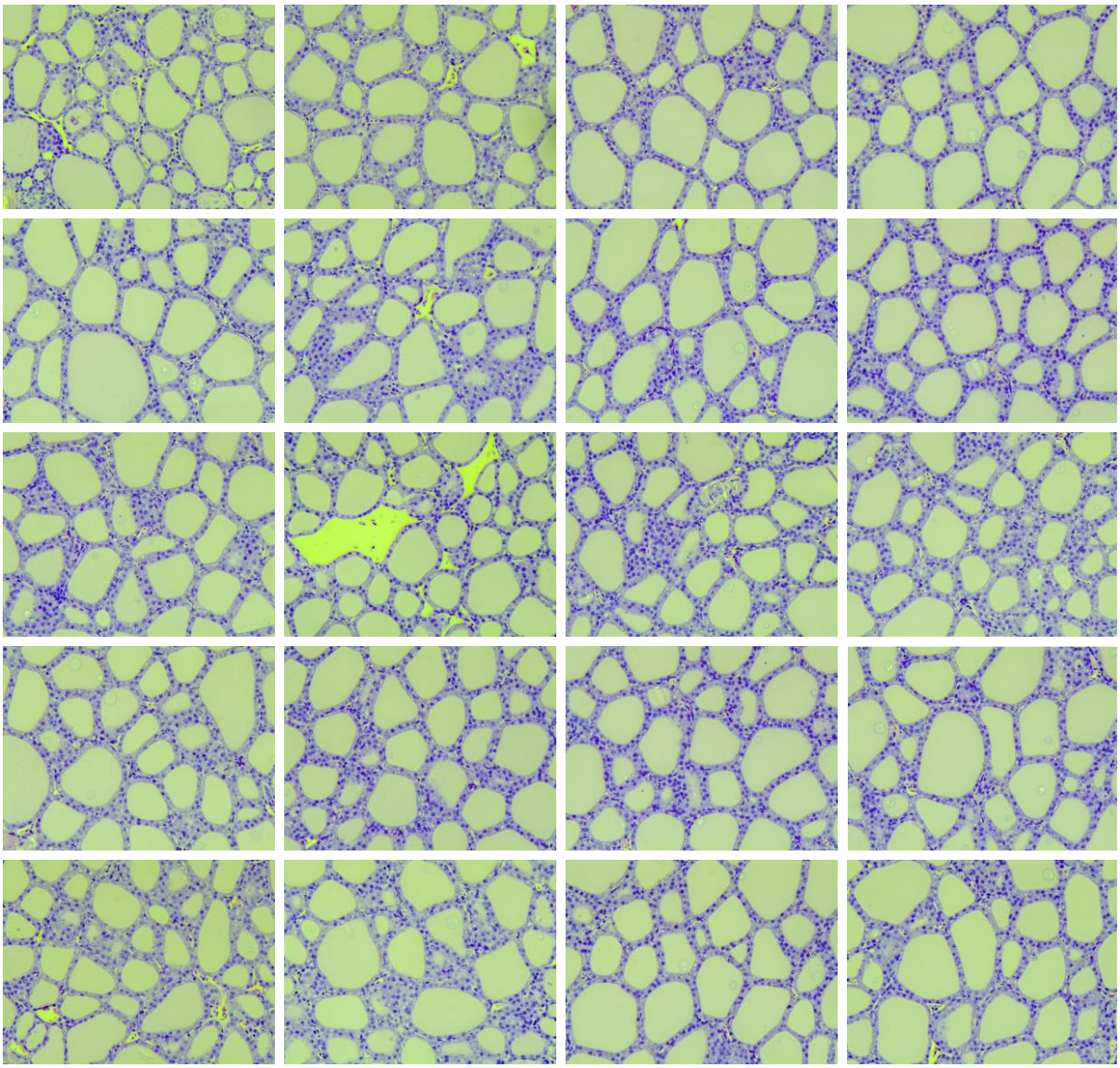

LH10, female
200x, HE stain
326 x 244 µm

Class A

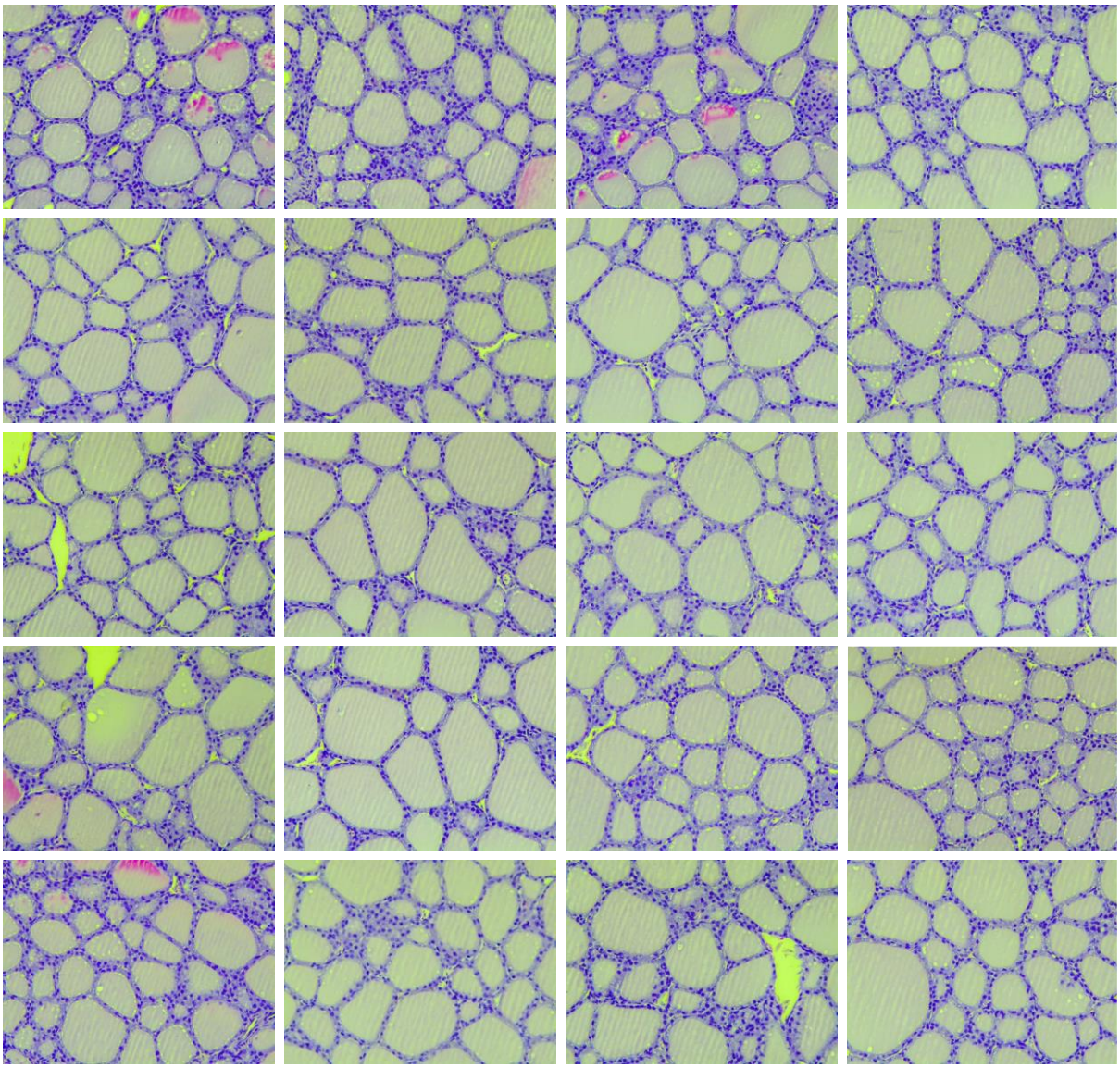

LH13, male
200x, HE stain
326 x 244 µm

Class B

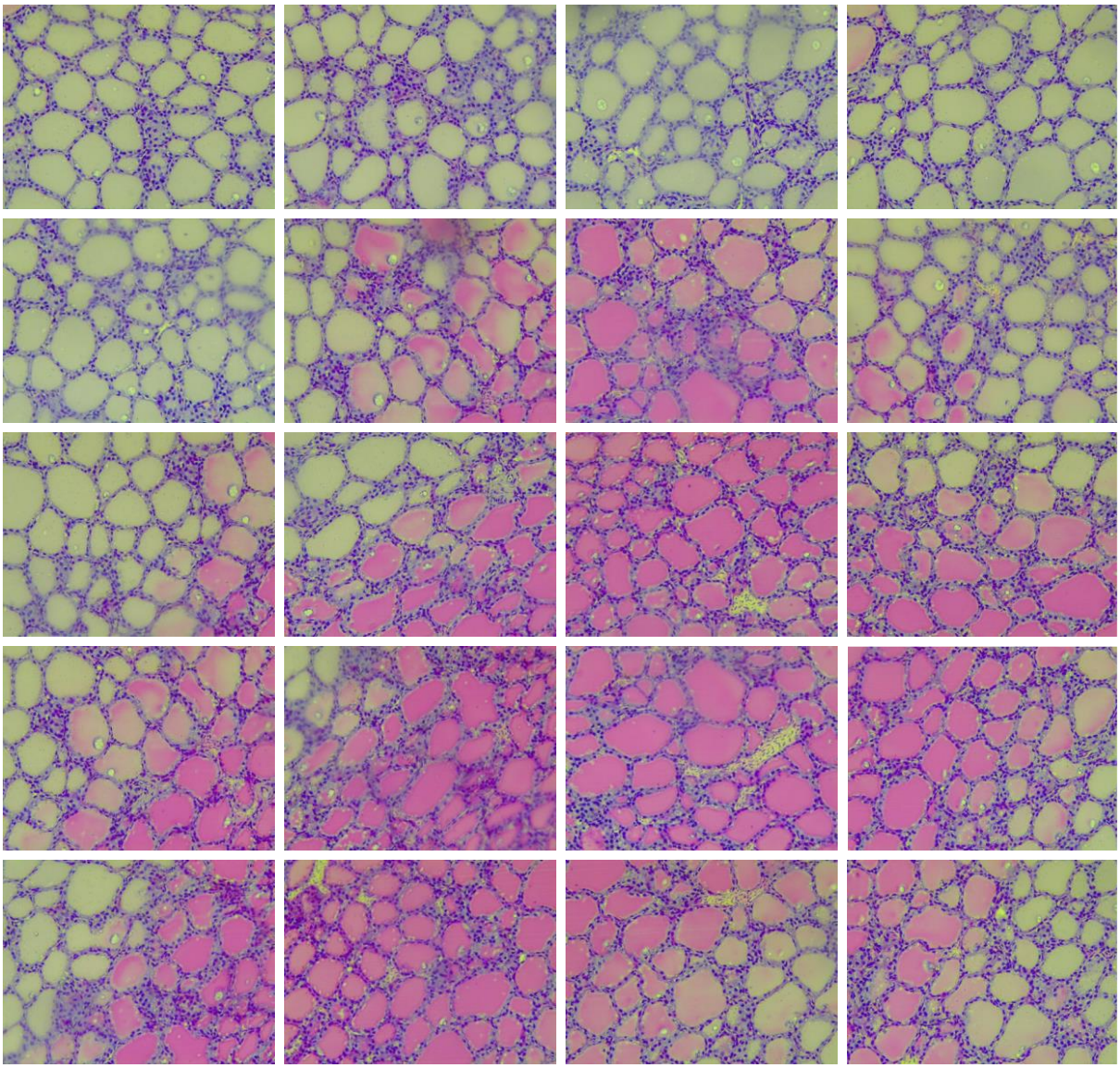

LH3, male
200x, HE stain
326 x 244 µm

Class B

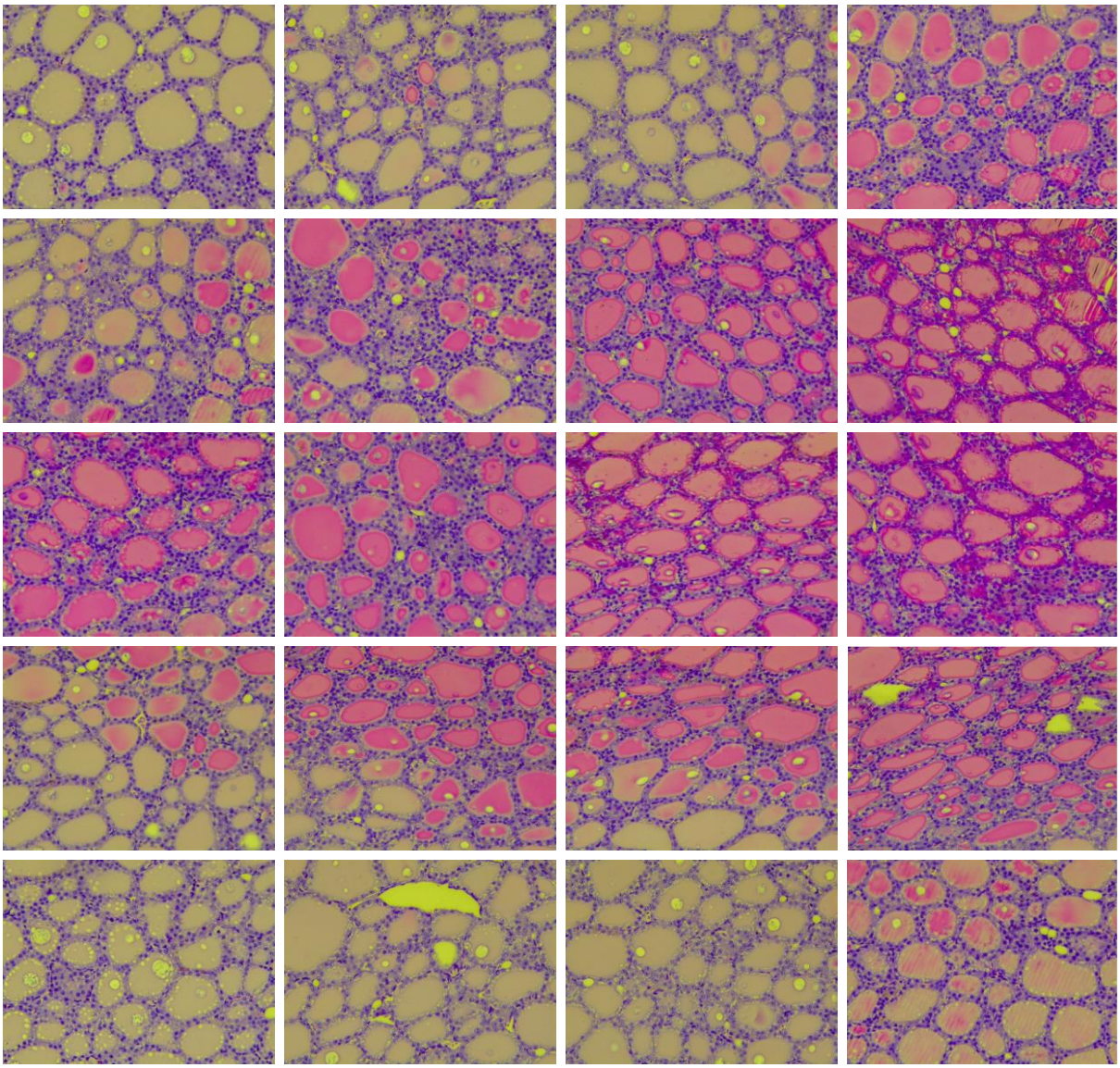

LH5, female
200x, HE stain
326 x 244 µm

Class B

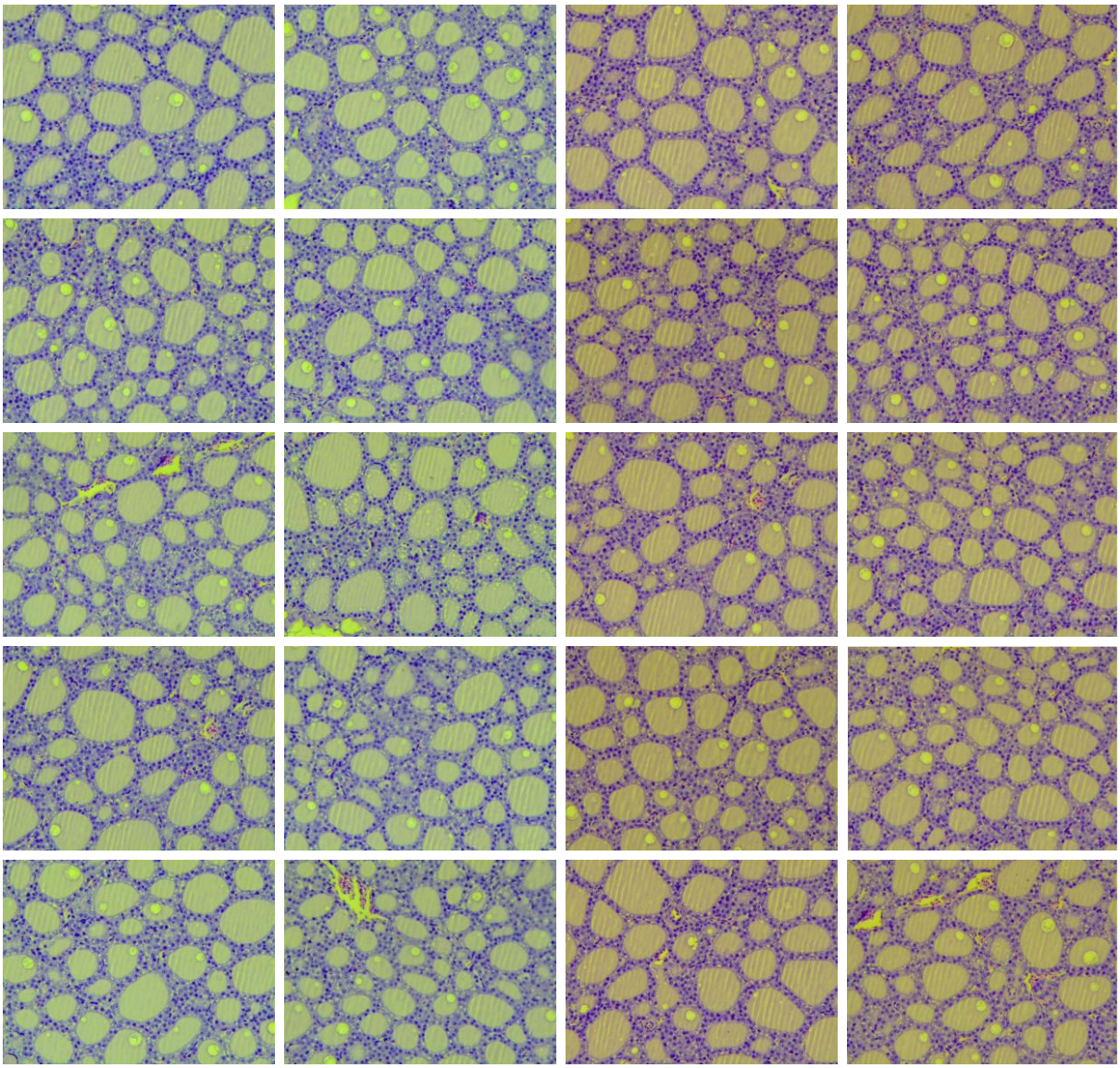

LH7, female
200x, HE stain
326 x 244 µm

Class B

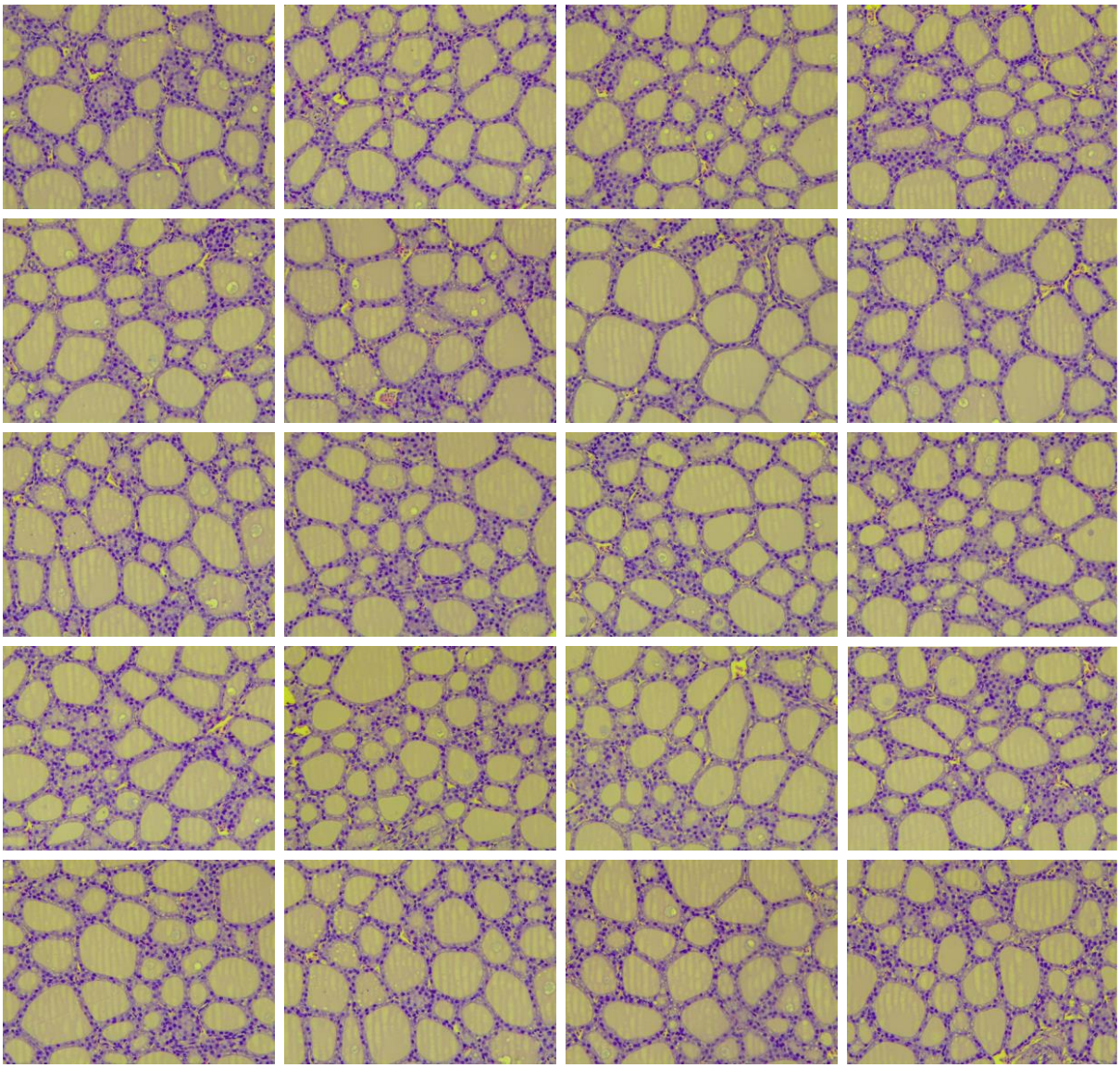

LH8, male
200x, HE stain
326 x 244 µm

Class B

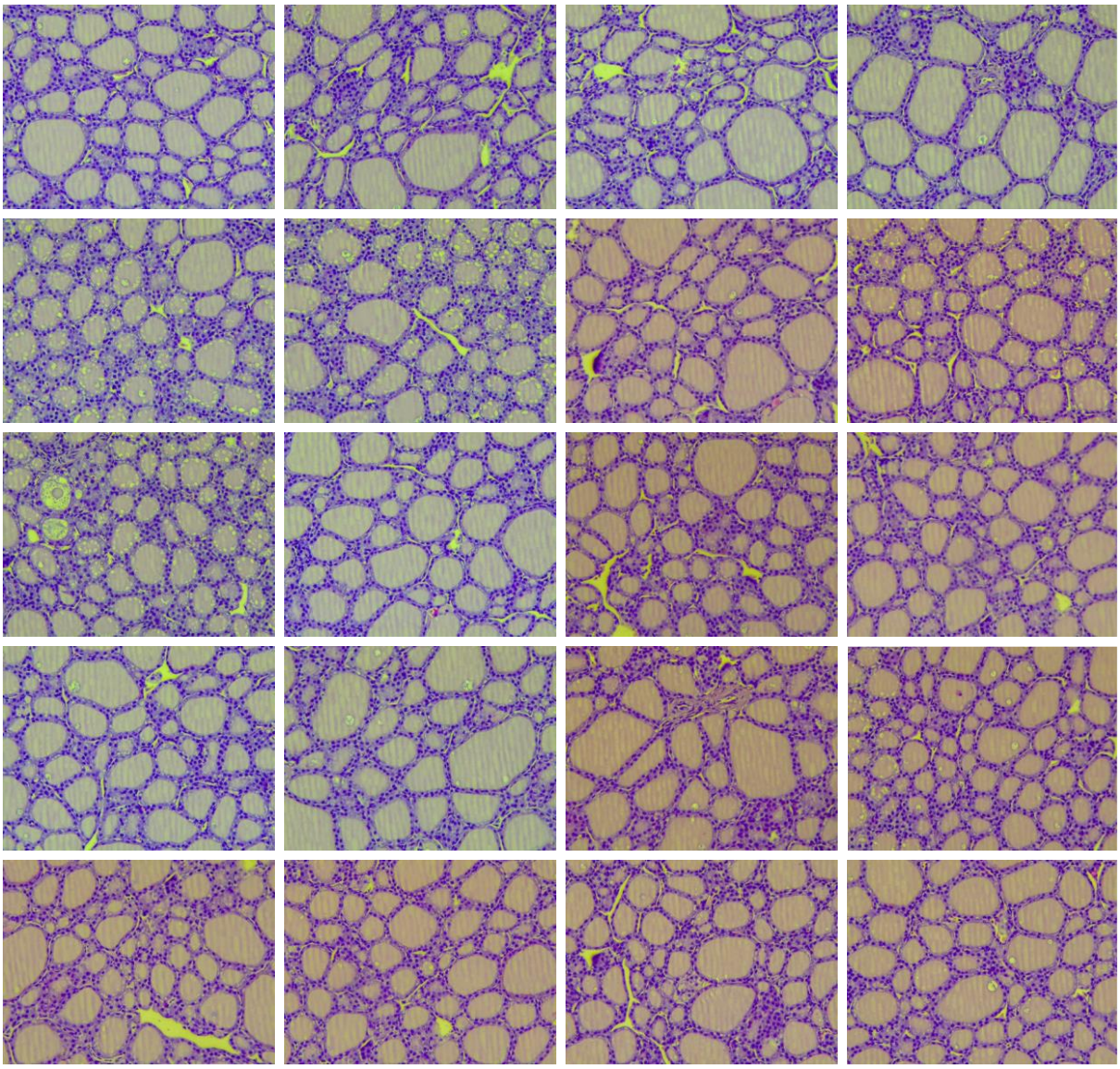

LH9, female
200x, HE stain
326 x 244 µm

Class B

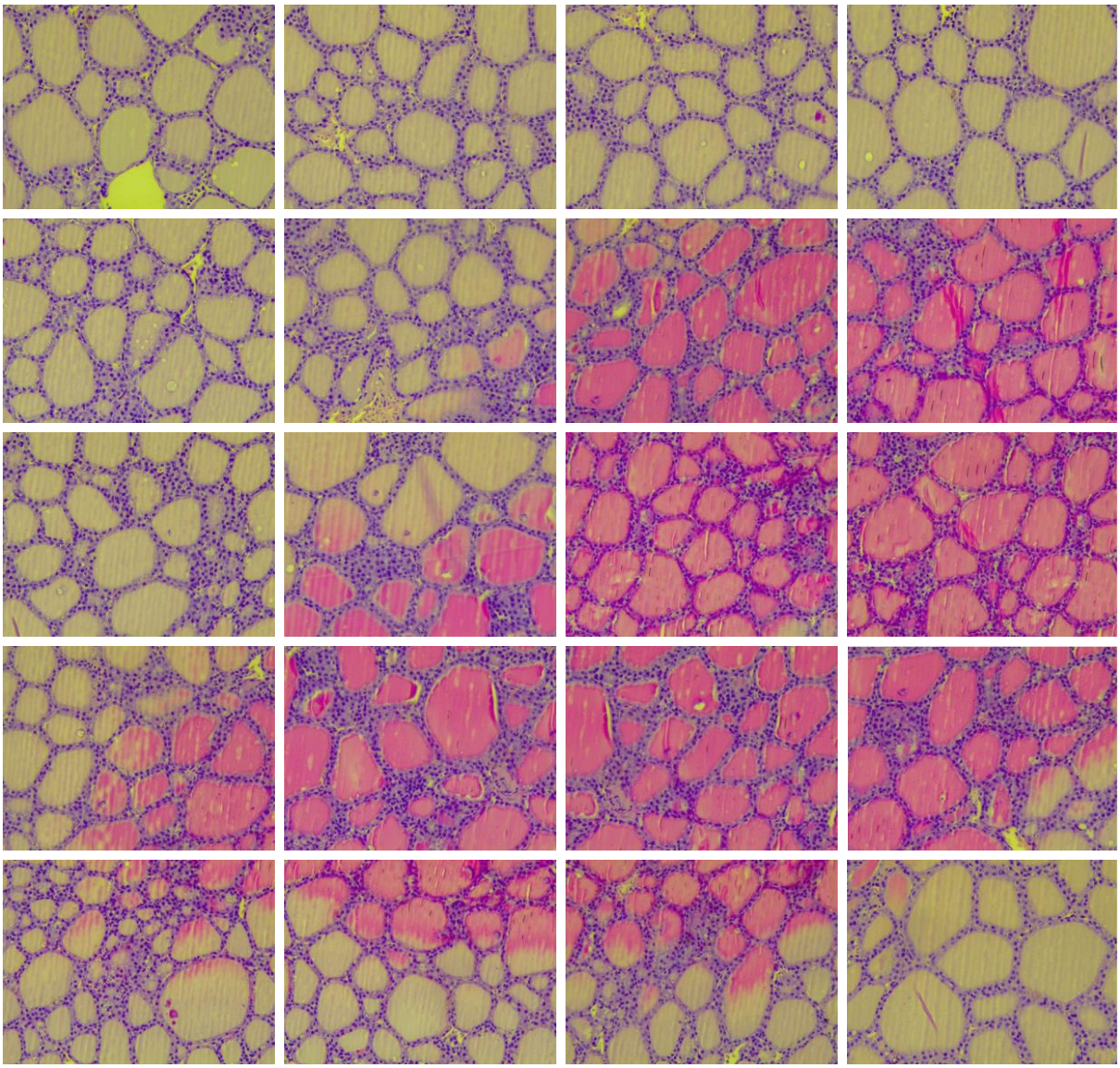

LH11, male
200x, HE stain
326 x 244 µm

Class B

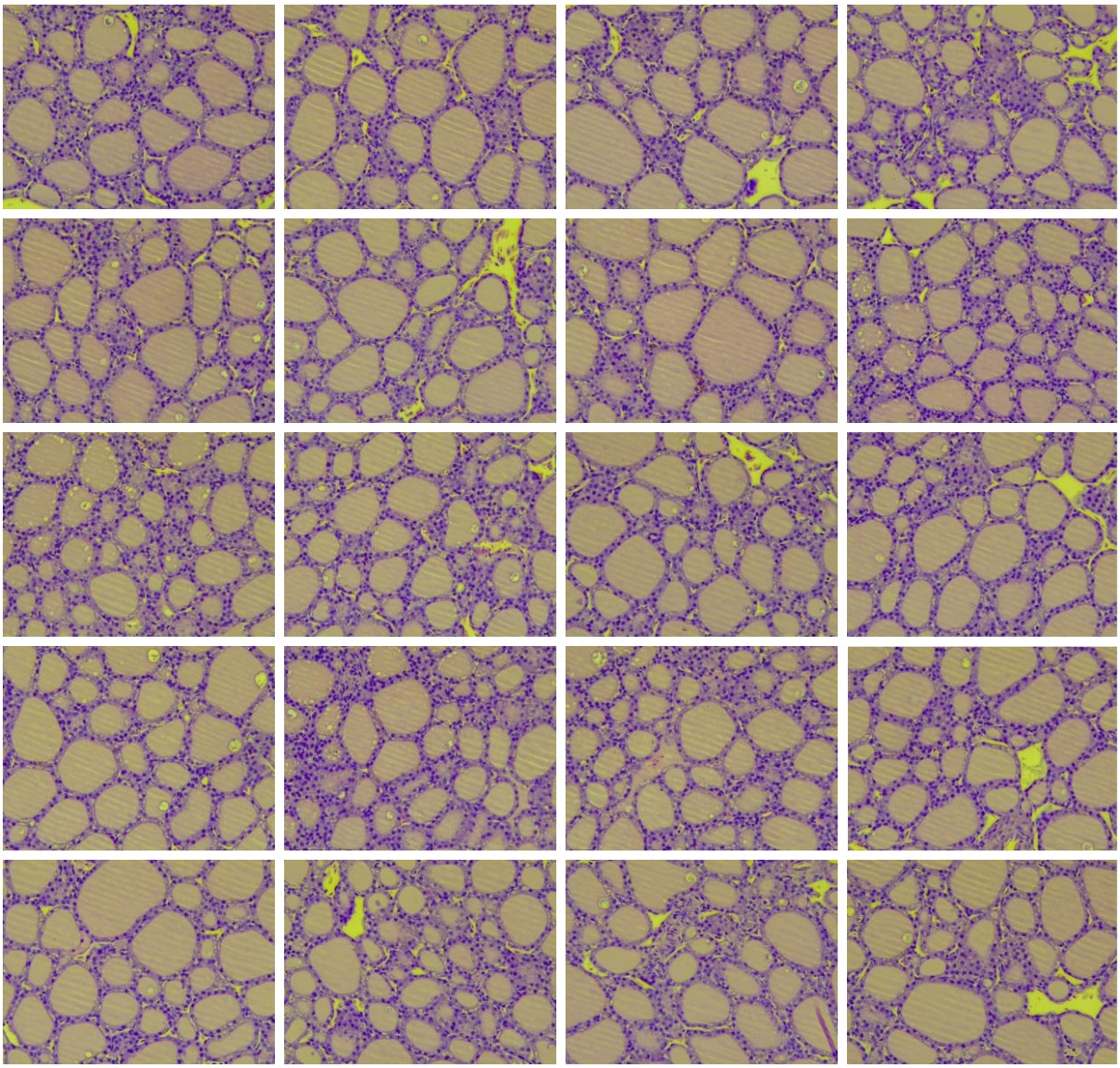

LH14, male
200x, HE stain
326 x 244 µm

Class B

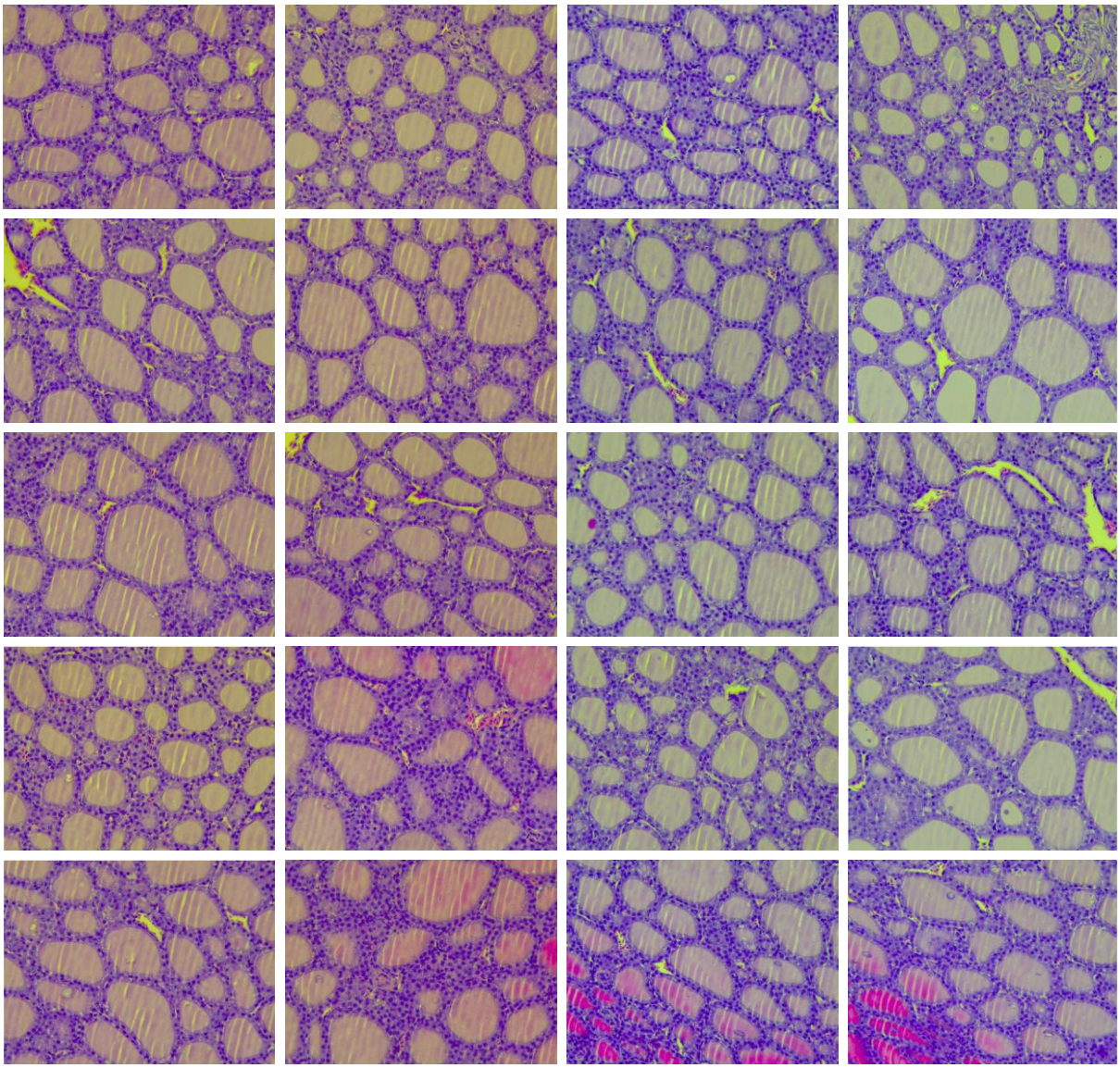

LH15, male
200x, HE stain
326 x 244 µm

Class C

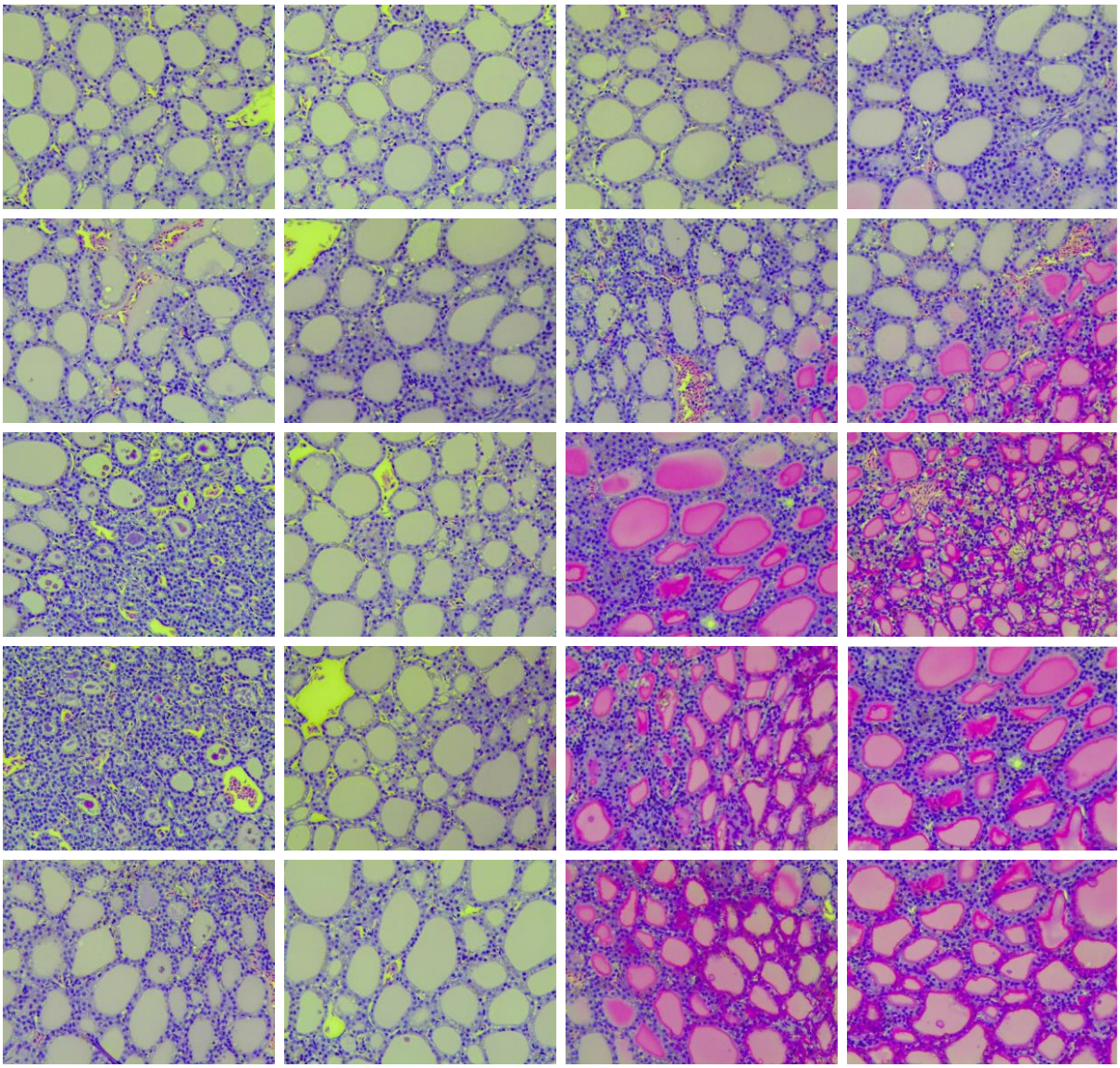

LH6, female
200x, HE stain
326 x 244 µm